124 p.

PROTON-NEUTRON DAMAGE

CORRELATION IN SEMICONDUCTORS

N63 18856

CODE-1

Prepared

by

J. R. Bilinski

E. H. Brooks

U. Cocca

R. J. Mai[illegible]

D. W. Seigworth

Radiation Effects Operation

Defense Systems Department

General Electric Company

Syracuse, New York

RQ+ 6756

OTS PRICE

XEROX $ ~~10.10~~ ph

MICROFILM $ ~~3.92~~ mf

Final Report

June 10, 1962

Period covered: November 24, 1961 through June 1, 1962

Contract No. NAS 1 -1595

Reproduced by
NATIONAL TECHNICAL
INFORMATION SERVICE
Springfield, Va. 22151

Prepared

for

National Aeronautics and Space Administration

Langley Research Center

Langley Air Force Base, Virginia

CR-50,422

I. FOREWORD

This report was prepared by the Radiation Effects Operation, Defense Systems Department of the General Electric Company on NASA Contract NAS 1 - 1595. The work was administered under the direction of W. C. Hulten of the National Space and Aeronautics Administration at Langley Field, Virginia.

The studies presented began on November 24, 1961 and were concluded on June 1, 1962.

In addition to the principal contributors listed on the preceding page, a substantial consulting effort, particularly on solar cell instrumentation was contributed by Dr. R. R. Bobone of our General Engineering Laboratory in Schenectady, New York. J. C. Peden of our Missile Space and Vehicle Department in Philadelphia has also assisted greatly in the solar cell measurements. Dr. J. W. Corbett, General Electric Company Research Laboratory in Schenectady has provided valuable advice and direction in the early stages of this study. The cooperation of W. Rosenzweig of the Bell Telephone Laboratories in Murray Hill, New Jersey, is appreciated.

II. ABSTRACT

18856

A study program to determine a proton-neutron damage correlation in semiconductors is presented. Three approaches were undertaken: Theoretical, empirical using data from existing literature, and experimental.

The results of the theoretical studies show that damage processes between the neutrons and protons are basically different in silicon. Damage to minority carrier lifetime from neutron irradiation is characterized by the effective cross sectional area of the cluster of displaced atoms and is relatively independent of the type of defect. Damage from protons, on the other hand, is dominated by the type of defect introduced (e.g. impurity trapping center). For this reason, theoretically derived damage "cross sections" for each different type of bombarding particle must be based on different (and independent) physical properties of the basic material.

In the empirical study using the data from the literature, it was not possible to determine a reliable proton-neutron correlation. Spread in neutron data due to irradiation of different types of devices, inadequate data reporting and no data on similar semiconductors under both neutron and proton irradiation contributed to this result.

The experimental program was carried out on silicon solar cells under fission and moderated neutrons and proton energies of 48.5, 68.9, and 96.5 Mev. A proton-neutron correlation for the diffusion length damage was determined and the ratios of the proton to neutron damage varied from 0.6 to 4.8 depending on the proton energy and neutron spectrum.

TABLE OF CONTENTS

I	Foreword	1
II	Abstract	1
III	Introduction	2
IV	Discussion	4
	A. Theoretical Calculation of Damage	5
	B. Analysis of Presently Existing Data	6
	C. Experimental Program	30
	1. Design of Experiment	
	a. Description of Solar Cells	40
	b. Description of Radiation Facilities	42
	c. Experimental Set-up	44
	d. Description of Measurements	51
	e. Diffusion Length Measurement Using a One Micron Photon Source	55
	2. Results of Experiment	57
	D. Discussion of Results	61
V	Conclusions	65
VI	Recommendations	66
VII	Appendix	
	A. Proton and Neutron Radiation Damage Data on Silicon and Germanium	68
	B. Experimental Data	89
VIII	References	
	A. Report References	111
	B. General References	116

III. INTRODUCTION

The discovery of large intensities of ionizing radiation in space has shown the need for rather extensive radiation damage studies on the electrical and mechanical components used on space vehicles. Space radiation consists primarily of electrons and protons. Radiation damage studies using electrons are fairly straightforward; there are many sources of high energy electrons available for this kind of experimental work. This is not true for protons. Protons of energies up to around 3 Mev can be obtained from electrostatic accelerators, but for energies up to several hundred Mev cyclotron-type accelerators are generally required. These machines are not common, nor are they generally available for extensive radiation damage studies. Little data is available as to proton damage to equipment; experimental studies using protons are often slow, difficult, and expensive.

In organic materials it has been fairly conclusively demonstrated that equal doses of radiation (where the dose is expressed in terms of absorbed energy) will cause equal damage irrespective of the type of radiation involved. To date no such equivalence has been demonstrated in inorganic materials.

If a damage equivalence were established between protons and neutrons, then the enormous amount of neutron damage data and the comparably economical and convenient reactor facilities could be utilized to obtain irradiation information on materials and devices to, in turn, predict their damage in the proton environment in space. Recently questions about the latter approach have been proposed. To this end, this study was undertaken for NASA.

The objective of this study program was to determine if a damage correlation existed between protons and neutrons in semiconductor materials. A

two-fold approach, theoretical and empirical, was undertaken early in this study:

1. A study of the basic proton and neutron damage processes in semiconductor material to determine a basic theoretical correlation.

2. Using the existing experimental proton and neutron damage data in the literature on semiconductors to arrive at an empirical correlation.

The correlation determined by both approaches then would be tested through carefully controlled radiation experiments.

During the study program, it was found that both of the above tasks would not yield a useful proton-neutron correlation. It was then decided to use the experimental program to carefully determine the damage correlation. Silicon solar cells were chosen as the test item for two reasons: They have a convenient basic diode structure from which we could obtain clean basic data and the data on the cells themselves would be useful to NASA from the space radiation environment considerations. Tests were conducted under fission and moderated neutrons and various energies of protons.

Thus, the report presents the results of the study program at determining a neutron-proton correlation by three approaches: Theoretical, empirical using data from existing literature, and experimental, the latter yielding a correlation.

IV. DISCUSSION

A. THEORETICAL CALCULATION OF DAMAGE

This section describes and compares the neutron and proton damage production processes in silicon. We will show, within the state-of-the-art, that a proton damage is basically different from neutron damage in silicon.

The production of permanent damage in silicon by nuclear particles is a three phase process. First the incident particle has a primary interaction with an atom of the lattice, creating a recoil atom, or primary knockon. This primary knockon collides with other atoms giving secondary and tertiary knockons. The vacancies formed by this cascade diffuse a few interatomic distances from the impact site almost immediately, and can be trapped by stress centers such as impurities, and other vacancies, to form defects.

The primary interactions are well understood except for a few notable exceptions such as proton spallation. There are no exact models for the partitioning of the energy of a knockon into lattice vibrations, electronic excitation and additional displacements. Electronic excitation models are particularly poor. With some simplifying assumptions, some approximate calculations of the formation of defects can be made. We will discuss each of the processes in the order in which they occur.

PRIMARY INTERACTIONS

To calculate the number and energy of primary knockons, the cross sections for all important interactions are needed. To process these cross sections we need the formulas given below for interactions in center of mass coordinates and corresponding recoil energy.

ELASTIC SCATTERING

The differential scattering cross section is normally given as a function of cos θ. To convert cos θ to the energy of the recoil we need:

$$T = KE \sin^2 \frac{\theta}{2} = .133\ E \sin^2 \frac{\theta}{2} \qquad (1)$$

where:

$$K = 4 \frac{M_i M_{si}}{(M_i + M_{si})^2} = .133 \text{ for non-relativistic velocities.}$$

$$KE = 2 \frac{M_i}{M_{si}} \left(\frac{E + 2M_i C^2}{M_i C^2} \right) E = 2 \frac{M_i^2}{M_{si}} V^2 (1-\beta^2) \text{ for}$$

relativistic velocities, with the approximation M_{si} much greater than M_i.

Where:

θ = scattering angle of the neutron or proton in the center of mass system,

E = energy of the neutron or proton,

M_i = mass of the neutron or proton,

M_{si} = mass of the silicon atom.

When we can convert θ to T, the energy of the energy of the recoil [illegible]:

$$\cos\theta = 1 - T/KE$$

$$d\Omega = \sin\theta = 2T/KE \qquad (3)$$

PROTON COULOMB SCATTERING AND SEPARATION

It can be shown that coulomb scattering [illegible] damage production [illegible] less than about 500 Mev. The non-relativistic differential coulomb [illegible] cross section is:

$$d\sigma = \frac{b^2}{16} \frac{d\Omega}{\sin^4 \theta/2} \qquad (4)$$

Where:

$$b = \frac{2Z z e^2}{v^2} \frac{M_p + M_{si}}{M_{si}}$$

Z = atomic number of silicon

z = atom number of a proton

e = electron charge.

For relativistic velocities this is modified by a factor:

$$\eta \cong (1 - \beta^2) \left[1 - \beta^2 \sin^2 \frac{\theta}{2} + \pi\alpha\beta \sin \frac{\theta}{2} \left(1 - \sin \frac{\theta}{2} \right) \right] \qquad (5)$$

Where:

$\beta = V/C$ and $\alpha = Z/137$.

Applying equations (1) and (2):

$$d\sigma = \frac{\pi b^2}{4} \frac{T_m}{T^2} dT = \frac{P_1}{E} \frac{dT}{T^2} \qquad (6)$$

Where:

$T_m = KE,$

$P_1 = 4.56 \times 10^{-13} (ev\text{-}cm)^2$

For relativistic velocities it must be noted that b is proportional to v^{-2} and not the inverse energy. This is because the momentum transfer is an increasing function of the time spent in the electrostatic field. The full relativistic cross section is then:

$$d\sigma = \frac{2\pi (Zze^2)}{(M_{si} c^2) \beta^2} \left[1 - \beta^2 \frac{T}{T_m} + \pi\alpha\beta \left\{ \left(\frac{T}{T_m} \right)^{\frac{1}{2}} - \frac{T}{T_m} \right\} \right] \frac{dT}{T^2} \qquad (7)$$

To obtain the cross section for recoils of energy greater than some energy T, we integrate:

$$\sigma (T > T_i) = \int^{T_m} d\sigma$$

$$= \frac{T_i P_2}{\beta^2} \left[\frac{1}{T_i} - \frac{1}{T_m} - \frac{\beta^2 + \pi\alpha\beta}{T_m} \ln \frac{T_m}{T_i} + \frac{1}{2} \frac{\pi\alpha\beta}{T_m^{1/2}} \left(\frac{1}{T_i^{1/2}} - \frac{1}{T_m^{1/2}} \right) \right]$$

T_m = 1.3 mev for 10 mev proton; T_1 = 12 ev

$T_m \gg T_1$

$$\sigma (T > T_1) \cong \frac{P_2}{T_1 \beta^2} = \frac{81.54}{\beta^2} \text{ barns}$$

For silicon:

$$P_2 = \frac{2\pi (Ze^2)^2}{(M_{si} c^2)} = .98 \times 10^{-21} \text{ ev-cm}^2$$

The density of silicon is ~ $.052 \times 10^{24}$ atoms/cm^3

$$\Sigma = N\sigma = 4.24 / \beta^2 \text{ cm}^{-1} \qquad (9)$$

TABLE I

PROTON COULOMB COLLISION CROSS SECTION

E (Mev)	β	β^2	Σ cm^{-1}
10	.14485	.020981	20.2
50	.31406	.098633	43.0
100	.42821	.183362	23.1
200	.56617	.320533	13.2
400	.71307	.508468	8.34
700	.81976	.672009	6.31
Spallation			.033

For energies greater than about 500 Mev, the spallation cross section can be important. The silicon nucleus is about 3×10^{-13} cm in radius. This is larger than the wave length $\lambda' = \lambda/2\pi$ of the proton. For purposes of getting an upper limit on the spallation cross section, we can use the cross section of a sphere, i.e., $\pi (R_{si} + R_p)^2$. This results in an upper limit of .64 barns. How important this is depends on the number of defects produced by one primary interaction.

NEUTRON CROSS SECTIONS

We are interested in the neutron cross sections at neutron energies, found in a reactor. The fission spectrum averaged total cross section for silicon is 3.12 barns. The average cross section for neutrons from the "1/E" spectrum is 2.45 barns. As it will be seen from succeeding sections, these are the only numbers we need.

2. THE CASCADE

If the energy of a knockon is below about 20 kev for silicon (where screened Rutherford scattering sets in) the scattering off other atoms is approximately isotropic in the center of mass coordinates. For scattering of two identical particles, this corresponds to constant distribution over all energies below the energy of the incident knockon for both the energy of the recoil atom and the energy of the scattered atom. Below some energy T_e, there is little energy loss in energy due to electronic excitation.

Where:

m_o = mass of electron

I = ionization potential for insulators.

For estimating the energy where electronic excitation becomes a major fraction of the energy loss, Schweinler (3) has calculated thresholds for protons with several directions of motion in the crystal. Here are:

Direction	Proton Energy	Silicon Equivalent Energy
< 100 >	125 ev	3.5 Kev
< 110 >	190 ev	5.3 Kev
< 111 >	340 ev	9.5 Kev

Though the moving silicon atom has a different potential than a proton, the main features such as thresholds, maxima, etc., would occur at approximately the same velocity because of momentum considerations in the center of mass of the silicon atom-electron system. Equation (12) gives T_e = 7.6 Kev, using the 1.19 ev excitation threshold energy given by Schweinler.

The values of $(dE/dx)_e$ are not known. It is known that for energies above the threshold, it is a major fraction of the energy loss. We are forced by this lack of knowledge to use the approximation of Seitz and Koehler (4) and assume all energy above T_e is lost to electronic excitation, i.e.

$$G(T) = T_e, \quad T \geq T_e \tag{13}$$

For the above conditions, the methods of G. H. Kinchin and R. S. Pease (1) give the following results:

Given a primary knockon of energy, $T = T_e$ the number $\nu(T)$ of displacements in the cascade is:

$$\nu(T) = 1 \qquad T_1 \leq T \leq 2T_1$$
$$\nu(T) = T/2T_1 \qquad 2T_1 \leq T \leq T_e \tag{10}$$

Where T_1 is the energy to displace one atom $T_1 \approx 12$ ev. For energies greater than T_e according to Dienes and Vineyard (2)

$$\nu(T) = G(T)/2T_1$$

Where:

$$G(T) = \int_0^T (dE/dx)_c \Big/ \left\{ (dE/dx)_e + (dE/dx)_c \right\} dE \tag{11}$$

$(dE/dx)_e$ = the energy loss per cm to recoil atoms

$(dE/dx)_e$ = the energy loss per cm to electrons.

3. ELECTRONIC EXCITATION

Kinchin and Pease (1) quote Seitz's formula for the electron excitation threshold as:

$$T_e = \frac{1}{8} \frac{M_{zi}}{m_o} I \qquad \text{for insulators} \tag{12}$$

4. CROSS SECTIONS FOR DISPLACEMENTS

To calculate the cross section for displacements by protons, we integrate the differential cross section for a primary knockon of energy T times the number of secondary knockons in the cascade over T.

$$\sigma_d = \int_{T_i}^{T_m} \left(\frac{d\sigma}{dT} \right) \nu(T) dT$$

$$= \frac{P_2}{\beta^2} \left[\int_{T_i}^{2T_i} \left(\frac{d\sigma}{dT} \right) dT + \frac{1}{2T_i} \int_{2T_i}^{T_e} \left(\frac{d\sigma}{dT} \right) T \, dT + \frac{T_e}{2T_i} \int_{T_e}^{T_m} \left(\frac{d\sigma}{dT} \right) dT \right]$$

$$\cong \frac{P_2}{T_i \beta^2} \left[\frac{1}{2} + \frac{1}{2} \ln \frac{T_e}{2T_e} + \frac{1}{2} \right]; \text{ for } T_e \ll T_m \qquad (14)$$

$$\cong \frac{P_2}{T_i \beta^2} (3.88) = \frac{16.45}{\beta^2} \quad (\text{Displacements}/\text{cm}^3)/(\text{proton}/\text{cm}^2)$$

This cross section is very insensitive to the choice of T_e. For protons we do not have to be too concerned about our choice of T_e and the shape of the threshold of electronic excitation.

These cross sections are shown in Figure 1.

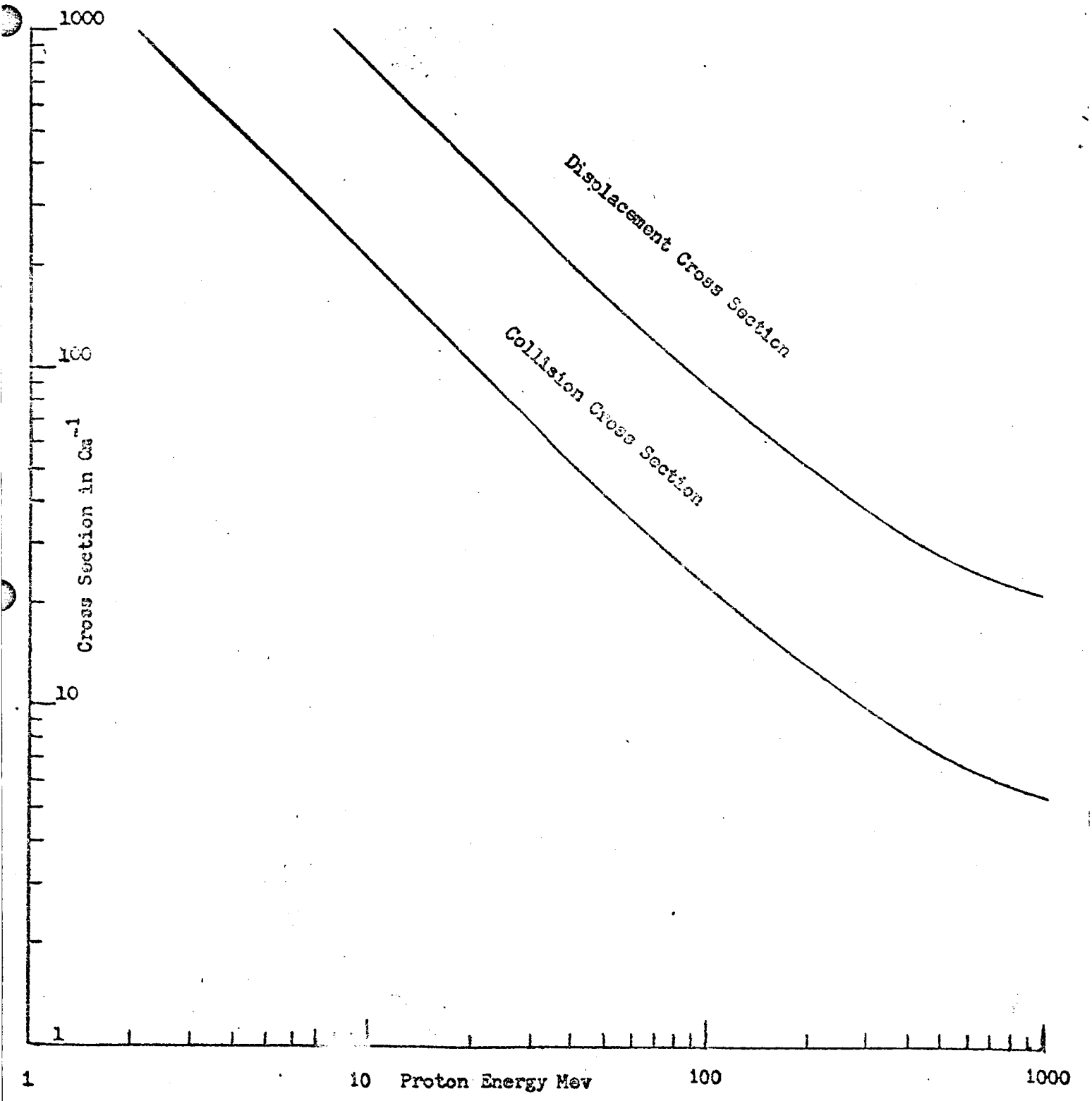

Figure 1

Proton Collision and Displacement Crossections Versus Proton Energy

For neutron displacement cross sections, we are concerned about the source spectrum. The normal source of neutrons is a reactor. Most reactor spectra can be well represented by three components, the fast or fission neutrons, the epithermal or 1/E tail neutrons and the thermal neutrons. Except in the presence of lithium or boron, the thermal neutrons do very little damage in silicon because of the small capture cross section. This leaves us with the following spectrum:

$$\phi(E)\,dE \cong \phi_1(E)\,dE + \phi_2(E)\,dE$$

$$\phi_1(E) = \phi_f\left[.453\, e^{-E/.965} \sinh\sqrt{2.25E}\right]$$

$$\phi_2(E) = \phi_e\left[N/E\right] \qquad .025\ ev < E < 1.5\ mev$$

$$= 0 \qquad \text{Otherwise}$$

Where:

$N = .05583$

ϕ_f = number of fission neutrons

ϕ_e = number of epithermal neutrons

ϕ_2 is very approximate, however, the error incurred by using it is small compared to other errors.

Up to about 1.5 mev neutron scattering is isotropic in the center of mass coordinates. For isotropic center of mass scattering, the distribution function of knockons from a neutron of energy E is:

$$f(T)\,dT = \frac{1}{KE}\,dT \qquad 0 < T < .133E$$
$$= 0 \quad \text{otherwise.} \qquad (16)$$
$$K = .133$$

For a neutron energy of 1.5 mev this results in only 4% of the knockons below 7.6 kev. With a small error, we can assume all of the $\phi_1(E)$ (fission) neutrons result in knockons of greater than 7.6 Kev. This results in uniform damage clusters of 317 displacements per neutron collision. The cross section for displacements is then:

$$317 \equiv (3.12 \text{ barns}) = 989 \ \frac{\text{displacements-barns}}{\text{neutron}}$$

From the epithermal neutrons, we receive a spectrum of primary knockons with the distribution function:

$$f(T)\,dT = \frac{N}{K}\int_{\text{Max}\,(T/K;\ .0033\ \text{ev})}^{1.5\ \text{mev}} \frac{dE}{E^2}$$
$$= N\left(\frac{1}{T} - \frac{1}{T_m}\right) dT; \quad .0033\ \text{ev} \leq T \leq 199\ \text{Kev} \qquad (17)$$
$$= 16.79\ dT \qquad 0 \leq T \leq .0033\ \text{ev}$$

It is of interest to note the fraction of primary knockons in each interval.

$T < 12$ ev	.513
12 ev $< T <$ 7.6 Kev	.359
7.6 ev $< T <$ 199.5 Kev	.128

The average number of displacements per epithermal neutron collision is then:

$$\bar{\nu} = \int_{T_1}^{T_m} \nu(T)\, f(T)\, dT$$

$$= N \left[\int_{T_1}^{2T_1} \left(\frac{1}{T} - \frac{1}{T_m} \right) dT \right]$$

$$= N \left[.69 + 317 + 729 \right] \qquad (18)$$

$$= 58$$

Where $N = .05583$

The cross section for displacement is 149 barns. There are 119 displacements, if only primaries which are knocked out of their site are considered, but when the 51.3% of the collisions which produce no displacement are averaged in, there are only 58. Approximately 74% of the primary displacements result in damage clusters smaller than the 317 displacements per cluster for fast neutrons.

The cascade from one collision will contain all the displacements in a small region. The median range of a primary knockon is about 23 Å per Kev (5 and 6) for primaries of greater than a Kev. The distribution of final locations of monoenergetic primary knockons is approximately spherically symmetric about the median range (6). It follows that the distribution of all the displacements in the cascade will be approximately spherically symmetric. The volume of this cluster will be $5.1 \times 10^{-20}\ T^3$ cm.^{3}, T in Kev (19)

The density of silicon is 5.2×10^{22} atoms/cc.

$$N = 2650\ T^3 \text{ atoms, T in Kev} \qquad (19a)$$

5. TRAPPING OF VACANCIES TO FORM DEFECTS

There is ample evidence (7 thru 10) that the vacant lattice site, created by knocking an atom out of position, can move about the lattice at room temperature. This motion is the result of an adjacent atom jumping into the vacant site leaving a vacant site in its former position. The vacancy, though a stress center itself, can partially relieve the stress in other stress centers (lattice defects) such as impurity atoms, lattice dislocations, interstitials, and other vacancies. In the stress field of the stress center the random jumps of the vacancy have a preferred direction toward a lower energy state. Once in the lower energy state the vacancy is trapped unless the thermal energy (kT) is the order of the binding energy of this state. The vacancy will diffuse through the lattice until trapped to form stable defects.

The best example of trapping is the SiA center. This is the result of trapping by an oxygen interstitial atom. The ground state of this center has the oxygen atom occupying a lattice site. Identification of some trapped centers by spin resonance techniques has been made. These are shown in Figure 2, in their approximate locations.

In Table III are listed the defect electronic levels and their approximate production rates. Little work has been done since 1959 to discover any more levels.

TABLE III (11)

LOCATION	CONDUCTIVITY CROSS SECTION	NATURE (IF KNOWN)
$E_c - .03$	$\sigma(4.5\ mev)$ $< 14\ cm^{-1}$	
	$\sigma(9.6\ mev)$ $< 670\ cm^{-1}$	
$E_c - .16$	$\gamma(Co^{60})$ $< .001\ cm^{-1}$	Substitutional Oxygen atom
	$\sigma(.7)$ $.18\ cm^{-1}$	
$E_c - \sim.4$	No rates available	1) (-) Charge state of divacancy * 2) Phosphorous Substitutional with adjacent Vacant site
$E_v + .3$	$\sigma(.7)$ $.005\ cm^{-1}$	
	$n(pile)$ $.35\ cm^{-1}$	(+) Charge state of divacancy *

* (tenative)

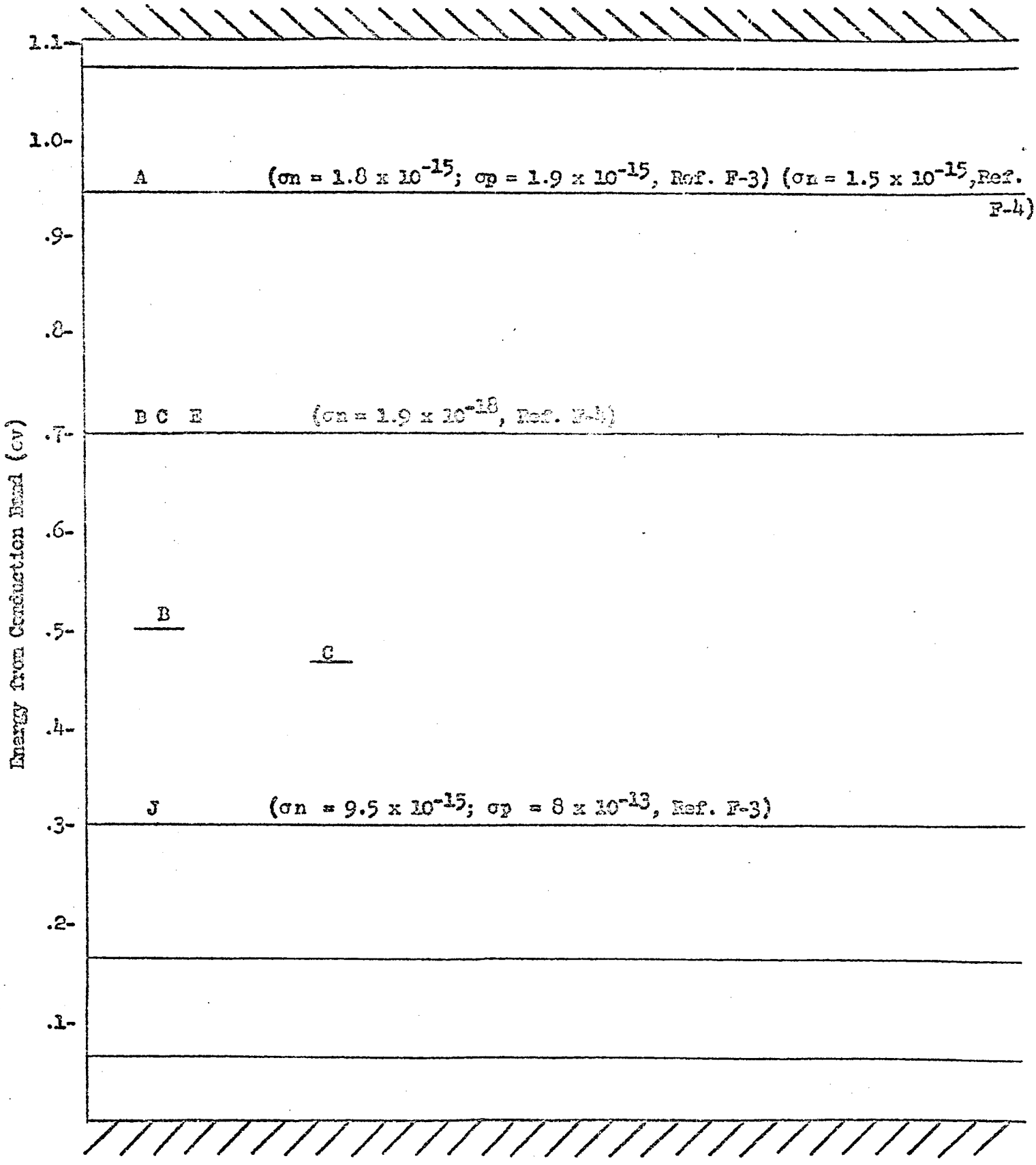

FIGURE 2

RADIATION INDUCED ENERGY LEVELS

TABLE II (11) Contd.

LOCATION	INTRODUCTION CROSS SECTION	NATURE (IF KNOWN)
$E_v + .16$	n(pile) $.35\ cm^{-1}$	
$E_v + .05$	$\sigma(4.5) < 18\ cm^{-1}$	
	$\sigma(9.6) < 750\ cm^{-1}$	
	n(pile) $> .65\ cm^{-1}$	

Little is known how the vacancies partition into different defects. We believe that all vacancies will in time find a more stable state, but how many of each type of defect can only roughly be estimated.

Protons will produce very small clusters averaging 3.88 vacancies per collision. The vacancies would have a moderate probability (.2 - .8 or so) to escape from this small cluster out into the undisturbed lattice. However, we would expect some to form divacancies (two adjacent vacant lattice sites) instead of escaping. With any particle (e.g., electron, proton, and neutron) divacancies can be produced by knocking two adjacent atoms out of their sites during the primary interaction or during the cascade. We would expect protons to produce a higher percentage of divacancy defects than electrons both from trapping and initial production. From Table II we see that electrons (.7 mev) produce .18/.005 = 32 (Ec - .16) levels per (Ev + .3) levels. We expect a lower ratio for protons. These two levels are important because of their effect on lifetime.

Neutrons produce 100 or more displacements in a small spherical region. Monte Carlo studies by Delaney and Beeler (12) showed that the vacancies were trapped in highly disordered region of the ordered binary lattice of BeO. Similarly, we would expect on the basis of the stress model the vacancy will be trapped in the highly stressed region of a neutron cluster. If this is the case, then only the trapping centers in the volume of the cluster can capture vacancies. The density of impurity trapping centers in silicon is from 10^{15} to 10^{18} centers/cc. The volume of the 2.5 kev cluster contains only 41,000 silicon atoms. There are 10^{-7} to 10^{-4} trapping impurities per silicon or 4×10^{-3} to 4 in the cluster. Thus, in pulled silicon (10^{+18} oxygen interstitials) there can only be about 4 S_iA centers per neutron collision. The rest of the vacancies must find a silicon interstitial or another vacancy. One can see that somewhat less than half would result in divacancies.

The fast neutron will create uniform clusters of 317 displacements corresponding to 7.6 kev of energy. The cluster occupies the space of 1.2×10^{6} silicon atoms. There can be a maximum of 120 SiA centers in this case, for pulled silicon.

6. ANALYSIS OF DAMAGE DATA

In semiconductors we are most concerned with lifetime damage. This is the property most affected by radiation and the property which device operation depends most strongly on. G. K. Wertheim (13) has analyzed electron damage data to obtain the lifetime damage per defect and the hole and electron capture cross sections using:

$$\frac{1}{\tau} = \frac{1}{\tau_o} + \frac{1}{\tau_b} \qquad (20a)$$

and

$$\tau_b = \tau_{p_o}\left(\frac{n_o + n_1}{n_o + p_o}\right) + \tau_{n_o}\left(\frac{p_o + p_1}{n_o + p_o}\right) \qquad (20b)$$

Where:

n_o & p_o = the equilibrium election and hole concentrations

n_1 & p_1 = The electron and hole concentrations if the fermi level was at the defect level.

$\tau_{po} = 1/N < v_p > \sigma_p$

$\tau_{no} = 1/N < v_n > \sigma_n$

$< v_n >$ & $< v_p >$ = the thermal electron and hole velocities

σ_n & σ_p = the defect electron and hole capture cross sections

N = the defect concentration.

He found $\sigma_n = 9.5 \times 10^{-15}$ cm^2 and $\sigma_p = 8 \times 10^{-13}$ cm^2 for a level at (Ev + .27) ev in N-type silicon. It is difficult to understand how with 7 ohm-cm N type silicon the divacancy which would be in the (-) charge state would have a level at (Ev + .27). We must assume there are some selection rules preventing the transition to the ground state.

In 5 ohm-cm p type silicon we obtained $\sigma_n = 1.8 \times 10^{-15}$ cm^2 and $\sigma_p = 1.9 \times 10^{-15}$ cm^2 for a level at $(E_c - .16)$ev. He had difficulty analyzing his data because of effects from the $(E_v + .3)$ev level. For 5 ohm-cm p type silicon the fermi level is at about $(E_v + .21)$ev at room temperature. In 2 ohm material with the fermi level at about $(E_v + .18)$ we could expect this level to be more troublesome. In p type material the divacancy is in the +1 charge state. We do not have the capture cross sections for this defect state.

Using $\langle v_n \rangle = 2 \times 10^{+7}$ cm/sec; $\langle v_p \rangle = 1.6 \times 10^{+7}$ for room temperature thermal velocities. Lifetime degradation per defect per cm^3 for n and p type silicon of one and two ohm-cm resistivities were calculated and ignoring the +1 charge state divacancy using the above single level formula. These are listed in Table III.

$$\tau_T = \frac{1}{N\tau_b} \qquad \frac{(\text{sec per defect})^{-1}}{\text{cm}^3}$$

TABLE III

	N_o	N Type λ_T	P_o	P type λ_T
1 Ω-cm	$4.4 \times 10^{+15}$	3.3×10^{-6}	1.2×10^{16}	2.4×10^{-8}
2 Ω-cm	$2.2 \times 10^{+15}$	1.9×10^{-6}	$.7 \times 10^{16}$	1.4×10^{-8}

We do not know how many vacancies are trapped in each type of defect. So using solar cell data and cross sections calculated according to preceding sections, we calculated the lifetime damage per vacancy per cm^3 (i.e., displacement), by dividing the lifetime damage constant by the displacement cross section. These calculations are listed in Table IV. K_L the diffusion length damage constant can be reduced to a lifetime damage constant by multiplying by the diffusion constant.

$$K_\tau = K_L \; D \; \frac{cm^2}{sec} \qquad D = 25 \; cm^2/sec \text{ for electrons}$$

$$10 \; cm^2/sec \text{ for holes.}$$

TABLE IV

SELECTED SOLAR CELL [illegible]

Energy	Cross Section	cm^{-1}	K_L [illegible]		$K_L D/\Sigma_d$	
Mev	Σ c Collision	Σ d Displacement	N Type	P Type	N Type	P Type
35	60	232.8		[illegible]		.97 x 10^{-7}
45	47.4	183.9	8 x 10^{-5}	[illegible]	4.37x10^{-7}	1.29 x 10^{-7}
55	39.4	152.9		[illegible]		1.38 x 10^{-7}
65	33.8	131.1	6.4x10^{-5}	[illegible]	[illegible]x10^{-7}	1.47 x 10^{-7}
80	28.0	108.6	5.0x10^{-5}	[illegible]	4.6[illegible]x10^{-7}	1.70 x 10^{-7}
100	23.1	89.6	5.5x10^{-5}	.95 x 10^{-5}	6.1[illegible]x10^{-7}	1.06 x 10^{-7}
120	19.8	76.8		.88 x 10^{-5}		1.15 x 10^{-7}
135	18.0	69.8	3.3x10^{-5}	.88 x 10^{-5}	4.73x10^{-7}	1.86 x 10^{-7}
450	7.8	30.2		.25 x 10^{-5}		.93 x 10^{-7}
				Average $K_L D/\Sigma d$ =	4.94x10^{-7}	1.12 x 10^{-7}

$K_L D/\Sigma d$ is then the lifetime damage per vacancy (i.e. displacement). If we divide by the lifetime damage per defect, λ_τ from Table III should obtain defects per vacancy.

$$\frac{K_L D}{\Sigma d \; \lambda_\tau} = .15 \text{ for 1 ohm N type (defects/vacancy)}$$

$$= 5.3 \text{ for 1 ohm P type}$$

$$= .26 \text{ for 2 ohm N type}$$

$$= 8 \text{ for 2 ohm P type.}$$

It is not possible to obtain 5.3 SIA defects per vacancy, the maximum is one per vacancy. For two ohm material, the disagreement is worse. The material used was undoubtedly between 1 and 2 ohm-cm. This is not surprising considering that we suspect there is another level contributing to the degradation. We have no knowledge which tells us that .15 - .26 divacancies per displacement is unreasonable.

For neutrons the simple one level formula (Eq. 20 b) for the lifetime damage does not work. The temperature dependence of the lifetime damage indicates that a broad band of defect levels is created. The problem is that neutrons produce the damage in a cluster. In Figure 5 the forbidden gap in a cluster is shown. The probability that a defect level is occupied by an electron is related by fermi statistics to the energy of the defect level and the energy of the fermi level. If the level is charged + or - when unoccupied or occupied, the conduction and valence bands are shifted with respect to the fermi level by the electrostatic potential. A cluster of such defects will act as a spherical capacitor with donor or acceptor states supplying the outside plate. The divacancy is believed to have a - charge state in the upper half of the forbidden gap and a + charge state in the lower half. These states are probably the source of the potential.

The model for recombination is to consider the cluster black to minority carriers. The cross section is then πR^2 where R is the radius of the cluster. For $R = 237 \mathring{A}$ the cross section of a cluster from an (T_e = 7.6 Kev) ionization threshold knocked fission neutron is 9.6×10^{-12} cm^2. Though the cluster is black to minority carriers, the potential hill repels majority carriers. The recombination occurs only if a majority carrier is absorbed before the absorbed

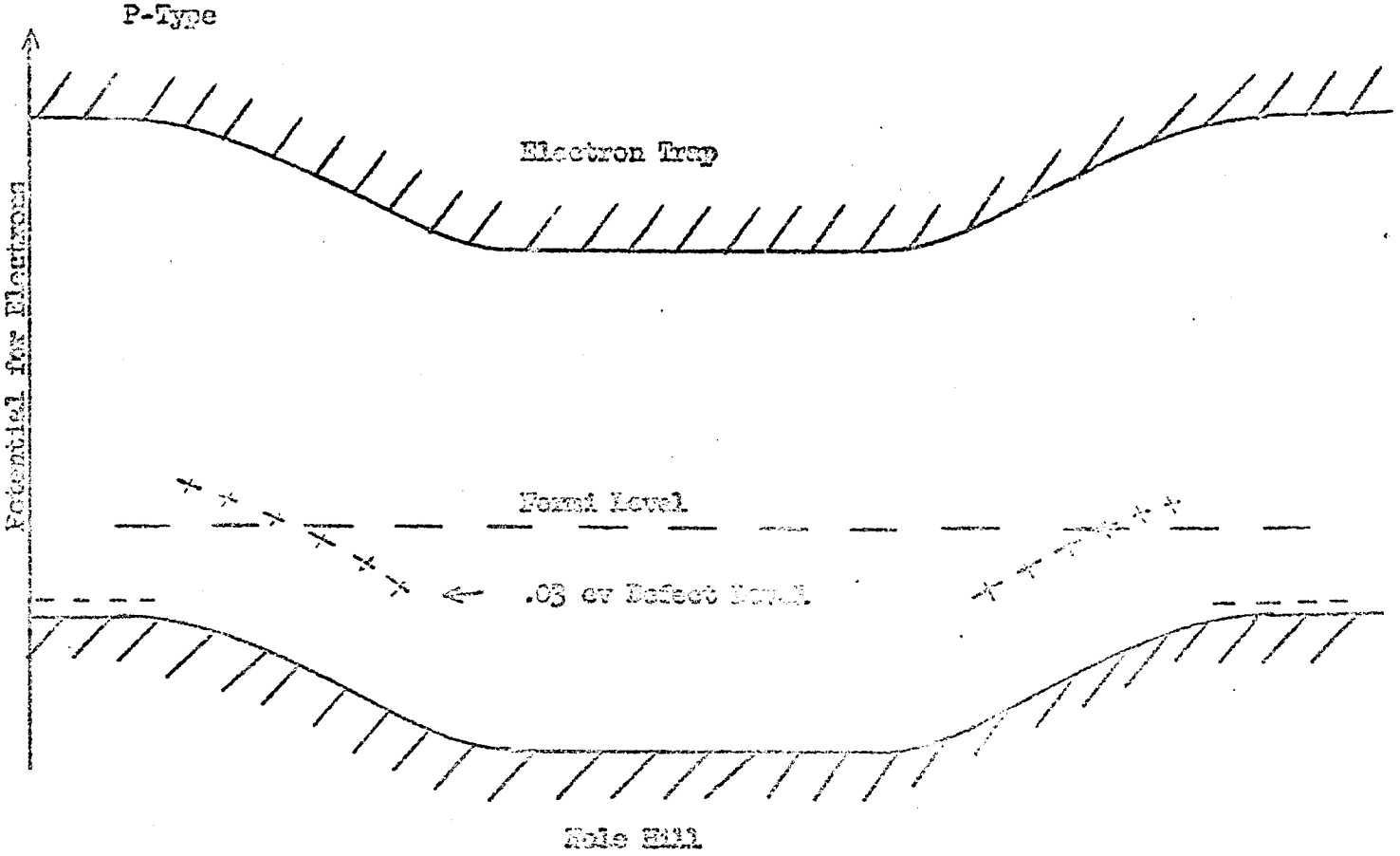

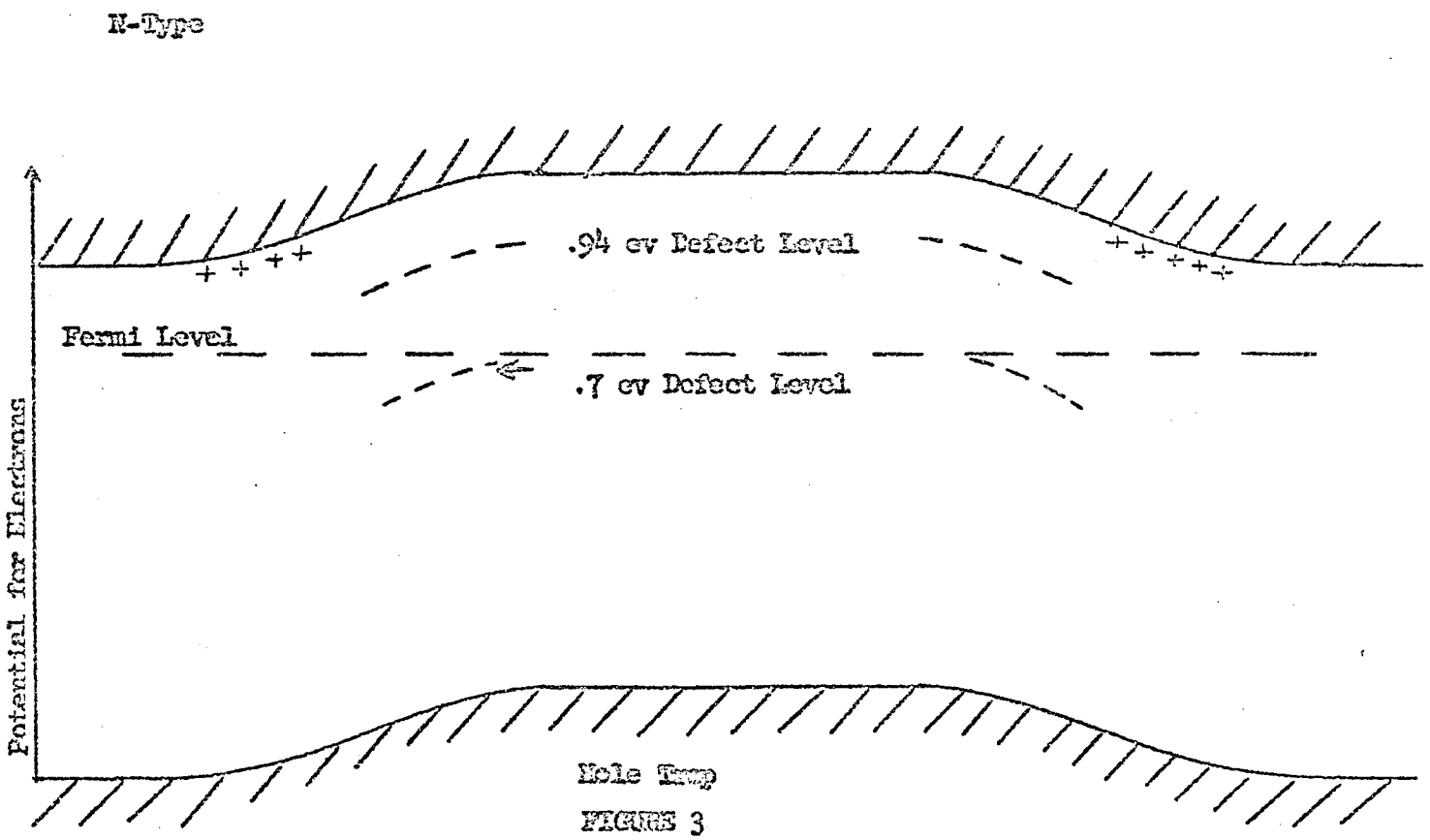

FIGURE 3

ELECTRON CLUSTERS

hole is thermally emitted. This is a complex situation. However we can check this model by comparing to low temperature data where the probability of thermal emission is low.

G. K. Wertheim (17) irradiated 2 ohm-cm samples of silicon to fission plate neutrons. The maximum lifetime damage constants were $.66 \times 10^{-5}$ cm^2 (sec-neutron)$^{-1}$ at 110 K° in n type and $.55 \times 10^{-5}$ cm^2 (sec-neutron)$^{-1}$ at 120 K° in p type. The neutron spectrum had about 60% of the neutrons above .4 Mev. The cross section for fission neutrons is 3.12 barns or $\Sigma = .16$ cm^{-1}. Using electron and hole thermal velocities of $1.2 \times 10^{+7}$ cm/sec and $1.0 \times 10^{+7}$ cm/sec.

$$K_T = \Sigma \langle v \rangle \sigma$$
$$= 1.5 \times 10^{-5} \text{ for holes}$$
$$= 1.8 \times 10^{-5} \text{ for electrons.}$$

Since only 60% of the neutrons had a high probability of causing a 7.6 Mev primary

$$K_T = .9 \times 10^{-5} \text{ for n type}$$
$$= 1.1 \times 10^{-5} \text{ for p type.}$$

The values are on the high side as they should be since all trapped minority carriers will not be recombined even at this lower temperature.

7. SUMMARY

In summary, neutron damage is basically different from proton damage. Neutron damage on minority carrier lifetime is more dependent on the size (cross section area) of the cluster than the type of defect in the cluster. Changes in impurity concentrations will have little effect on the electron and hole recombination capture cross sections. Proton damage results in defects which can affect the lifetime according to type of defect. Thus, the capture cross sections are influenced by impurity concentration.

B. ANALYSIS OF PRESENTLY EXISTING DATA

Presently existing irradiation data on semiconductors has been analyzed to determine an empirical neutron-proton correlation constant. The bulk of the neutron irradiation damage data is on transistors while the proton irradiation damage data is on solar cells. The electrical parameter which is common to both of these devices and is an indicator of radiation damage is the minority carrier lifetime degradation of the base region. The radiation damage can be expressed in the form of a damage constant K. The lifetime degradation constant K_τ is defined by the expression:

$$1/_\tau = 1/_{\tau o} + K_\tau \phi$$

where τ_o = initial minority carrier lifetime

τ = final minority carrier lifetime

ϕ = accumulated dose

In the case of solar cells an additional damage constant is introduced because of its more direct relationship to the mechanism of device failure. This is the minority carrier diffusion length damage constant, K_L. It is defined by the expression:

$$1/_L{}^2 = 1/_{Lo}{}^2 + K_L \phi$$

where Lo = initial minority carrier diffusion length

L = final minority carrier diffusion length

and is related to the lifetime damage constant, K_τ, by

$$K_\tau = DK_L$$

where D = minority carrier diffusion constant.

For p on n cells, D_n = 10 cm^2/sec, and for n on p cells, D_e = 25 cm^2/sec, for 2 ohm-cm silicon (16)

1. SOLAR CELL ANALYSIS

In the solar cell analysis, the diffusion length damage constant is related to the proton energy. In most cases the damage constant is reported directly by the experimenters. In the cases where the damage constant was not given and some information of the spectral response change is known, one can determine the diffusion length damage constant by means of the spectral response - diffusion length relationships as derived by Dale and Smith in Reference 18.

No analysis of diffusion length degradation could be performed from data where only the degradation of power output or short circuit current response to one sun or tungsten lights was reported.

The data analyzed is summarized in Tables A-I through A-V in appendix and in Figure 4.

No information on the effects of neutrons on solar cell degradation is available.

In Tables A-III and A-IV, the value K_L, is the damage constant calculated by RCA from their spectral response data.

In the data presented in Tables A-III, the discrepancy between damage constants K_τ determined from lifetime measurements and those from spectral response data was believed to be due either to the method by which lifetimes were measured, or to the difference between equilibrium and transient lifetimes. Values of damage constants obtained from spectral response data were considered by the experimenters to be more reliable than values obtained from the pulse injection method of measuring lifetimes.

Figure 4 is a plot of the average values of K_L vs. proton energy, (Tables A-I through A-V) with spread in data indicated by vertical lines, regardless of the source of information or the experimental conditions. No attempt was made to draw any "average" curves, but this figure gives an idea of the order-of-magnitude of the spread in damage constant values, and of the n/p vs. p/n variation. For comparison, the transistor data of Hulten, et.al., (23) is shown.

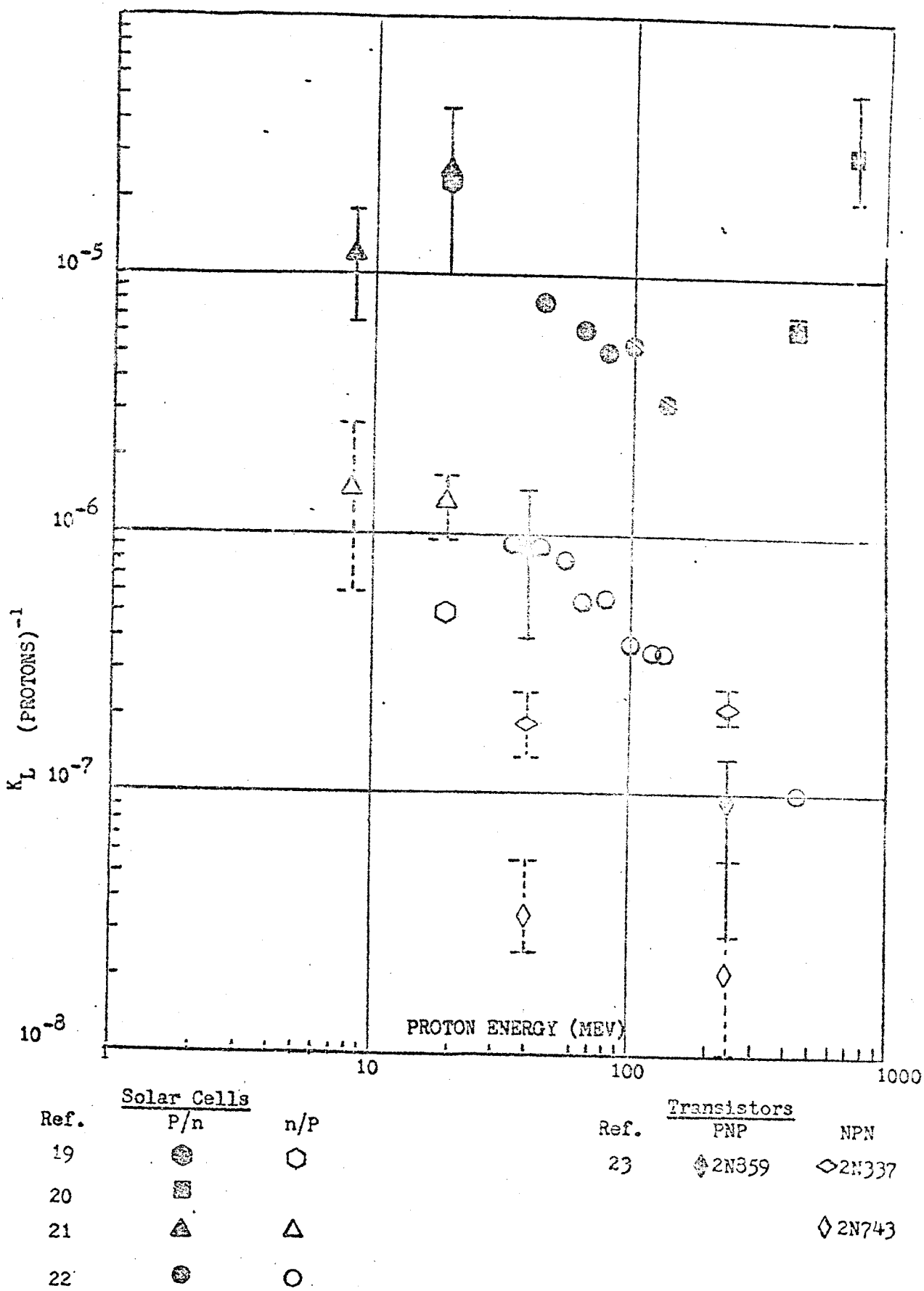

Figure 4 Proton Damage in Silicon as defined by $1/L^2 = 1/L_o^2 + K_L \phi$

2. TRANSISTOR ANALYSIS

The approach to the analysis of the literature on nuclear radiation effects in transistors was to relate the lifetime damage constant K_τ to the proton energy or the reactor neutron spectrum. In many reports the damage constant K_τ was reported directly. In others, the constant was calculated when sufficient data was reported, by the following method.

The effect of nuclear radiation on the common emitter forward current gain (h_{FE}), as developed by Loferski (24) can be related by the following expression:

$$1/h_{FE} = 1/h_{FEo} + \bar{t}\phi K_\tau,$$

neglecting emitter efficiency and surface effects where,

h_{FE} = current gain after bombardment

h_{FEo} = current gain initially

$\bar{t}$ = average transit time of minority carriers in base

ϕ = radiation dose

K_τ = lifetime damage constant

and K_τ is related to minority carrier lifetime τ by

$$1/\tau = 1/\tau_O + K_\tau\phi$$

The average transit time of minority carriers in the base region of the transistor has been calculated by Moll and Ross (25) as follows:

for uniform base,

$$\bar{t} = W^2/2D = 1/2\pi f_{\alpha b}$$

for linear graded base,

$$\bar{t} = W^2/4D = 1/\sqrt{2}\,\pi f_{\alpha b}$$

where

W = base width

D = minority carrier diffusion length

$f_{\alpha b}$ = alpha cutoff frequency

The above expressions agree well with experiment, except in the case of P-N-P germanium transistors where the effect of depletion layer widening of the collector region is appreciable. This case has been treated by Easley and Dooley (26) for the germanium alloy transistor with uniform conductivity base region. His results may be written in the form:

$$1/h_{FE} = (1/h_{FEo} + Wo^2 K_\tau \phi/2D) \quad (W^2/Wo^2)$$

for the case when $\tau o \gg 1/K_\tau \phi$.

Or in terms of frequency cutoff parameters

$$1/h_{FE} = \left[1/h_{FEo} + (1/2\pi f_{\alpha bo}) \quad (K\tau\phi)\right] \quad f_{\alpha bo}/f_{\alpha b}$$

Thus, the lifetime damage constant for silicon and germanium transistors is given by

$$K_\tau = (h_{FEo} - h_{FE}) \qquad 2\pi f_{\alpha b}/ h_{FEo} h_{FE} \phi$$

and for the case of P-N-P germanium transistors exhibiting depletion layer widening (i.e., a change in $f_{\alpha b}$) is given by

$$K_\tau = (h_{FEo} f_{\alpha b}/f_{\alpha bo} - h_{FE}) \quad 2\pi f_{\alpha b}/h_{FEo} h_{FE} \phi$$

The results of the calculation of the damage constant for proton irradiations of silicon and germanium transistor is tabulated in Tables A-VI to A-X. For the PNP germanium devices no damage constant was calculable for those transistors exhibiting depletion layer widening for which a final alpha cutoff frequency measurement is missing.

3. SUMMARY

The average values of proton damage constants for germanium and silicon are shown in figures 5 and 6 as a function of proton energy. In figure 5, the RCA and BTL solar cell data is shown for comparison.

The results of the calculations of damage constant for neutron irradiations is shown in Tables A-XI to A-XV. No plots of this data were made because of the lack of adequate neutron spectra information. The estimated resistivity and carrier concentration of several transistor base regions is shown in Table A-XVI.

Referencing the open literature data on neutron and proton radiation damage on silicon and germanium it was not possible to determine a reliable neutron-proton correlation. The reasons for this are:

a) The spread in the neutron damage data indicated in Tables A-XI to A-XV. Experimenters had used different neutron spectra which were not reported adequately for analysis. The neutron irradiations on different types of semiconductor devices and materials also introduces a wide spread in data.

b) There was no data which was taken on similar semiconductor samples under both proton and neutron irradiations.

Other investigations have also found difficulty in analyzing existing data to determine a proton-neutron correlation as indicated below.

With reference to Table V RCA (21) pointed out the similarity of the electron and proton values and the difference between these and the neutron values. The values of K_τ for electrons and protons are very nearly proportional to n_d, the total number of displacements, whereas if electrons and protons are compared with neutrons, the values of K_τ are more nearly proportional to n_c, the total number of collisions, than to n_d, since the total number of lattice displacements per centimeter was nearly the same for neutrons and for protons, this suggested to them that the electrical damage resulting from the high density displacement spikes occuring in neutron-irradiated silicon was far less than that produced by the same number of individually displaced atoms produced over larger distances in proton irradiated silicon.

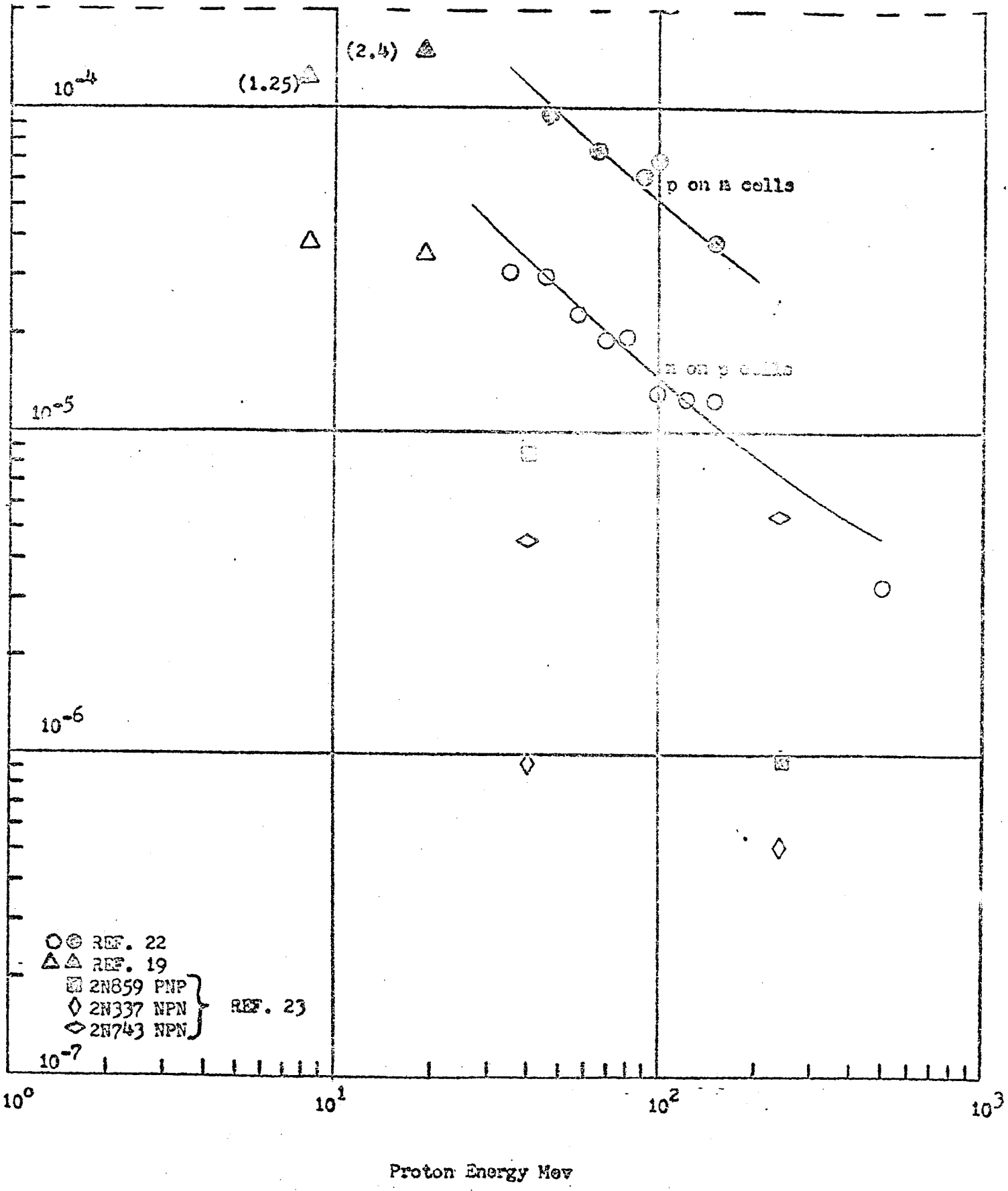

Figure 5 - Proton Damage in Silicon, as defined by $1/\tau = 1/\tau_o + K_\tau \phi$

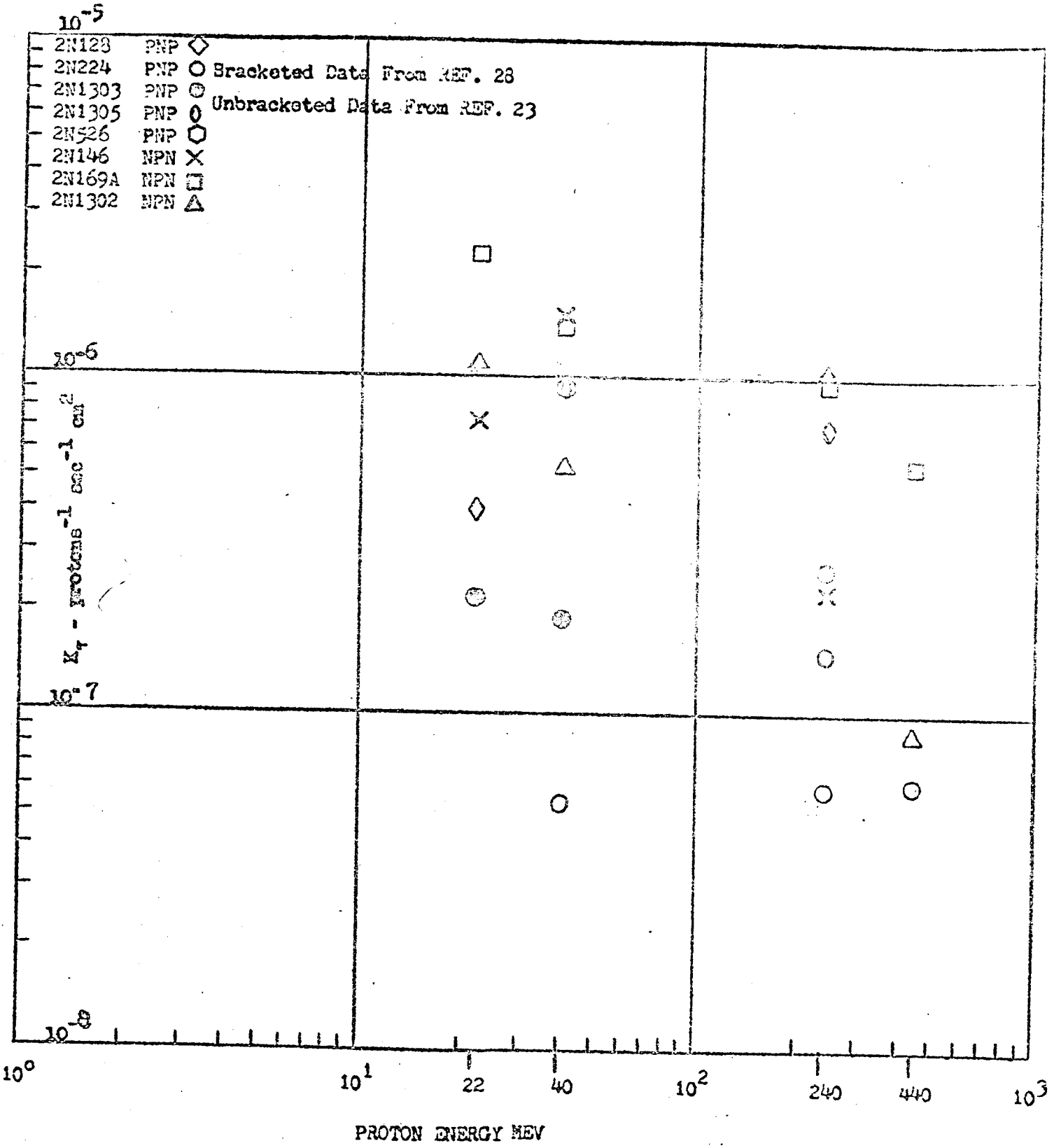

Figure 6 - Proton Damage in Germanium as defined by $1/\tau = 1/\tau_0 + K_\tau \phi$

TABLE V

COMPARISON OF DAMAGE CONSTANTS IN SILICON

PARTICLE	ENERGY Mev	θ min	n_c	n_d	$K_{n\tau}$ n-type	K_{τ} p-type	REF. NO.
Electrons	0.75	46°	0.65	0.65	1.6×10^{-7}	10^{-8}	19
Protons	17	0.21°	185	$1\text{-}2 \times 10^{3}$	10^{-4}	2×10^{-5}	
Neutrons	17	0.21°	0.1	$2\text{-}4 \times 10^{3}$	10^{-6}	4.4×10^{-7}	

θ min = minimum scattering angle for which the recoiling silicon atom possesses sufficient energy to be displace.

n_c = number of collisions per centimeter of traversal of the crystal for which $\theta \geq \theta$ min

n_d = total number of displaces silicon atoms per centimeter of traversal of the crystal, including both primary and all succeeding displacement processes.

Note: the reference report does not specify whether the above values of K_τ were derived from spectral response or lifetime measurements. From comparison with otherdata we assume they relate to spectral response measurements.

Brown (22) made some rough comparisons between the effects of particles, but cautioned that they must not be interpreted as much more than guides. For p-types silicon of about 5 ohm-cm, the comparisons were approximately:

40 Mev protons: $1/cm^2$

1 Mev electrons: $3 \times 10^3/cm^2$

1 Mev neutrons: $5 \times 10^2/cm^2$

Co^{60} gamma rays: 2×10^{-3} rads

He pointed out that many more comparisons of this sort must be made in detail before a correlation could be established with any confidence.

A similar comparison was made by Battelle (27) and is tabulated in Table VI. Although no direct estimate of proton-neutron damage was reported, an estimated value is inferred from comparison of the proton-electron with neutron-electron damage rates.

They also warn that these values should be used as order-of-magnitude estimates since the quantities were selected on the basis of compatibility of data, a certain amount of theoretical consideration, and a lot of guesswork.

TABLE VI

RELATIVE DAMAGE RATES IN SILICON

TYPE OF RADIATION		ESTIMATED DAMAGE RATE RATIO (A/B)
A	17 mev protons	900 (see note 1)
B	0.75 mev electrons	
A	40 mev protons	340 (see note 1)
B	1 mev electron	
A	Fission Neutrons	50 (see note 2)
B	0.75 mev electron	
A	Fission neutron	50 (see note 3)
B	1 mev electron	
A	17 mev proton	18 (see note 4)
B	Fission neutron	
A	40 mev proton	6.8 (see note 4)
B	Fission Neutron	

Notes:

1 values estimated from data on degradation of solar cell efficiency
2 value based on data on damage constants for solar cells by electrons and p-i-n junction by neutrons
3 value based on carrier removal rates
4 values inferred by comparison

C. EXPERIMENTAL PROGRAM

1. DESIGN OF EXPERIMENT

a. DESCRIPTION OF SOLAR CELLS

Several types of solar cells were used in the proton and neutron irradiation experiments. Approximately equal numbers of p on n cells and n on p cells were used. The p on n cells were made by Hoffmann with an Advent designed grid structure. These cells are 1 cm wide x 2 cm long and are approximately 20 mils thick. Before the irradiations were performed, the short circuit currents under a carbon arc source was measured and also the short circuit current under a tungsten source was obtained. Only those cells whose tungsten short circuit currents fell within a range of 60 to 65 milliamps of current were selected for the irradiation test. These cells all have similar V-I characteristics and have conversion efficiences under a space sun source which are scattered about 9%. The n on p cells were made by RCA and were used because of the increased radiation resistance of this type cell. The short circuit currents of this type cell exhibited a larger spread than the p on n type cells. The cells used in these measurements had short circuit currents which varied from about 55 milliamps to 65 milliamps, with the majority of these currents centered about 60 milliamps. It was also observed that during the V-I characteristics measurements a good portion of the cells exhibited a very erratic current. In general, the breakdown voltage in both the forward and reverse directions was lower than for the p on n type cells.

c. EXPERIMENTAL TECHNIQUES

At the McGill 100 mev cyclotron the energy was measured by Mr. W. Link a fewdays before the experiment was performed. He found that the energy of the beam at the exit tube was 98 mev initially. At this energy there was an energy spread of less than 1 mev. In order to obtain the desired uniform beam over a large area and also reduce the beam intensity to a useable level a 10 mil brass scatterer was inserted at the exit port before the drift tube. The protons then entered the drift tube and traveled to the exit window which was about 10 mils of aluminum. Coming out of the aluminum window the energy was 96.5 mev and the beam filled the entire 4 inch diameter tube. Two x-ray sensitive emulsions were exposed at the end of the drift tube and the density was then read on a Densitometer transmission densitometer. The transmission density is proportional to the proton flux. Thus, the intensity of the beam can be determined by a measurement of the optical density. A plot of this beam intensity in the horizontal and vertical direction is given in Figure 8.

An aluminum bracket (Figure 9) was made to fit on the end of the drift tube and contained a holder into which the brass plate containing the solar cells were inserted during the irradiation. The solar cells were mounted on the aluminum plate and occupied a total area slightly over 4 cm^2 approximately at the center of the beam tube. By considering the variation in the beam intensity over the area in question it is found that the proton flux incident on the 2 cells varies by less than 5%. According to Dr. R.E. Bell of the McGill Radiation Laboratory the beam should remain fixed in space over a very long period of time so that the variation in beam intensity as represented here should be that which existed during the entire irradiation.

The proton flux to which the cells were exposed was measured by a Farraday cup which was connected to a Keithly electrometer, the output of which was fed

b. DESCRIPTION OF RADIATION FACILITIES

1) Proton Accelerator

The proton accelerator at the McGill University in Montreal, Quebec, Canada is a synchro-cyclotron having a pole diameter of 82 inches and a magnetic field of 16,500 gauss. The RF frequency is modulated sinusoidually between 28 and 21. megacycles by a mechanical rotating condenser, and the proton acceleration occurs in the 25 to 22 megacycle range. The accelerator is pulsed at a frequency of 400 cycles/sec. In order to obtain a variable beam current a scaling unit was used on the modulation frequency which could scale down the beam current by a factor of two up to a factor of 32. In our experiment the initial radiations were scaled down a factor of four and at full beam current the time was increased in order to obtain a higher total integrated flux. The proton energy at the outlet of the accelerator but still inside the vacumn system is 98 mev. A 10 mil brass disc was inserted at the entrance of the drift tube. The energy loss through this brass was 1.1 mev. A 10 mil aluminum window was attached to the end of the drift tube. The energy lost through this window was 0.4 mev so that the total energy loss of the protons was 1.5 mev making the available energy of the beam 96.5 mev.

2) Reactor Facility

The fission plate at the Batelle Research Reactor Facility is mounted on the end of a four foot square thermal column of graphite. A large sheet of boral is inserted between the fission plate and the thermal column to absorb the thermal neutrons before they reach the fission plate when irradiation is not desired. The fission plate itself is a circular plate .0199 inches thick and 28 inches diameter. consisting of uranium-235 of 93.14% enrichment. For all practical purposes the fission plate is a plane source. Measurements of the fast neutron does rates off center line from the fission plate indiate that at 10 cm off center line the fast

neutron dose rate is only $2\frac{1}{2}\%$ less than on the center line. Our samples were located not more than 5 cm off the center line so that it can reasonably be assumed that the neutron flux was uniform to within about $\pm$ 1% over the sample holder. The reactor itself has a maximum power of 2 megawatts and is a water moderated, water cooled enriched uranium fuel type reactor. It is shielded by the water in the pool plus concrete. One side of the reactor is adjacent to the thermal column, the end of which is the fission plate facility. The 5 inch diameter aluminum tube in which the irradiations were performed was located approximately 24 inches from the corner of the reactor which is approximately rectangular in shape. The center of the samples was located several inches above the center line of the reactor.

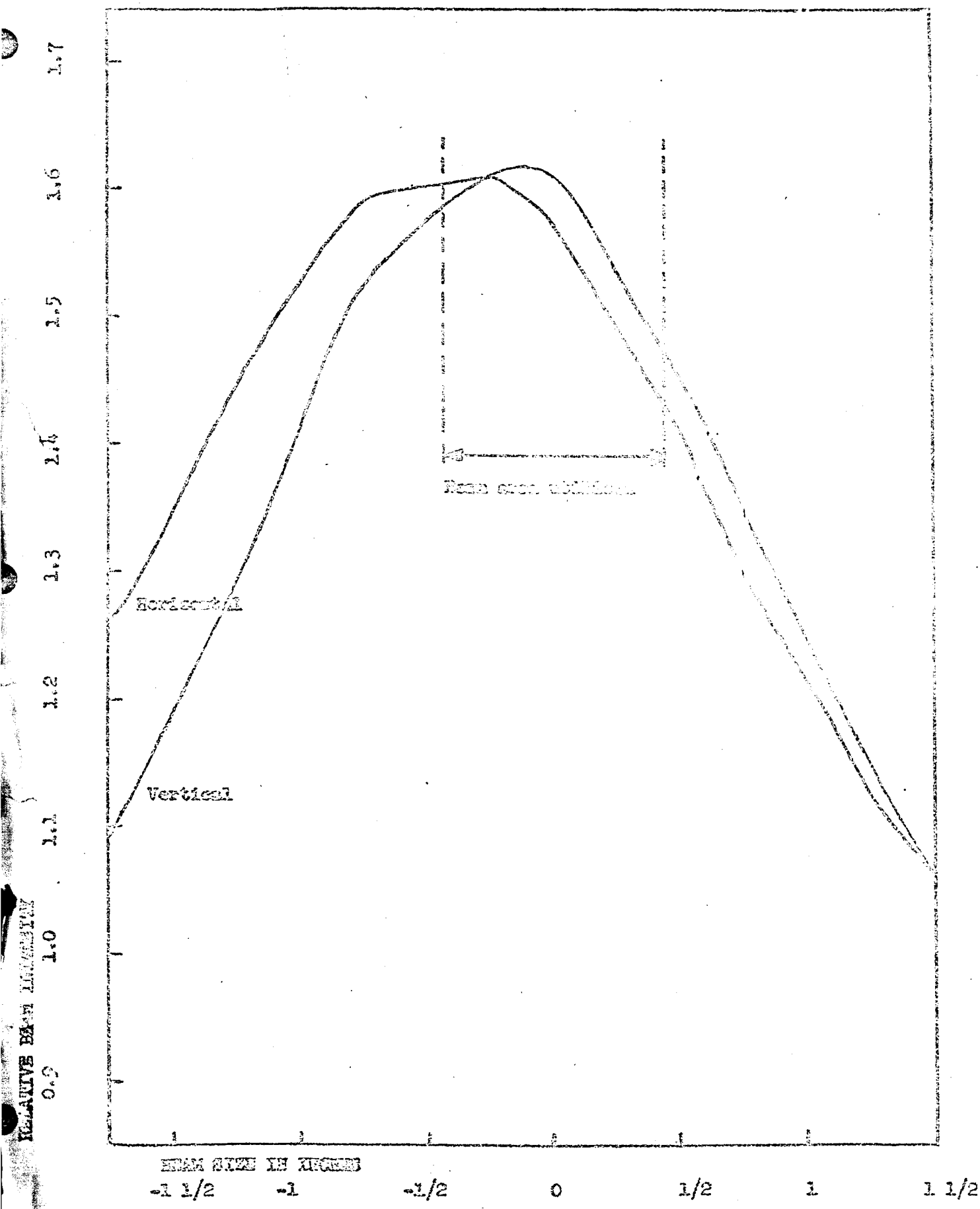
1.7
1.6
1.5
1.4
1.3
1.2
1.1
1.0
0.9
RELATIVE BEAM INTENSITY
Horizontal
Vertical
BEAM SIZE IN INCHES
-1 1/2
-1
-1/2
0
1/2
1
1 1/2

into a Leeds & Northrup strip chart recorder. A brass plate one inch thick with a square hole through the center 7/8 inch on each side, was placed behind the sample holder near the beam tube exit. This hole was carefully aligned with the samples when they were mounted in the fixture such that the protons passing through the solar cells would also pass through the 7/8 inch square hole in the brass plate and from there into the Faraday cup. Any protons not passing through the square hole were stopped in the brass plate and not collected by the Faraday cup. Thus the beam current as measured was that of protons coming through the 7/8 inch square hole. In order to obtain the total integrated proton flux received by the cells during a given exposure the output of the electrometer as recorded on the strip chart recorder was integrated over the time of the exposure using a planimeter to measure the area under the curve. In order to determine the reproducibility of the results each curve was measured over the top portion of the curve and again over the bottom portion of the curve at least twice. If the results on successive measurements did not agree to within 2% then the measurements were repeated until such agreement was obtained. Once this was completed the average of the two readings was taken to be the actual area under the curve. It is believed that the proton flux determined in this manner is accurate to within 5%. Also it is believed that the Faraday cup measured accurately the total protons incident on the entrance window of the cup since it was determined that by varying the voltage on the entrance window with respect to the cup itself no appreciable effects were observed for voltages ranging from +300 volts to -300 volts.

The neutron irradiations were performed at the Battelle Memorial Institute Research Reactor Facility at West Jefferson, Ohio. At the Battelle Reactor the fission plate was used as a source of neutrons and a tube in the pool near the reactor was used to obtain the moderated neutrons. Eight cells of each type were exposed in both the fission plate and the pool. In the fission plate, the 6-inch inside diameter aluminum tube reached from the surface of the pool in which the fission

plate was contained to 2 1/4 inches below the center of the fission plate. The solar cells and the monitoring foils were mounted in the holder as shown in Figure 10. For the distance of approximately 4 inches about the center of the fission plate the neutron flux is constant to within about one per cent. (41) The samples were lowered into the tube by means of a 1/4 inch diameter aluminum tube attached to the sample holder. The top of the aluminum tube was bent so that the samples could always be oriented in the same direction during the exposure. For all practical purposes the neutron spectrum at the fission plate is a Watt's fission spectrum. Sulphur and nickel threshold foils were used to monitor the flux during the irradiation and a knowledge of the fission spectrum was used to obtain the total fast flux from these measurements. The water temperature during the fission plate exposures was 70°F.

The tube in the pool was approximately 5 inches inside diameter and at the bottom of the tube a cadmium basket 40 mils thick and approximately 12 inches deep was inserted to remove the thermal neutrons. Uranium-238, nickel, sulphur, and aluminum foils were used to obtain points on the spectral curve at the high neutron energies. A cadmium difference technique utilizing cobalt foils was used to obtain the resonance and thermal flux. Figure 11 shows the Watt's fission spectrum and the moderated spectrum as hardened by the 24 inches of water between the reactor core and the tube as it was located during the irradiations. The neutron flux was monitored with sulphur foils during the irradiations and the measured spectrum was used to obtain the integral fast flux. The solar cells were mounted on the sample holders as in the case of the fission plate experiment and approximately 24 feet of 1/4 inch diameter aluminum tube was attached to the sample holder to insert the samples into the tube. Again, these samples were maintained in the same orientation by means of a bend at the end of the tube. The water temperature in the reactor pool was approximately 116°F. It is assumed that the samples were at approximately this temperature during the exposure since the samples were in the pool for at least one minute prior to the exposure.

FIGURE IX INTEGRAL NEUTRON FLUX VS. NEUTRON ENERGY

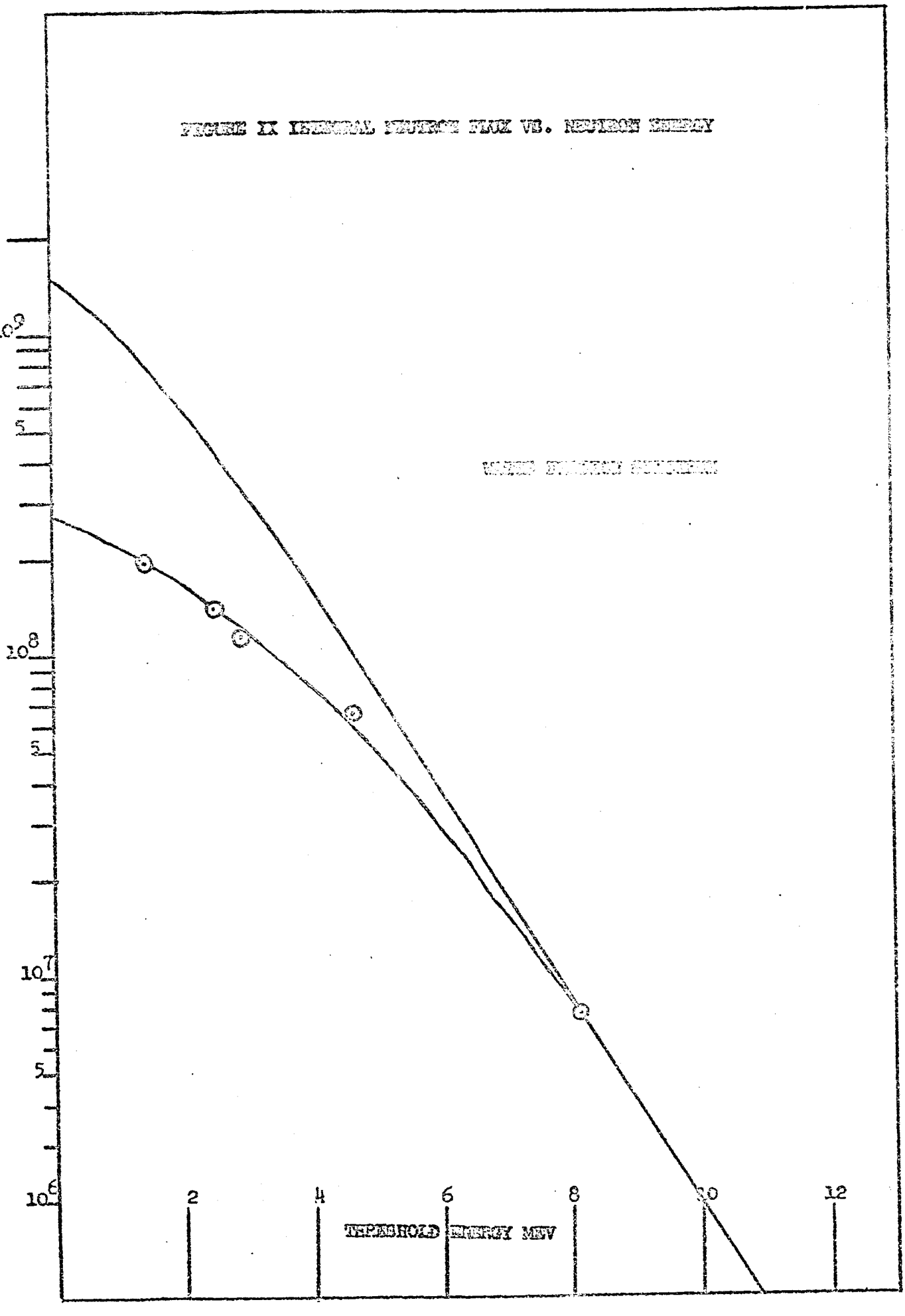

d. DESCRIPTION OF MEASUREMENTS

None of the measurements performed on the solar cells were made during irradiation. At the McGill cyclotron a large amount of radio frequency interference was present. This noise was more than the expected signal from the solar cells and in time occurred almost simultaneously with the beam of protons coming from the cyclotron. As a result, it would have been extremely difficult to separate the interference signal from the signal obtained from the solar cells for lifetime measurements. Since the neutron irradiation was steady state, no lifetime measurement could be made using the carrier decay technique. Since it would have been extremely difficult to determine the gamma photon flux, no diffusion length measurements during irradiation were made.

The measurements made on the solar cells consisted of the dark and illuminated conditions, voltage and current characteristic curves, both forward and reverse. The forward bias curves extended from zero up to approximately 0.7 volt and the reverse bias curves from zero up to 35 volts.

The forward bias curve was also obtained under an equivalent one sun illumination which was produced by a tungsten flood lamp (Figure 12) operating at about 2800° K. located about 15 inches above the solar cell. The solar cells were mounted in a brass block which was used as a heat sink to maintain a uniform temperature during the one sun measurements. The temperature was maintained at 27° C. + 2° by running water through a brass block on which the sample rested during the measurements. Thermocouples were attached to the brass block and the output of the thermocouple was compared against a reference junction which was maintained at 0°C by means of an ice bath. The output of the solar cells was connected across a one ohm resistor and a Hewlett-Packard millivolt meter measured the voltage drop across the one ohm resistor. This particular reading gave the solar cell short circuit current under a one sun illumination. Complete voltage current curves under the same illumination were obtained by connecting the output of the solar cell in series with a one ohm

resistor and an external power supply. As the voltage from the power supply was varied, the voltage across the one ohm resistor was fed to the vertical axis of an X-Y recorder and the voltage across the solar cell was fed into the horizontal axis of the X-Y recorder. The X-Y recorder calibration was checked against a mercury standard cell and also against the Hewlett Packard and Keithly microvolt meter used with the one micron sources. The agreement between all three meters was generally the order of 2 percent which is within the rated accuracy of the individual instruments.

The short circuit current from the solar cells was also obtained using a penetrating light source of 1.03 microns wavelength (Figure 13.) This was obtained by using a tungsten lamp in an iodine vapor atmosphere as the light source. The light passed through a condensing lense and a Bausch and Lomb 1.03 micron interference filter. Two Corning trimming filters removed the light having wavelengths above and below the 1.03 micron wavelength. The transmission was measured in the range of wavelengths from 0.35 to 2.7 microns by using a Beckman DK-2A spectrograph and the range from 2 to 10 microns utilized a Perkin-Elmer 235 instrument. The transmission was essentially zero except at about 1.03 microns. At 1.03 micron the transmission was 5.5%. The half-width of the transmission peak was about 0.05 microns. A thermopile was used to determine the radiant energy falling on the surface of the solar cells and from this measurement, the short circuit current can be used to determine the diffusion lengthof the cell provided the various other quantities are know. A description of this technique follows.

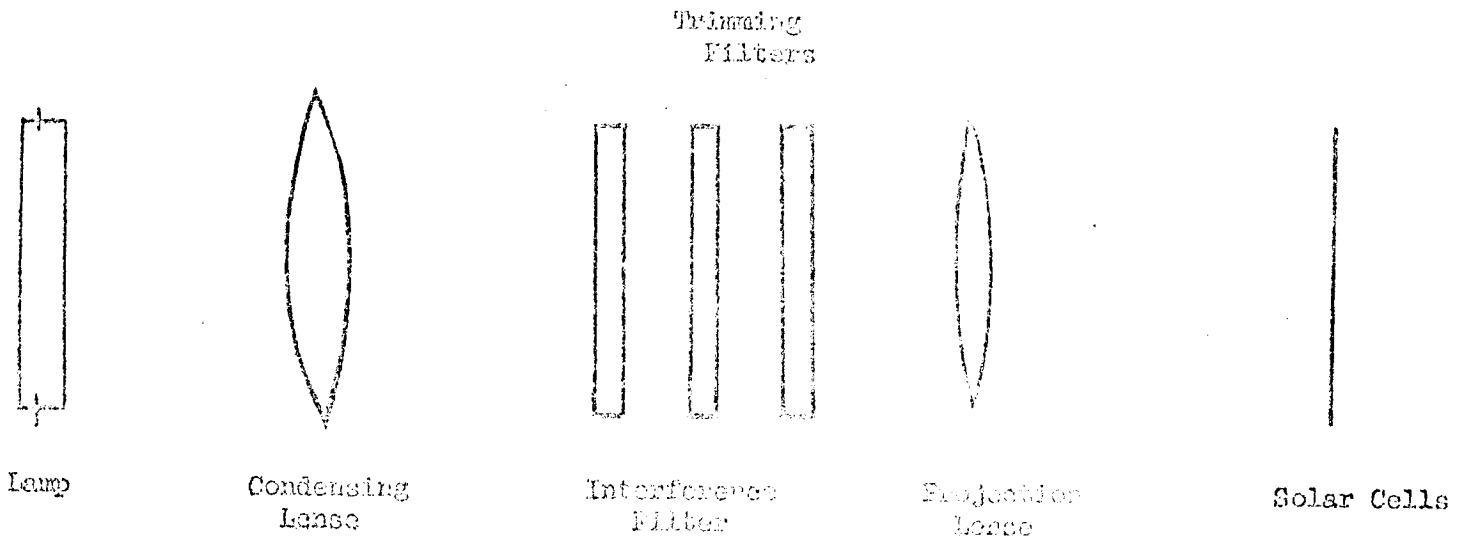

FIGURE 13

SCHEMATIC REPRESENTATION OF ONE MICRON SOURCE

e. DIFFUSION LENGTH MEASUREMENTS USING A ONE MICRON PHOTON SOURCE

The theoretical expression for the spectral response of the short circuit current of the base region of a silicon solar cell is:

$$I_{sc} = Ne\,(1-R)\frac{\alpha L}{1+\alpha L}\,e^{-\alpha d} \qquad (21)$$

where I_{sc} = short circuit current density in amp/cm^2

N = incident photon flux density in photons/cm^{2}sec

e = electronic charge in coulombs

R = reflectivity

α = absorption constant = 110 cm^{-1} 60μ

L = diffusion length in cm

d = junction depth in cm

At 1μ and for the junction depths in commercial solar cells, the exponential term can be neglected, i.e., $e^{-\alpha d} \simeq 1$. The photon flux N is obtained from a measurement of the absolute energy density H at 1μ, by the expression:

$$N = H/1.6^{0} \times 10^{-19}\,h\nu$$

where H = absolute energy density in watts/cm^2

$h\nu$ = photon energy at 1μ = 1.242 ev

The diffusion length in terms of measured parameters is therefore given by

$$(L)^{-1} = (110\,H\,(1-R)/1.242\,I_{sc}) - 1$$

At 1.03 microns the absorption coefficient of silicon, α, is 110 cm^{-1}. The reflectivity of several p/n cells was measured and was found to vary from 4.56 to 11.0% with the mean falling at 7.1%. The reflectivity of the n/p cells varied from 8.2 to 12.9%, with a mean of 10.8%. Delivery and test schedule timing prevented pre- and post- measurements from being made on all the cells.

The incident energy on the solar cells from the one micron source was determined to be 60 microwatts/cm^2 estimated to be accurate to within less than 20%. It was also found that the intensity varied by about 6% at the two positions at which the cells were measured.

Four cells were obtained from Bell Telephone Laboratories the diffusion lengths of which had been determined by the electron accelerator technique. The diffusion lengths of these same cells were measured with the one micron source. The results are given in Table VII.

TABLE VII

Cell	BTL Values	REO Values
9437L	143 microns	232 microns
9445R	133 "	140 "
877L	7.33 "	5.85 "
879 R	7.60 "	4.78 "

If one considers the expression for the diffusion length:

$$L = \frac{1}{\alpha \frac{NE(1-R)}{Isc} - 1}$$

and substitues actual values for α, N, e, R and Isc for an undamaged cell it is apparent that the measurement of L is dependent on the difference between two numbers which are nearly equal, that is, $\frac{1}{(1.5-1)}$ for a cell with a diffusion length of about 180 microns. Under these conditions then the accuracy of the diffusion length is strongly dependent on the value of N, and to a smaller degree, the reflectivity. Under these conditions a 1% error in the value of N results in about 6% error in the diffusion length. However, as the diffusion length decreases due to radiation damage the error in the diffusion length approaches the error in the N. Also, the error introduced by the reflectivity becomes less important.

2. RESULTS OF EXPERIMENT

The diffusion length of the minority carriers in the base region of the solar cells was calculated from the short circuit current response at one micron wavelength by means of Equation (21). The experimental data showing the diffusion lengths of each cell at the various energy levels of irradiation is presented in tables B-1 and B-2 in Appendix B. It will be noted that there is considerable variation in the initial diffusion lengths. The larger values of diffusion length are probably due to error in experimental technique. Preliminary analysis of our 1 micron source measurement reveals that for the larger initial solar cell diffusion lengths, the accuracy of the measurement decreases.

The damage constants for the observed changes in the diffusion lengths of each solar cell, as calculated from the defining equation

$$(1/L^2 = 1/L_o^2 + K_L \phi)$$

are also presented in tables B-1 and B-2 in Appendix B. The damage constant constant was calculated at each dose level using the initial value of diffusion length in each case. For a particular type of cell (p/n or n/p) and particle energy, all damage constants were averaged. These averages with maximum and minimum values are presented in table VIII, and illustrated in figure 14.

The degradition of solar cell short circuit current at 1 sun illumination due to proton and neutron irradiation is shown in Figures B-1 through B-8 in Appendix B. The complete voltage current characteristics of typical cells are shown in Figures B-9 through B-20 in Appendix B. The degradation of short circuit current is in agreement with existing knowledge of solar cell damage mechanisms, i.e., decrease in short circuit current through reduction in diffusion lengths. These curves present a common base for comparison with data of other experimenters.

The complete voltage-current characteristics reveals that the permanent damage to solar cell dark characteristics is not similar to permanent damage in

TABLE VIII SUMMARY OF PROTON AND NEUTRON

DAMAGE IN SILICON SOLAR CELLS

CELL	PARTICLE ENERGY	DAMAGE CONSTANT K_L - (PARTICLES^{-1}) AVERAGE	MAXIMUM	MINIMUM
p/n	48.5 Mev Protons	21.2×10^{-6}	27.5×10^{-6}	$1[illegible].5 \times 10^{-6}$
n/p	48.5 Mev Protons	2.9×10^{-6}	4.53×10^{-6}	1.72×10^{-6}
p/n	68.9 Mev Protons	10.8×10^{-6}	13.8×10^{-6}	$8.9[illegible] \times 10^{-6}$
n/p	68.9 Mev Protons	2.29×10^{-6}	3.82×10^{-6}	1.51×10^{-6}
p/n	96.5 Mev Protons	8.0×10^{-6}	16.4×10^{-6}	4.17×10^{-6}
n/p	96.5 Mev Protons	1.35×10^{-6}	2.04×10^{-6}	0.46×10^{-6}
p/n	Fission Plate Neutron Spectrum	8.23×10^{-6}	15.7×10^{-6}	4.57×10^{-6}
n/p	Fission Plate Neutron Spectrum	1.70×10^{-6}	4.10×10^{-6}	0.87×10^{-6}
p/n	Moderated Neutron Spectrum	4.46×10^{-6}	6.57×10^{-6}	2.33×10^{-6}
n/p	Moderated Neutron Spectrum	2.20×10^{-6}	7.40×10^{-6}	0.49×10^{-6}

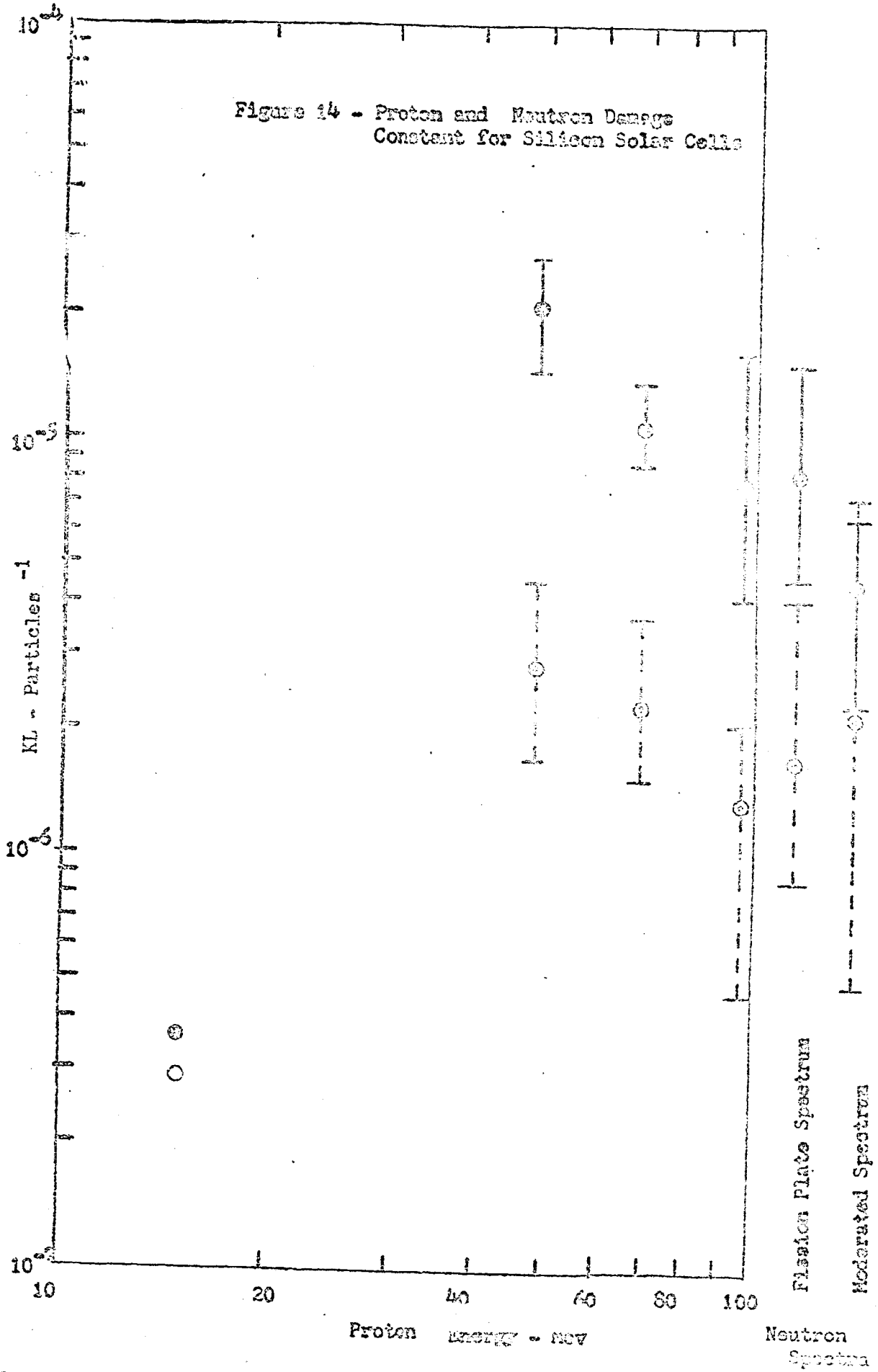

Figure 14 - Proton and Neutron Damage Constant for Silicon Solar Cells

diode characteristics. These curves also indicate little change in characteristics throughout the irradiations, which indicates that all cells functioned properly after each irradiation.

D. DISCUSSION OF RESULTS

A proton-neutron damage correlation for the diffusion length change in silicon solar cells was determined through the previously discussed experimental program. Table IX gives the correlation for the different proton energies versus the neutron spectrum. This was done by comparing the respective diffusion length damage constants. Figure 14 also shows the respective damages in graphical form.

TABLE IX - RATIO OF PROTON DAMAGE CONSTANT TO NEUTRON DAMAGE CONSTANT

Ratio	SOLAR CELL TYPE p/n	n/p
96.5 Mev Protons / Fission Neutrons	0.97	0.795
68.9 Mev Protons / Fission Neutrons	1.31	1.35
48.5 Mev Protons / Fission Neutrons	2.58	1.71
96.5 Mev Protons / Moderated Neutrons	1.80	0.61
68.9 Mev Protons / Moderated Neutrons	2.42	1.04
48.5 Mev Protons / Moderated Neutrons	4.76	1.32

One should be cautious in using these damage correlations. As was pointed out in the theoretical studies and substantiated by our empirical work on the data from literature, the correlation will vary depending on:

1) Basic Material Resistivity - This varies among semiconductor devices and types, dependent on bulk material resistivity, manufacturer and manufacturing process.

2) Basic Material Doping and Impurities - Different types of semiconductor devices use various doping materials such as indium, boron, etc. Material processing depending on whether it is manufactured by the floating zone or pulled process will have an impurity predominance, such as oxygen, which, in turn, will act as a trapping center for vacancies creating defects.

Table X gives a comparison of the proton-neutron correlations that have been published to date by other experimenters. It is difficult to make direct comparisons as the particle energies, type material and method of determination vary.

TABLE X - COMPARISON OF NEUTRON-PROTON CORRELATIONS

	TYPE OF SEMICONDUCTOR BASE MATERIAL		
RCA (21)	n-Type	[illegible]	No Type Stated
17 Mev Protons / 17 Mev Neutrons	100	.45	
BTL (22)			
40 Mev Protons / 1 Mev Neutrons		.002	
Batelle (27)			
17 Mev Protons / Fission Neutrons			18
40 Mev Proton / Fission Neutron			6.8

In the case of RCA, their determination was based on 17 Mev neutrons and an assumption of isotropy. They also had considered the neutron damage to be uniform and no clustering. Bell had use, for comparison, a semiconductor material of 5 ohm-cm and we had used in our experiment a value of 2 ohm-cm. Batelle estimates were made

primarily based on literature data, in which, they do caution the reader of the guesswork they used. In none of the above references, were there controlled experiments conducted on the same samples with both protons and neutrons.

An additional observation was made during this study which does not pertain to the proton-neutron damage correlation; however, it does concern the diffusion length damage constants which we have determined. We have not agreed with the BTL (22) data. This is probably due to the difference in diffusion length length measurement technique. We used the one micron technique whereby they used an accelerator method. We also know that the experimental data disagrees among various experimenters depending on whether the minority carrier lifetime damage comes from diffusion length measurements or from a direct transient method. Lifetime damage from diffusion length is a factor 6-10 greater than the lifetime from a direct transient method even when measured on the same cells (Ref. 16). Our fission plate neutron damage measured by the diffusion length is a factor 20-40 larger than Wertheim's (Ref. 17 and 18) fission plate neutron damage by a transient method. There is not enough known about his measurement technique to determine where the error lies.

In the theoretical discussion, we calculated the number of defects per vacancy from theoretical models and proton data. We can do the same with our proton data. In Table XI, our results for the proton data are shown.

TABLE XI

Energy Mev	Cross Section cm^{-1}		$K_L D$		$K_L D/\Sigma d$	
	Σ c Collision	Σ d Displacement	N Type	P Type	N Type	P Type
48.5	44.2	172.	21.2×10^{-5}	7.2×10^{-5}	1.24×10^{-6}	$.42 \times 10^{-6}$
68.9	32.1	125.	16.8	6.73	1.35	.46
96.5	23.8	93.	8.	3.38	.86	.37
			Average $K_L D/\Sigma d = 1.15 \times 10^{-6}$			$.42 \times 10^{-6}$

When the lifetime damage per vacancy per cm^3 from Table XI is divided by the lifetime damage per defect per cm^3 from Table III, we again obtain an estimate of the number of defects.

	P Type	N Type
1 ohm-cm	19.5	.35
2 ohm-cm	25.3	.60

These numbers are still not reasonable. This could be because the theoretical models are wrong or incorrectly applied. We already know we are not accounting for the damage due to all defects. We have assumed that all damage in the P type is due to the oxygen defect and all damage in N type is due to the divacancy.

V. CONCLUSIONS

The study program has determined a proton-neutron damage correlation in silicon solar cells which ranges from .6 to 4.8 depending on p or n type base material, proton energy and neutron spectrum. It is not known whether this correlation would apply to other semiconductor devices.

The attempts at arriving at a correlation from theoretical considerations using the basic mechanisms of damage by protons and neutrons in semiconductor material was unsuccessful. The damage processes of the two particles are basically different. Damage to minority carrier lifetime from neutron irradiation is characterized by the effective cross sectional area of the cluster of displaced atoms and is relatively independent of the type of defect. Damage from protons, on the other hand, is dominated by the type of defect introduced (e.g., impurity trapping center). For this reason, theoretically derived damage "cross sections" for each different type of bombarding particle must be based on different (and independent) physical properties of the basic material. This possibly indicates that the development of radiation-hardened semiconductor devices will proceed in different directions for neutrons and protons.

In the study involving use of existing data in the literature, it was not possible to arrive at a reliable empirical neutron-proton correlation. There was too wide a spread in the neutron damage data due to the use of various semiconductor devices and types of materials, inadequate reporting of data and no data available on similar semiconducting material under both proton and neutron irradiation.

VI RECOMMENDATIONS

Further studies need to be performed in this area in order to establish adequate neutron-proton correlation in semiconductors such as:

1. Additional refinement needs to be performed on this study program. With the large amount of experimental data that has been taken, a statistical analysis could be made. An additional effort should also be applied to more thoroughly connecting our theoretical studies with the experimental work.
2. A correlation has been determined for silicon solar cells. Does this correlation hold for another type device, such as a diode or transistor, with the same impurities and resistivity material? Such questions still should be answered for a meaningful correlation and if there is a variation, what does it depend on.
3. Theoretical and experimental studies on semiconductor bulk material to determine better damage models for both neutrons and protons. Effort is also needed to relate the basic material changes, such as displacements, vacancies, etc., to property changes such as minority carrier lifetime, etc. This effort, which has been started on this program, could have far reaching importance in the development of radiation-hardened components.
4. In our study program, we have developed a one micron diffusion length measurement technique for solar cells and bulk material which looks promising in that the associated instrument is convenient, economical, fast, and portable. To date, BTL is the only organization making diffusion

length measurements and these necessitate the use of an electron accelerator.

5. A serious discrepancy exists between minority carrier lifetime measurements using the transient method and the minority carrier lifetime which is calculated from the diffusion length measurements. Studies are needed to investigate this further.

VIII. APPENDIX

A. Proton and Neutron Radiation Damage Data on [illegible]

TABLE A-I - PROTON DAMAGE TO SILICON SOLAR CELLS

CELL MFGR	CELL TYPE	PARTICLE	L BEFORE IRRAD. μ	L AFTER IRRAD. μ	τ BEFORE IRRAD. μsec.	τ AFTER IRRAD. μsec.	EFFICIENCY η max	K_L PROTON^{-1}	K_τ (cm^2/sec proton) FROM L MEASUREM.	K_τ (cm^2/sec proton) FROM τ MEASUREM.	REF. NO.
RCA (L2)	n/p	19 Mev Protons	100	15	10	1.7	8.5	5×10^{-7}	1.25×10^{-5}	5.44×10^{-6}	19
HOFF. (13)	p/n	19 Mev Protons	40	3	3	0.2	9.0	2.26×10^{-5}	2.26×10^{-4}	9.52×10^{-5}	19
IRC (43)	p/n	19 Mev Protons			8	0.7	10.5			1.47×10^{-5}	19
RCA (L3)	n/p	19 Mev Protons			10	2.2	8.5			2.08×10^{-6}	19

TABLE A-II - PROTON DAMAGE TO SILICON SOLAR CELLS

CELL MFGR.	CELL TYPE	EFFICIENCY η	PARTICLE	L μ	ϕ p/cm^2	K_L PROTON^{-1}	REF. NO.
HOFF.	p/n	9% ungridded	740 Mev Protons	44.4	0		20
				13.5	7.5×10^{10}	6.67×10^{-6}	
				2.55	6.1×10^{11}	2.52×10^{-5}	
				0.255	1.4×10^{12}	1.1×10^{-3}	
HOFF.	p/n	11% gridded	740 Mev Protons	59.3	0		20
				4.15	2.8×10^{11}	2.06×10^{-5}	
				2.02	1.0×10^{12}	2.46×10^{-5}	
				1.0	4.4×10^{12}	2.27×10^{-5}	
				0.48	8.1×10^{12}	5.38×10^{-5}	
HOFF.	p/n	11% gridded	450 Mev Protons	46.9	0		20
				29.0	1.2×10^{10}	6.13×10^{-6}	
				10.4	1.5×10^{11}	6.0×10^{-6}	
				5.6	4.9×10^{11}	6.41×10^{-6}	
				2.72	1.9×10^{12}	7.1×10^{-6}	

TABLE A-III - PROTON DAMAGE TO SILICON SOLAR CELLS

CELL TYPE	PARTICLE	L BEFORE IRRAD. μ	L AFTER IRRAD. μ	K_L PROTON^{-1}	K_τ (cm^2/sec proton) FROM L MEAS.	FROM τ MEAS.	REF. NO.
p/n	19 Mev Protons	120	5	1.2×10^{-5}	1.2×10^{-4}	2.6×10^{-5}	29
p/n		170	4	2.1×10^{-5}	2.1×10^{-4}	2.5×10^{-5}	29
p/n		130	5.5	1.0×10^{-5}	1.0×10^{-4}	2.4×10^{-5}	29
p/n		110	5	4.0×10^{-5}	4.0×10^{-4}	3.6×10^{-5}	29
p/n		95	7	4.4×10^{-5}	4.4×10^{-4}	4.4×10^{-5}	29
p/n		130	5	4.5×10^{-5}	4.5×10^{-4}	1.2×10^{-4}	29
p/n		95	3	1.3×10^{-5}	1.3×10^{-4}	1.4×10^{-5}	29
n/p		105	10	1.7×10^{-6}	4.2×10^{-5}	6.7×10^{-6}	29
n/p		45	22	9.6×10^{-7}	2.4×10^{-5}	2.0×10^{-5}	29

average for p/n 2.64×10^{-5}
average for n/p 1.33×10^{-6}

TABLE A-IV - PROTON DAMAGE TO SILICON SOLAR CELLS

CELL MFGR	CELL TYPE	EFFICIENCY η	PARTICLE	τ_L BEFORE IRRAD. μ	τ_L AFTER IRRAD. μ	K_L $(\text{PROTON})^{-1}$	K_T $(\text{cm}^2/\text{sec proton})$ FROM L MEAS.	REF. NO.
HOFF	p/n	9.5%	8.3 Mev Protons	93 93	7 7	1.2×10^{-5}	1.2×10^{-4}	21
IRC	p/n	10.5%		100	7	1.2×10^{-5}	1.2×10^{-4}	21
IRC	p/n	11%		144	7.4	1.8×10^{-5}	1.8×10^{-4}	21
IRC	p/n	11%		126	7.5	6.9×10^{-6}	6.9×10^{-5}	21
USASRDL	n/p	6.4%		48	13	1.2×10^{-6}	3.0×10^{-5}	21
USASRDL	n/p	7.8%		48	13	2.72×10^{-6}	6.8×10^{-5}	21
USASRDL	n/p	5.6%		200	10	6.0×10^{-7}	1.5×10^{-5}	21

TABLE A-VI

TRANSISTORS IRRADIATED IN ORNL 22 MEV CYCLOTRON CO.01 μA BEAM CURRENT (2.5×10^{10} PROTONS/CM^2/SEC) REF. 28

TRANSISTOR TYPE	SAMPLE NO.	DOSE PROTONS/CM^2	COLLECTOR CURRENT μA	GAIN h_{FE} BEFORE IRRAD.	GAIN h_{FE} AFTER IRRAD.	DAMAGE CONSTANT, K (PROTONS/CM^2/SEC)$^{-1}$	REMARKS
2N128	217	7.5×10^{12}	20	76	65	9.1×10^{-8}	Dose questionable
PNP Surface	219	1.5×10^{13}	20	37	Destroyed		$f_{\alpha b}$ = 50 mc
Barrier Germanium	200	2.25×10^{13}	20	35.5	12.3	7.15×10^{-7}	(quoted by author)
2N393	32						I_{ceo} data only
PNP, Micro-Alloy, Ge	100					4.0×10^{-7}	
2N1303	11	3×10^{12}	30	220	2.1	4.0×10^{-7}	$f_{\alpha b}$ = 4.5 mc*
Ge, PNP	54	3×10^{12}	30	15.5	103	3.2×10^{-8}	
Alloy, Junct.	52	4.73×10^{12}	30	13.6	3.7	1.18×10^{-7}	
						2.16×10^{-7}	
2N146	61	7.5×10^{12}	[illegible]	21	2	1.14×10^{-6}	$f_{\alpha b}$ = 3 mc
Germanium, NPN	134	1.5×10^{13}	[illegible]	40	4	3.14×10^{-7}	(quoted by author)
	43	2.25×10^{13}	50	64	1	7.7×10^{-7}	
						7.4×10^{-7}	
2N169A	71	7.5×10^{12}	50	45	3	2.3×10^{-6}	$f_{\alpha b}$ = 9 mc*
Germanium, NPN	73	1.5×10^{13}	20	43	1	3.7×10^{-6}	
Rate, Grown	90	2.25×10^{13}	50	55	2.5	1.0×10^{-6}	
						2.3×10^{-6}	
2N1302	50	7.5×10^{12}	100	27	2.9	1.15×10^{-6}	$f_{\alpha b}$ = 4.5 mc*
Ge, NPN	53	1.5×11^{13}	100	45	1.4	1.3×10^{-6}	
Alloy, Junct.	36	2.25×10^{13}	100	23.5	1.6	7.7×10^{-7}	
						1.07×10^{-6} av.	

*manufacturer's specifications

TABLE A-V - PROTON DAMAGE TO SILICON SOLAR CELLS

CELL TYPE	PARTICLE PROTONS, IN MEV	K_L	REF. NO.
n/p	35	9.3×10^{-7}	22
	45	9.2×10^{-7}	22
	55	7.0×10^{-7}	22
	65	5.5×10^{-7}	22
	80	5.7×10^{-7}	22
	100	3.8×10^{-7}	22
	120	3.5×10^{-7}	22
	135	3.5×10^{-7}	22
	450	1.0×10^{-7}	22
p/n	45	7.9×10^{-6}	22
	65	6.2×10^{-6}	22
	80	5.1×10^{-6}	22
	100	5.5×10^{-6}	22
	[illegible]	3.3×10^{-6}	22

TABLE A-VII

TRANSISTORS IRRADIATED IN UNIVERSITY OF ROCHESTER

240 MEV SYNCHROCYCLOTRON AT TOTAL PROTON FLUX OF 9.3×10^{11} PROTONS/CM^2 REF. 28

TRANSISTOR TYPE	SAMPLE NO.	BASE CURRENT μA	GAIN h_{FE} BEFORE IRRAD.	GAIN h_{FE} AFTER IRRAD.	DAMAGE CONSTANT, K_T $(PROTON/CM^2/SEC)^{-1}$	REMARKS
2N128	1	30	45	42	7.1×10^{-7}	fab = 50 mc (author's quote)
PNP, Ge, S.B.	3	30	20	21		Note increase in h_{FE}
2N146	17	50	27	21	2.1×10^{-7}	fab = 3 mc (author's quote)
NPN, Ge	42	50	41	25	3.1×10^{-7}	
	52	50	40	31	1.47×10^{-7}	
					2.3×10^{-7} av.	
2N224	175	75	96	32	6.2×10^{-8}	fab = 0.5 mc*
PNP Ge, Alloy Junction	176	75	93	36	5.9×10^{-8}	
					6.0×10^{-8} av.	

*manufacturer's specification

TABLE A-VIII

TRANSISTORS IRRADIATED AT UNIVERSITY OF ROCHESTER - 240 MEV CYCLOTRON, REF. 29

TRANSISTOR TYPE	SAMPLE NO.	PROTON DOSE PROTONS/CM^2	BASE CURRENT μA	GAIN h_{FE} BEFORE IRRAD.	GAIN h_{FE} AFTER IRRAD.	DAMAGE CONSTANT, K_τ (PROTON/SEC/CM^2)$^{-1}$	REMARKS
2N1303	159	4.27×10^{11}	50	138.8	92.4	4.83×10^{-7}	h_{FE} = 50*, $f_{\alpha b}$ = 4.5 mc,*
PNP Ge	160	4.27×10^{11}	50	92.4	76.4	3.33×10^{-7}	$f_{\alpha b}$ = 5 to 15 mc for 40 mev,
Alloy Junct.	161	4.27×10^{11}	50	103.6	92.0	1.79×10^{-7}	used $f_{\alpha b}$ = 10 for values of K_τ
	162	4.27×10^{11}	50	45.0	44.0	1.45×10^{-7}	
	163	4.27×10^{11}	50	104.0	93.6	1.91×10^{-7}	
						2.66×10^{-7} av.	
2N1302	109	4.02×10^{11}	30	142.7	74.0	1.01×10^{-6}	h_{FE} = 50*, $f_{\alpha b}$ = 4.5 mc*,
NPN Ge	111	4.02×10^{11}	30	52.0	33.3	1.68×10^{-6}	$f_{\alpha b}$ = 10 mev for 40 mev,
Alloy Junct.	111	4.02×10^{11}	30	166.0	105.5	5.4×10^{-7}	used $f_{\alpha b}$ = 10 for K_τ
	112	4.02×10^{11}	30	84.0	58.7	8.0×10^{-7}	
	113	4.02×10^{11}	30	78.7	50.0	11.36×10^{-7}	
						1.03×10^{-6} av.	
2N224	1	4.27×10^{11}	50	104.0	53.2	1.35×10^{-7}	h_{FE} = 90*, $f_{\alpha b}$ = .5 mc*,
PNP Ge	2	4.27×10^{11}	50	111.6	48.4	1.72×10^{-7}	$f_{\alpha b}$ = 1 mc for 40 mev,
Alloy Junct.	3	4.27×10^{11}	50	160.8	67.6	1.26×10^{-7}	decreased when irrad.,
	4	4.27×10^{11}	50	154.0	66.4	1.26×10^{-7}	used $f_{\alpha b}$ = 1 for K_τ
	5	4.27×10^{11}	50	121.6	45.2	2.04×10^{-7}	
	6	4.27×10^{11}	50	130.0	60.4	1.30×10^{-7}	
						1.49×10^{-7} av.	
2N169A	3	4.02×10^{11}	75	34.7	34.4		h_{FE} = 72*, $f_{\alpha b}$ = 9 mc*,
NPN, Ge.	4	4.02×10^{11}	75	36.8	30.1	8.48×10^{-7}	$f_{\alpha b}$ agrees w/40 mev.
Rate Grown	5	4.02×10^{11}	75	42.4	38.2	5.15×10^{-7}	
	6	4.02×10^{11}	75	39.2	24.8	20.8×10^{-7}	
	7	4.02×10^{11}	75	42.0	39.0	3.51×10^{-7}	
						9.48×10^{-7} av.	

TABLE A-VIII (cont'd)

TRANSISTOR TYPE	SAMPLE NO.	PROTON DOSE PROTONS/CM^2	BASE CURRENT μA	GAIN h_{FE} BEFORE IRRAD.	GAIN h_{FE} AFTER IRRAD.	DAMAGE CONSTANT, K_τ (PROTON/SEC/CM^2)$^{-1}$	REMARKS
2N859	1	3.39×10^{11}	50	41	34	1.14×10^{-6}	$f_{\alpha b}$ = 14 mc*
Si PNP	2	3.39×10^{11}	50	43	38	0.91×10^{-6}	
	3	3.39×10^{11}	50	44	42	0.28×10^{-6}	
	4	3.39×10^{11}	50	46	39	1.02×10^{-6}	
	5	3.39×10^{11}	50	45	39	1.41×10^{-6}	
						$.95 \times 10^{-6}$ av.	
2N743	61	3.39×10^{11}	50				
Si NPN	62	3.39×10^{11}	50	34	33	6.65×10^{-6}	$f_{\alpha b}$ = 400 mc*
	63	3.39×10^{11}	50				
	64	3.39×10^{11}	50	40	39	4.75×10^{-6}	
	65						
	66			39	38	5.0×10^{-6}	
						5.50×10^{-6} av.	
2N337	51	4.02×10^{11}	50	57	36	4.75×10^{-7}	$f_{\alpha b}$ = 30 mc*
Si NPN	52	4.02×10^{11}	50	62	42	3.58×10^{-7}	
	53	4.02×10^{11}	50	75	52	2.78×10^{-7}	
	54	4.02×10^{11}	50	68	56	13.9×10^{-7}	
	55	4.02×10^{11}	50	74	48	3.45×10^{-7}	
	56	4.02×10^{11}	50	81	56	2.56×10^{-7}	

*specification value

TABLE A-XI

SUMMARY OF LIFETIME

DAMAGE CONSTANT K_τ FOR SILICON FROM NEUTRON IRRADIATION

TRANSISTOR TYPE	SEMICONDUCTOR BASE TYPE	K_τ $(NVT\ SEC)^{-1}$	REFERENCE	AUTHOR
Not Specified	n	3.57×10^{-7}	30	Messenger & Spratt
	n	2.56×10^{-6}	31	Wertheim
	p	3.12×10^{-7}	30	Messenger & Spratt
	p	2.32×10^{-6}	31	Wertheim
	p	1.75×10^{-6}	32	Easley
T 1257	n	3.20×10^{-7}	33	Hicks, et.al.
905	p	2.28×10^{-7}	33	Hicks, et.al.
952	p	6.25×10^{-7}	33	Hicks, et.al.
MTN Experimental	p	1.60×10^{-7}	33	Hicks, et.al.
2082 (2N1675)	p	3.71×10^{-6}	34	Blair
2N1675	p	3.46×10^{-6}	34	Blair
1N462 Diode		5.6×10^{-8}	35	Kavipurapu
1N463 Diode		4.6×10^{-8}	35	Kavipurapu
1N486A Diode		3.96×10^{-8}	35	Kavipurapu
Single Crystal	n	4.4×10^{-7}	36	Beck, et.al.
Single Crystal	p	1.2×10^{-6}	36	Beck, et.al.

Table A-IX Transistors Irradiated at Carnegie Institute of Technology - 440 Mev Synchrocyclotron, REF. 29

Transistor Type	Sample No.	Proton Dose Protons/cm^2	h_{FE} Before Irrad.	Gain Before Irrad.	h_{FE} After Irrad.	Damage Constant, K_5 (Protons sec/cm^2)$^{-1}$	Remarks
2N169A	1	1.90×10^{11}	75	47.5	44.6	8.94×10^{-7}	h_{FE} $f_{\alpha b}$
NPN Ge	2	2.63×10^{11}	75	39.5	36.8	4.0×10^{-7}	72*, 9*, agrees
Rate Grown	3	3.45×10^{11}	75	51.3	48.0	2.19×10^{-7}	with 40 Mev data.
	4	4.10×10^{11}	75	42.1	34.7	7.00×10^{-7}	
						5.53×10^{-7} av.	
2N1302	5	9.96×10^{11}	30	208	192	2.38×10^{-8}	50*, 4.5*, f_b = 10 for
NPN Ge	6	2.20×10^{11}	30	197	187	7.35×10^{-8}	40 Mev data.
Alloy Junction	7	2.63×10^{11}	30	202	172	19.5×10^{-8}	
						8.69×10^{-8} av.	
2N393	8	5.50×10^{11}	20	152	161		95*, 60 ($f_{\alpha b}$ max.)
PNP Ge Micro alloy							increase in h_{FE} due to depletion layer widening. 33 (h_{fe})*
2N146	9	3.61 *	75	51.3	49.6		
NPN Ge	10	4.03 *	75	54.5	40.6		
Grown Junction	11	5.07 *	75	42.1	38.8		No 40 Mev $f_{\alpha b}$ data.
2N128	12	3.21 *	30	38.7	39.3		40 (h_{fe})*, 60 (f_{max})*,
PNP Ge	13	3.91 *	30	45.6	45.4		depletion layer widening
Surface Barrier	14	4.90 *	30	33.7	34.7		from 40 Mev f b = 70 and decreased.
2N224	15	5.37 *	75	82.4	51.9	8×10^{-8}	90*, 0.5*, mev data
PNP Ge	16	6.36 *	75	92.5	62.4	5.26×10^{-8}	showed $f_{\alpha b}$ = 1 and
Alloy Junction	17	7.35 *	75	84.5	54.6	5.32×10^{-8}	decreased when irrad.
						0.19 av.	
2N1303	18	2.42 *	50	68.8	72.4		50* 4.5*
PNP Ge	19	3.42 *	50	128.0	141.6		depletion layer widening,
Alloy Junction	20	4.42 *	50	128.0	128.8		f_b = 5 to 15

* Specification Values

TABLE A-X

TRANSISTORS IRRADIATED AT UNIVERSITY OF MINNESOTA

40 MEV LINAC ACCELERATOR AT A TOTAL FLUX OF 1.8 X 10^{12} PROTONS/CM^2, REF. 29

TRANSISTOR TYPE	TRANSISTOR NO.	GAIN h_{FE} BEFORE IRRAD.	GAIN h_{FE} AFTER IRRAD.	$f_{\alpha b}$ (mc) BEFORE	$f_{\alpha b}$ (mc) AFTER	K_τ $(PROTON/SEC/CM^2)^{-1}$
2N1302, NPN GERMANIUM	1	169	47	11.2	11.1	5.9×10^{-7}
	2	92	47	11.7	11.7	4.2×10^{-7}
	3	147	50	14.6	14.5	6.7×10^{-7}
	4	83	37	10.3	10.1	5.3×10^{-7}
	5	88	48	11.3	11.2	3.8×10^{-7}
	6	114	35	10.0	9.9	7.1×10^{-7}
	7	73	28	6.7	6.5	5.0×10^{-7}
						5.4×10^{-7} = average
2N1303, PNP GERMANIUM	8	68	49	12.2	11.9	2.4×10^{-7}
	9	71	38	5.2	5.1	2.2×10^{-7}
	10	150	118	16.5	16.7	1.0×10^{-7}
	11	115	84	9.7	9.8	1.1×10^{-7}
	12	135	71	15.3	14.9	3.6×10^{-8}
	13	73	71	8.5	8.4	1.1×10^{-7}
	14	71	50	5.8	8.5	1.2×10^{-7}
	15	51	26	5.6	5.4	3.6×10^{-7}
						1.9×10^{-7} = average
2N1305, PNP GERMANIUM	16	116	19	8.0	7.4	1.2×10^{-6}
	17	105	20	6.0	5.5	9.1×10^{-7}
	18	63	14	6.7	6.1	1.2×10^{-6}
	19	81	26	10.7	99.9	9.1×10^{-7}
	20	86	38	8.6	8.0	4.3×10^{-7}
	21	61	17	6.4	5.8	9.1×10^{-7}
						9.3×10^{-7} = average
2N146, NPN GERMANIUM	22	26	6.8			1.3×10^{-6}
	23	18	3.2			2.6×10^{-6}
	24	27	3.5			2.6×10^{-6}
	25	21	4.7			1.2×10^{-6}
	26	65	14			5.9×10^{-7}
	27	24	6.1			1.3×10^{-6}
	28	46	6.9			1.3×10^{-7}
						1.5×10^{-6} = average
2N743, NPN SILICON	29	40	34	400*		6.3×10^{-6}
	30	26	26			
	31	42	37			4.4×10^{-6}
	32	42	38			3.5×10^{-6}
	33	40	36			3.9×10^{-6}
	34	38	34			4.4×10^{-6}
						4.6×10^{-6} = average

TABLE A-X (cont'd.)

TRANSISTOR TYPE	TRANSISTOR NO.	GAIN h_{FE} BEFORE IRRAD.	GAIN h_{FE} AFTER IRRAD.	f_{α_b} (mc) BEFORE	f_{α_b} (mc) AFTER	K_τ (PROTON/SEC/CM^2)$^{-1}$
2N169A, NPN GERMANIUM	35	34	13	9.8	9.0	1.6×10^{-6}
	36	41	16	11.5	10.45	1.4 x "
	37	36	20	18.1	16.1	1.[illegible] x "
	38	36	13	10.9	9.6	1.8 x "
	39	36	14	11.0	11.1	1.[illegible] x "
	40	44	20	12.1	11.8	1.1 x "
	41	46	20	14.3	12.75	1.4 x "
	42	32	13	7.9	7.8	1.2 x "
						1.4 x " = average
2N337, NPN SILICON	43	52	8.6	30		1.0×10^{-6}
	44	69	6.4			1.4×10^{-6}
	45	78	12			7.7×10^{-7}
	46	78	13			6.7×10^{-7}
	47	78	13			8.3×10^{-7}
						9.3×10^{-7} = average
2N526 GERMANIUM	48	63	10	4.0	3.49	1.1×10^{-6}
	49	58	11	4.51	3.72	1.1×10^{-6}
	50	71	11	4.15	3.59	1.0×10^{-6}
	51	64	10	3.20	2.74	9.1×10^{-7}
	52	71	11	5.13	3.31	1.1×10^{-6}
	53	51	16	5.13	4.51	7.1×10^{-7}
	54	82	18	4.27	3.80	6.4×10^{-7}
	55	75	13	3.55	3.13	7.7×10^{-7}
						9.2×10^{-7} = average
2N224, PNP GERMANIUM	62	117	70	1.39	.71	
	63	131	12	1.05	.72	1.1×10^{-7}
	64	84	28	.97	.78	3.2×10^{-8}
	65	125	39	1.07	1.01	5.6×10^{-8}
	66	147	51	1.0	.79	1.7×10^{-8}
	67	127	49	1.15	.53	
	68	137	63	1.05	.52	
						5.4×10^{-8} = average
2N859, PNP SILICON	69	47	4.8	14*		9.1×10^{-6}
	70	48	9.8			4.0×10^{-6}
	71	46	6.6			6.2×10^{-6}
	72	47	3.2			1.4×10^{-5}
	73	50	5.2			5.9×10^{-6}
	74	42	9.4			4.0×10^{-6}
	75	48	3.0			1.54×10^{-5}
						8.4×10^{-6} = average

*manufacturer's value

Table A-XII - Neutron Irradiation of Silicon Diodes

Three types of Sylvania Silicon Diodes were irradiated at the Pennsylvania State University reactor at four integrated flux levels 1×10^{12}, 5×10^{12}, 1×10^{13}, and 1×10^{14} neutrons per cm^2. The values of lifetimes were measured before and after irradiation.

Diode Type	K_τ $(NVT\text{-}SEC)^{-1}$	Reference
1N462	5.6×10^{-8}	35
1N463	4.6×10^{-8}	
1N486A	3.96×10^{-8}	

TABLE A-XIII

NEUTRON IRRADIATION OF SILICON POWER TRANSISTORS

Transistor Type	I_c amp	W mil	ϕ nvt	α_o	α	Damage Constant K_T calc. (nvt. - sec.)	Damage Constant K_T cal. Average (nvt-sec)	Reference
2082 (2N1675) npn	0.1	0.09	1.2×10^{13}	0.98	0.875	7.35×10^{-6}		
		.10		.99	.90	5.47	5.17×10^{-6}	34
		.12		.96	.855	4.42		
		.13		.97	.865	3.79		
		.15		.97	.81	4.34		
	0.5	.09	1.2×10^{13}	.98	.91	5.17×10^{-6}		
		.10		.99	.93	3.68		
		.12		.975	.905	2.59	3.36×10^{-6}	34
		.13		.97	.90	2.54		
		.15		.97	.86	2.91		
	1.0	.09	1.2×10^{13}	.98	.91	5.17×10^{-6}		
		.10		.99	.93	3.68	3.31×10^{-6}	34
		.12		.98	.91	2.96		
		.13		.975	.900	2.71		
		.15		.965	.89	2.03		
2N1675 npn	0.1	.14	1.2×10^{13}	.93	.73	4.65×10^{-6}		34
		.12		.97	.85	5.17		
		.12		.92	.73	5.95	4.5×10^{-6}	
		.13		.97	.835	2.97		

Table A-XIII (Continued)

Transistor type	I_c amp	W mil	ϕ nvt	α_o	α	Damage Constant K_τ calc. $(nvt. - sec.)^{-1}$	Damage Constant K_τ calc. Average $(nvt\text{-}sec)^{-1}$	Reference
2N1675 npn		.12		.985	.89	3.78		
	0.5	.14	1.2×10^{13}	.93	.825	3.25×10^{-6}		
		.12		.955	.875	3.54	2.97×10^{-6}	34
		.12		.94	.855	3.61		
		.13		.97	.905	2.35		
		.12		.975	.925	2.12		

Neutron Source - BNL Water Tank Shielding Facility and Swimming Pool Reactor at the Pennsylvania State University

Table A-XIV

Summary of Lifetime

Damage Constant, K_τ, for Germanium from Neutron Irradiation

Transistor type	Semiconductor Base type	K_τ $(nvt\ sec)^{-1}$	Reference	Author
Not specified	n	1.69×10^{-8}	39, 40	Curtis
	n	2.0×10^{-8}	39	Messenger & Spratt
	n	4.75×10^{-8}	37	Easley & Dooley
	p	2.5×10^{-8}	38	Curtis
	p	4.2×10^{-8}	39	Messenger & Spratt
	p	5.5×10^{-8}	37	Easley & Dooley
T1166	n	2.7×10^{-8}	33	Eichin, et. al.
MACS	n	2.13×10^{-8}		"
2N139	n	2.38×10^{-8}		"
T1041	n	2.17×10^{-8}		"
4JD1A17	n	2.70×10^{-8}		"
2N174	n	2.00×10^{-8}		"
2N176	n	3.00×10^{-8}		"
2N94A	p	5.90×10^{-8}		"
HA5003	p	2.20×10^{-8}		"
Bulk Ge	n	1.44×10^{-8}	38	Curtis
"	n	5.15×10^{-8}		"
"	n	1.21×10^{-7}		"
"	n	4.63×10^{-6}		"
"	n	5.9×10^{-6}		"

Table A-XIV (continued)

Transistor type	Semiconductor Base Type	K_q (mrt sec)$^{-1}$	Reference	Author
Bulk Ge	p	1.14×10^{-8}	38	Curtis
"	p	4.1×10^{-8}		"
"	p	1.03×10^{-7}		"

TABLE A-XV

EFFECT OF IRRADIATION WITH 14-MEV NEUTRONS ON CARRIER LIFETIME IN GERMANIUM. REF. 38

Sample	Initial Properties: n cm^{-3}	Initial Properties: p cm^{-3}	Initial Properties: T_o usec	T^* usec	$1/T - 1/T_o$ sec $^{-1}$ x 10^{-3}	Estimated Equivalent Reactor Irradiation**	Calculated K_τ: Damage Const. $(nvt\text{-}sec)^{-1}$	Calculated K_τ: Damage Const.** $(nvt\ sec)^{-1}$
A5-1	5.1×10^{13}	4.9×10^{12}	1070	410	1.51	4×10^{11}	1.44×10^{-8}	3.79×10^{-9}
A6-1	1.5×10^{14}		960	155	5.41	8 x 10	5.15×10^{-8}	6.75×10^{-9}
AB7-1	3.1×10^{14}		410	66	12.7	1×10^{12}	1.21×10^{-7}	1.27×10^{-9}
A4-1	7.6×10^{14}		170	18.4	48.5	1.5×10^{12}	4.63×10^{-6}	3.21×10^{-9}
CH-6	2.6×10^{15}		44	11.8	62	1.1×10^{12}	5.9×10^{-6}	5.67×10^{-9}
D1-1	3.1×10^{12}	8.0×10^{13}	760	400	1.2	4×10^{11}	1.14×10^{-8}	3.00×10^{-9}
F2A-1		3.4×10^{14}	460	155	4.3	6×10^{11}	4.1×10^{-8}	7.15×10^{-9}
D3-1		1.6×10^{15}	220	65	10.8		1.03×10^{-7}	

* Carrier lifetime after irradiation with 1.05×10^{11} neut/cm^2 (energy 14 Mev)

** Average neutron energy approximately 1.5 Mev

Irradiations carried out at the ORNL Biology Division Cockcraft-Walton accelerator

Table A-XVI - Base Region Characteristics of Several Transistor Types

Transistor No.	Type	Estimated Base Resistivity	Estimated Base Carrier Concentration
2N337	NPN Si	1.8 ohm - cm	~ 4.2×10^{16}
2N128	PNP Ge	1 ohm - cm	~ 10^{15}
2N711	PNP Ge	Sheet resistance 300 - 400 ohm/sq	~ 4×10^{16}
2N169A	NPN Ge	1.7 ohm cm	2.1×10^{15}
2N224	PNP Ge		~ 6×10^{18}
2N526	PNP Ge	1.8 - 2.5 ohm cm	7×10^{14} - 1×10^{15}
2N1302			
2N1303	PNP Ge	1.8 - 2.1 ohm cm	9×10^{14} - 10^{15} Sb or As
2N1305	PNP Ge	1.8 - 2.1 ohm.	9×10^{14} - 10^{15} Sb or As

B. EXPERIMENTAL DATA

TABLE II-I PROTON DAMAGE DATA ON SILICON SOLAR CELLS

SAMPLE NO.	RUN NO.	DIFFUSION LENGTH (microns) RIGHT CELL	DIFFUSION LENGTH (microns) LEFT CELL	INTEGRATED PROTON FLUX (proton/cm^2)	DAMAGE CONSTANT K_L (proton^{-1}) RIGHT CELL	DAMAGE CONSTANT K_L (proton^{-1}) LEFT CELL	PROTON ENERGY (MeV)
2	0	271.0	144.2	0			
p/n	1	45.5	52.0	0.772×10^{10}	6.15×10^{-6}	4.17×10^{-6}	[illegible]
	2	27.8	32.5	1.62×10^{10}	7.90×10^{-6}	5.95×10^{-6}	"
	3	19.32	23.9	3.18×10^{10}	8.10×10^{-6}	6.55×10^{-6}	"
	4	10.70	13.45	9.92×10^{10}	8.8×10^{-6}	5.50×10^{-6}	"
	5	6.87	8.3	29.9×10^{10}	9.86×10^{-6}	6.65×10^{-6}	"
	6	4.0	4.86	73.3×10^{10}	8.50×10^{-6}	5.76×10^{-6}	"
3	0	278.0	227.0	0			
	1	40.9	49.2	0.764×10^{10}	7.50×10^{-6}	5.2×10^{-6}	"
p/n	2	27.8	33.5	1.56×10^{10}	8.20×10^{-6}	5.57×10^{-6}	"
	3	19.33	22.5	3.03×10^{10}	8.77×10^{-6}	6.46×10^{-6}	"
	4	10.70	13.13	9.31×10^{10}	9.36×10^{-6}	6.23×10^{-6}	"
	5	6.74	7.25	27.9×10^{10}	9.50×10^{-6}	6.82×10^{-6}	"
	6	2.88	4.47	73.7×10^{10}	10.4×10^{-6}	6.60×10^{-6}	"
4	0	171.6	253.0	0			
	1	35.2	40.2	1.06×10^{10}	7.47×10^{-6}	5.7×10^{-6}	"
p/n	2	16.12	17.66	3.60×10^{10}	10.0×10^{-6}	8.9×10^{-6}	"
	3	10.2	10.82	11.8×10^{10}	8.43×10^{-6}	7.22×10^{-6}	"
	4	5.53	5.53	38.6×10^{10}	8.5×10^{-6}	8.5×10^{-6}	"
5	0	318.0	327.0	0			
	1	35.1	34.6	1.14×10^{10}	7.02×10^{-6}	7.26×10^{-6}	"
p/n	2	16.3	16.15	4.30×10^{10}	8.72×10^{-6}	8.91×10^{-6}	"
	3	10.02	10.82	12.5×10^{10}	7.92×10^{-6}	6.8×10^{-6}	"
	4	5.28	5.90	39.5×10^{10}	9.05×10^{-6}	7.28×10^{-6}	"
6	0	177.0	202.0	0			
	1	32.4	36.5	1.17×10^{10}	7.87×10^{-6}	6.20×10^{-6}	"
p/n	2	17.66	15.84	3.85×10^{10}	7.46×10^{-6}	10.6×10^{-6}	"
	3	8.38	9.12	13.0×10^{10}	10.94×10^{-6}	9.23×10^{-6}	"
	4	5.03	5.35	40.6×10^{10}	9.70×10^{-6}	8.60×10^{-6}	"

TABLE B-I (CON'T.)

SAMPLE NO.	RUN NO.	DIFFUSION LENGTH (microns) RIGHT CELL	DIFFUSION LENGTH (microns) LEFT CELL	INTEGRATED PROTON FLUX (proton/cm^2)	DAMAGE CONSTANT K_L (proton^{-1}) RIGHT CELL	DAMAGE CONSTANT K_L (proton^{-1}) LEFT CELL	PROTON ENERGY (MEV)
7	0	182.0	239.0	0			
	1	31.9	32.2	1.16×10^{10}	8.2×10^{-6}	8.13×10^{-6}	96.5
p/n	2	17.47	19.15	3.62×10^{10}	8.95×10^{-6}	7.50×10^{-6}	"
	3	8.1	10.14	12.8×10^{10}	11.9×10^{-6}	7.6×10^{-6}	"
	4	5.07	5.63	35.5×10^{10}	10.94×10^{-6}	8.85×10^{-6}	"
8	0	227.0	244.0	0			
	1	20.6	25.7	1.01×10^{10}	2.31×10^{-5}	1.49×10^{-5}	48.5
p/n	2	11.22	12.6	3.29×10^{10}	2.40×10^{-5}	[illegible]	"
	3	6.14	7.6	10.9×10^{10}	2.43×10^{-5}	1.69×10^{-5}	"
	4	3.68	3.99	34.8×10^{10}	2.13×10^{-5}	1.81×10^{-5}	"
9	0	254.0	186.0	0			
	1	21.2	20.1	0.995×10^{10}	2.21×10^{-5}	2.45×10^{-5}	"
p/n	2	11.52	11.2	3.32×10^{10}	2.26×10^{-5}	2.40×10^{-5}	"
	3	5.85	5.74	10.6×10^{10}	2.35×10^{-5}	2.84×10^{-5}	"
	4	3.52	3.42	36.0×10^{10}	2.24×10^{-5}	2.38×10^{-5}	"
10	0	216.0	80.5	0			
	1	21.3	19.05	1.02×10^{10}	2.13×10^{-5}	2.55×10^{-5}	"
p/n	2	11.8	10.56	3.38×10^{10}	2.12×10^{-5}	2.61×10^{-5}	"
	3	6.62	6.06	10.78×10^{10}	2.12×10^{-5}	2.52×10^{-5}	"
	4	3.80	3.55	34.00×10^{10}	2.04×10^{-5}	2.33×10^{-5}	"
11	0	182.0	197.6	0			
	1	24.9	26.0	0.956×10^{10}	1.65×10^{-5}	1.53×10^{-5}	"
p/n	2	12.86	13.7	2.78×10^{10}	2.16×10^{-5}	1.91×10^{-5}	"
	3	6.87	7.15	11.00×10^{10}	1.92×10^{-5}	1.77×10^{-5}	"
	4	4.12	4.38	35.90	1.65×10^{-5}	1.45×10^{-5}	"
12	0	193.5	227.0	0			
	1	61.2	72.7	0.957×10^{10}	2.51×10^{-6}	1.78×10^{-6}	"
n/p	2	24.7	21.1	4.86×10^{10}	3.33×10^{-6}	4.53×10^{-6}	"
	3	12.92	14.35	17.3×10^{10}	3.44×10^{-6}	2.79×10^{-6}	"
	4	7.68	8.50	45.6×10^{10}	3.70×10^{-6}	3.02×10^{-6}	"

TABLE B-I (CON'T.)

SAMPLE NO.	RUN NO.	DIFFUSION LENGTH (microns) RIGHT CELL	DIFFUSION LENGTH (microns) LEFT CELL	INTEGRATED PROTON FLUX (proton/cm^2)	DAMAGE CONSTANT K_L (proton^{-1}) RIGHT CELL	DAMAGE CONSTANT K_L (proton^{-1}) LEFT CELL	PROTON ENERGY (MEV)
13	0	160.6	171.0	0			
	1	52.9	58.7	1.00×10^{10}	3.18×10^{-6}	2.55×10^{-6}	46.5
n/p	2	23.1	25.6	4.94×10^{10}	3.71×10^{-6}	3.04×10^{-6}	"
	3	12.38	13.8	17.2×10^{10}	3.78×10^{-6}	3.03×10^{-6}	"
	4	7.43	8.1	47.6×10^{10}	3.79×10^{-6}	3.19×10^{-6}	"
14	0	221.0	231.0	0			
	1	67.9	76.5	0.911×10^{10}	2.16×10^{-6}	1.67×10^{-6}	"
n/p	2	29.1	37.3	4.15×10^{10}	2.80×10^{-6}	1.72×10^{-6}	"
	3	14.55	15.9	16.8×10^{10}	2.80×10^{-6}	2.35×10^{-6}	"
	4	7.97	9.05	49.6×10^{10}	3.16×10^{-6}	2.46×10^{-6}	"
15	0	219.0	234.0	0			
	1	65.5	72.2	0.87×10^{10}	2.45×10^{-6}	2.00×10^{-6}	"
n/p	2	27.1	32.9	4.28×10^{10}	3.13×10^{-6}	2.11×10^{-6}	"
	3	14.1	15.5	15.8×10^{10}	3.16×10^{-6}	2.62×10^{-6}	"
	4	8.16	8.84	49.8×10^{10}	3.01×10^{-6}	2.57×10^{-6}	"
16	0	252.0	198.5	0			
	1	79.0	79.0	1.19×10^{10}	1.28×10^{-6}	1.13×10^{-6}	96.5
n/p	2	27.7	29.0	8.55×10^{10}	1.50×10^{-6}	1.36×10^{-6}	"
	3	14.85	15.16	30.2×10^{10}	1.50×10^{-6}	1.43×10^{-6}	"
	4	9.05	9.30	77.2×10^{10}	1.58×10^{-6}	1.49×10^{-6}	"
17	0	137.8	322.0	0			
	1	71.5	97.8	1.12×10^{10}	1.27×10^{-6}	0.843×10^{-6}	"
n/p	2	26.5	31.6	8.52×10^{10}	1.61×10^{-6}	1.162×10^{-6}	"
	3	14.66	16.96	26.3×10^{10}	1.75×10^{-6}	1.32×10^{-6}	"
	4	8.74	9.96	74.0×10^{10}	1.75×10^{-6}	1.35×10^{-6}	"
18	0	227.0	279.0	0			
	1	55.2	64.5	2.73×10^{10}	1.13×10^{-6}	0.465×10^{-6}	"
n/p	2	24.0	27.7	11.4×10^{10}	1.51×10^{-6}	1.13×10^{-6}	"
	3	14.24	16.2	34.3×10^{10}	1.43×10^{-6}	1.11×10^{-6}	"
	4	8.15	9.16	89.8	1.67×10^{-6}	1.33×10^{-6}	"

TABLE 2-V (CON'T.)

SAMPLE NO.	RUN NO.	DIFFUSION LENGTH (microns) RIGHT CELL	DIFFUSION LENGTH (microns) LEFT CELL	INTEGRATED PROTON FLUX (proton/cm^2)	DAMAGE CONSTANT K_L (proton^{-1}) RIGHT CELL	DAMAGE CONSTANT K_L (proton^{-1}) LEFT CELL	PROTON ENERGY (MEV)
19	0	174.6	207.0	0			
	1	47.2	55.1	3.32×10^{10}	1.26×10^{-6}	0.915×10^{-6}	96.5
n/p	2	23.1	26.3	12.9×10^{10}	1.43×10^{-6}	1.11×10^{-6}	"
	3	13.6	14.82	35.5×10^{10}	1.52×10^{-6}	1.27×10^{-6}	"
	4	7.16	7.86	95.7×10^{10}	2.04×10^{-6}	1.68×10^{-6}	"
20	0	156.5	145.1	0			
	1	45.2	39.9	2.08×10^{10}	2.16×10^{-6}	2.79×10^{-6}	48.5
n/p	2	17.9	19.4	8.85×10^{10}	3.48×10^{-6}	2.94×10^{-6}	"
	3	10.25	11.2	25.4×10^{10}	3.73×10^{-6}	3.12×10^{-6}	"
	4	6.60	7.16	65.4×10^{10}	3.5×10^{-6}	2.98×10^{-6}	"
21	0	169.4	212.0	0			
	1	39.2	43.5	2.18×10^{10}	2.82×10^{-6}	2.32×10^{-6}	"
n/p	2	19.8	21.8	8.05×10^{10}	3.12×10^{-6}	2.59×10^{-6}	"
	3	10.86	12.0	25.8×10^{10}	3.27×10^{-6}	2.67×10^{-6}	"
	4	6.85	7.70	70.6×10^{10}	3.00×10^{-6}	2.38×10^{-6}	"
22	0	187.2	206.0	0			
	1	26.5	31.8	1.01×10^{10}	1.378×10^{-5}	0.957×10^{-5}	83.5
p/n	2	14.66	17.2	3.64×10^{10}	1.276×10^{-5}	0.925×10^{-5}	"
	3	7.85	9.15	12.5×10^{10}	1.29×10^{-5}	0.952×10^{-5}	"
	4	4.48	5.17	42.0×10^{10}	1.18×10^{-5}	0.894×10^{-5}	"
23	0	172.0	241.0	0			
	1	25.6	28.0	1.34×10^{10}	1.12×10^{-5}	0.937×10^{-5}	"
p/n	2	14.86	16.3	3.85×10^{10}	1.17×10^{-5}	0.972×10^{-5}	"
	3	8.5	8.85	12.2×10^{10}	1.13×10^{-5}	1.066×10^{-5}	"
	4	4.75	5.17	40.1×10^{10}	1.11×10^{-5}	0.936×10^{-5}	"
24	0	157.4	202.0	0			
	1	44.2	48.1	2.71×10^{10}	1.74×10^{-6}	1.51×10^{-6}	"
n/p	2	19.35	22.3	10.45×10^{10}	2.51×10^{-6}	1.91×10^{-6}	"
	3	10.9	13.03	31.15×10^{10}	2.69×10^{-6}	1.88×10^{-6}	"
	4	6.6	7.57	83.6×10^{10}	2.74×10^{-6}	2.08×10^{-6}	"
25	0	125.2	180.2	0			
	1	39.3	47.2	2.40×10^{10}	2.42×10^{-6}	1.74×10^{-6}	"
n/p	2	18.4	22.4	10.41×10^{10}	2.77×10^{-6}	1.88×10^{-6}	"
	3	9.17	12.9	31.0×10^{10}	3.82×10^{-6}	1.93×10^{-6}	"
	4	6.22	7.65	86.6×10^{10}	2.98×10^{-6}	1.98×10^{-6}	"

TABLE B-2 NEUTRON DAMAGE DATA ON

SILICON SOLAR CELLS

SAMPLE NO.	RUN NO.		INTEGRATED NEUTRON FLUX (neutrons/cm^2)	DIFFUSION LENGTH (microns) RIGHT CELL	DIFFUSION LENGTH (microns) LEFT CELL	DAMAGE CONSTANT K_L (neutrons^{-1}) RIGHT CELL	DAMAGE CONSTANT K_L (neutrons^{-1}) LEFT CELL
29	0		0.00	314	129		
p/n	1	F*	9.3×10^{9}	42.8	25.6	5.8×10^{-6}	1.57×10^{-5}
	2		3.63×10^{10}	21.3	19.6	6.04×10^{-6}	7.0×10^{-6}
	3		9.03×10^{10}	14.2	13.6	5.48×10^{-6}	5.93×10^{-6}
	4		3.96×10^{11}	7.08	7.08	4.79×10^{-6}	4.79×10^{-6}
30	0		0.00	505	413		
p/n	1	F	9.3×10^{9}	48.3	45.0	4.57×10^{-6}	4.53×10^{-6}
	2		3.63×10^{10}	21.8	19.9	6.06×10^{-6}	6.94×10^{-6}
	3		9.03×10^{10}	13.5	12.8	6.03×10^{-6}	6.87×10^{-6}
	4		3.96×10^{11}	6.9	6.4	5.31×10^{-6}	6.16×10^{-6}
31	0	F	0.00	216	606		
p/n	1		9.3×10^{9}	40.8	47.8	4.95×10^{-6}	4.9×10^{-6}
	2		3.63×10^{10}	20.4	21.0	6.7×10^{-6}	6.26×10^{-6}
	3		9.03×10^{10}	13.4	14.2	6.16×10^{-6}	5.5×10^{-6}
	4		3.96×10^{11}	6.58	6.88	5.83×10^{-6}	5.35×10^{-6}
32	0		0.00	550	187		
p/n	1	F	9.3×10^{9}	37.2	33.4	7.74×10^{-6}	11×10^{-6}
	2		3.63×10^{10}	16.8	17.9	9.76×10^{-6}	8.6×10^{-6}
	3		9.03×10^{10}	11.1	12.4	9.15×10^{-6}	7.2×10^{-6}
	4		3.96×10^{11}	5.79	6.3	7.53×10^{-6}	6.36×10^{-6}
33	0		0.00	362	259		
p/n	1	M*	9.9×10^{9}	49.3	45.6	4.09×10^{-6}	4.71×10^{-6}
	2		4.79×10^{10}	22.5	21.0	4.13×10^{-6}	4.74×10^{-6}
	3		1.25×10^{11}	14.0	13.3	4.08×10^{-6}	4.53×10^{-6}
	4		4.15×10^{11}	7.76	7.45	4.01×10^{-6}	4.34×10^{-6}
34	0		0.00	284	259		
p/n	1	M	9.9×10^{9}	49.9	48.9	3.95×10^{-6}	4.07×10^{-6}
	2		4.79×10^{10}	20.2	20.2	5.1×10^{-6}	5.1×10^{-6}
	3		1.25×10^{11}	12.8	12.8	4.81×10^{-6}	4.81×10^{-6}
	4		4.15×10^{11}	7.57	7.64	4.18×10^{-6}	4.12×10^{-6}
35	0		0.00	124	909		
p/n	1	M	9.9×10^{-9}	49.9	65.4	3.66×10^{-6}	2.33×10^{-6}
	2		4.79×10^{10}	21.4	22.8	4.43×10^{-6}	4.01×10^{-6}
	3		1.25×10^{11}	13.5	14.2	4.34×10^{-6}	3.97×10^{-6}
	4		4.15×10^{11}	7.63	8.19	4.15×10^{-6}	3.60×10^{-6}
36	0		0.00	189	193		
p/n	1	M	9.9×10^{9}	47.3	52.2	4.23×10^{-6}	3.43×10^{-6}
	2		4.79×10^{10}	18.0	19.6	6.37×10^{-6}	5.38×10^{-6}
	3		1.25×10^{11}	11.0	12.1	6.57×10^{-6}	5.44×10^{-6}
	4		4.15×10^{11}	6.63	7.26	5.5×10^{-6}	4.58×10^{-6}

* F denotes Fission Spectrum; M denotes Moderated Spectrum

SAMPLE NO.	RUN NO.		INTEGRATED NEUTRON FLUX (neutrons/cm^2)	DIFFUSION LENGTH (microns) RIGHT CELL	DIFFUSION LENGTH (microns) LEFT CELL	DAMAGE CONSTANT K_L (neutrons^{-1}) RIGHT CELL	DAMAGE CONSTANT K_L (neutrons^{-1}) LEFT CELL
37	0			123	111		
	1	F	1.8×10^{10}	54.1	58.2	1.53×10^{-6}	1.28×10^{-6}
n/p	2		7.2×10^{10}	28.9	29.6	1.58×10^{-6}	1.47×10^{-6}
	3		2.16×10^{11}	15.7	17.2	1.85×10^{-6}	1.53×10^{-6}
	4		7.56×10^{11}	9.01	8.91	1.62×10^{-6}	1.65×10^{-6}
38	0		0	55.8	206		
	1	F	1.8×10^{10}	32.0	64.4	3.72×10^{-6}	1.20×10^{-6}
n/p	2		7.2×10^{10}	18.6	34.4	3.58×10^{-6}	1.14×10^{-6}
	3		2.16×10^{11}	10.5	20.4	4.06×10^{-6}	1.36×10^{-6}
	4		7.56×10^{11}	5.64	9.56	4.1×10^{-6}	1.44×10^{-6}
39	0			142	233		
	1	F	1.8×10^{10}	57.4	73.3	1.42×10^{-6}	9.34×10^{-7}
n/p	2		7.2×10^{10}	31.1	35.9	1.36×10^{-6}	1.05×10^{-6}
	3		2.16×10^{10}	16.4	19.2	1.70×10^{-6}	1.25×10^{-6}
	4		7.56×10^{11}	8.29	9.09	1.59×10^{-6}	1.60×10^{-6}
40	0			186	222		
	1	F	1.8×10^{10}	65.8	75.1	1.12×10^{-6}	8.72×10^{-7}
n/p	2		7.2×10^{10}	32.6	35.0	1.25×10^{-6}	1.11×10^{-6}
	3		2.16×10^{11}	18.4	19.9	1.35×10^{-6}	1.27×10^{-6}
	4		7.56×10^{11}	8.65	9.09	1.77×10^{-6}	1.60×10^{-6}
41	0			111	36.0		
	1	M*	2.9×10^{10}	48.6	20.8	1.18×10^{-6}	5.35×10^{-6}
n/p	2		1.10×10^{11}	24.2	11.5	1.48×10^{-6}	6.17×10^{-6}
	3		3.50×10^{11}	14.8	7.27	1.28×10^{-6}	5.17×10^{-6}
	4		1.08×10^{12}	7.76	4.17	1.53×10^{-6}	5.25×10^{-6}
42	0			35.9	276		
	1	M	2.9×10^{10}	19.4	77.0	6.5×10^{-6}	5.38×10^{-7}
n/p	2		1.10×10^{11}	10.7	35.0	7.25×10^{-6}	6.58×10^{-7}
	3		3.50×10^{11}	6.22	18.9	7.15×10^{-6}	7.96×10^{-7}
	4		1.08×10^{12}	3.52	9.56	7.40×10^{-6}	1.00×10^{-6}
43	0			233	133		
	1	M	2.9×10^{10}	78.4	61.4	5.01×10^{-7}	8.55×10^{-7}
n/p	2		1.1×10^{11}	42.4	35.0	4.89×10^{-7}	6.91×10^{-7}
	3		3.50×10^{11}	19.9	17.3	7.14×10^{-7}	9.38×10^{-7}
	4		1.08×10^{12}	11.7	10.1	6.74×10^{-7}	9.02×10^{-7}
44	0	M	2	222	222		
	1		2.9×10^{10}	71.6	71.0	6.04×10^{-7}	6.18×10^{-7}
n/p	2		1.10×10^{11}	35.8	35.4	6.91×10^{-7}	7.08×10^{-7}
	3		3.50×10^{11}	18.8	18.1	8.03×10^{-7}	8.65×10^{-7}
	4		1.08×10^{12}	10.2	10.1	8.88×10^{-7}	9.06×10^{-7}

* F denotes Fission Spectrum; M denotes Moderated Spectrum

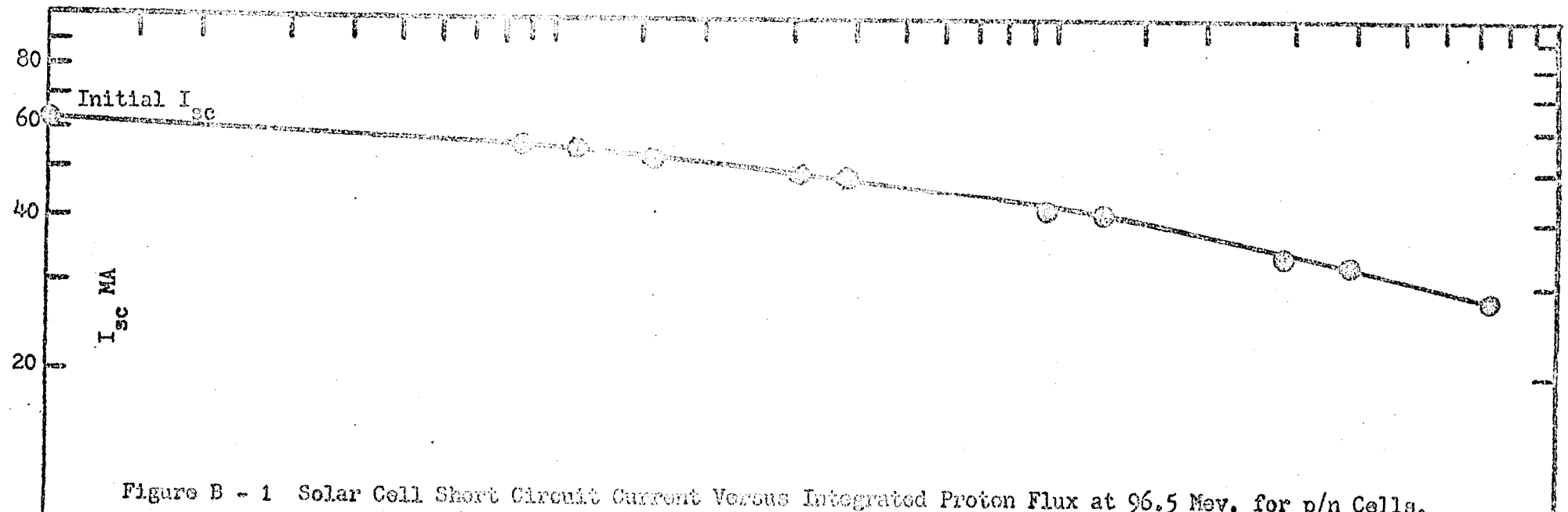

Figure B - 1 Solar Cell Short Circuit Current Versus Integrated Proton Flux at 96.5 Mev. for p/n Cells.

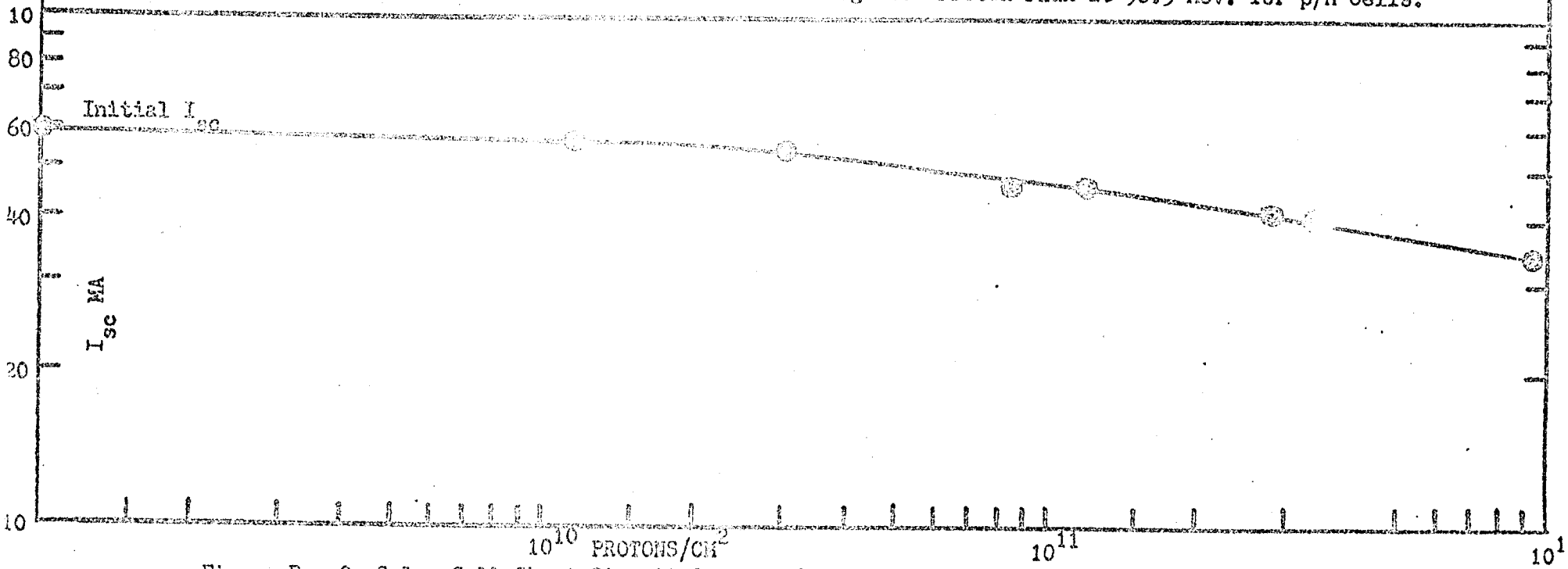

Figure B - 2 Solar Cell Short Circuit Current Versus Integrated Proton Flux at 96.5 Mev for n/p Cells

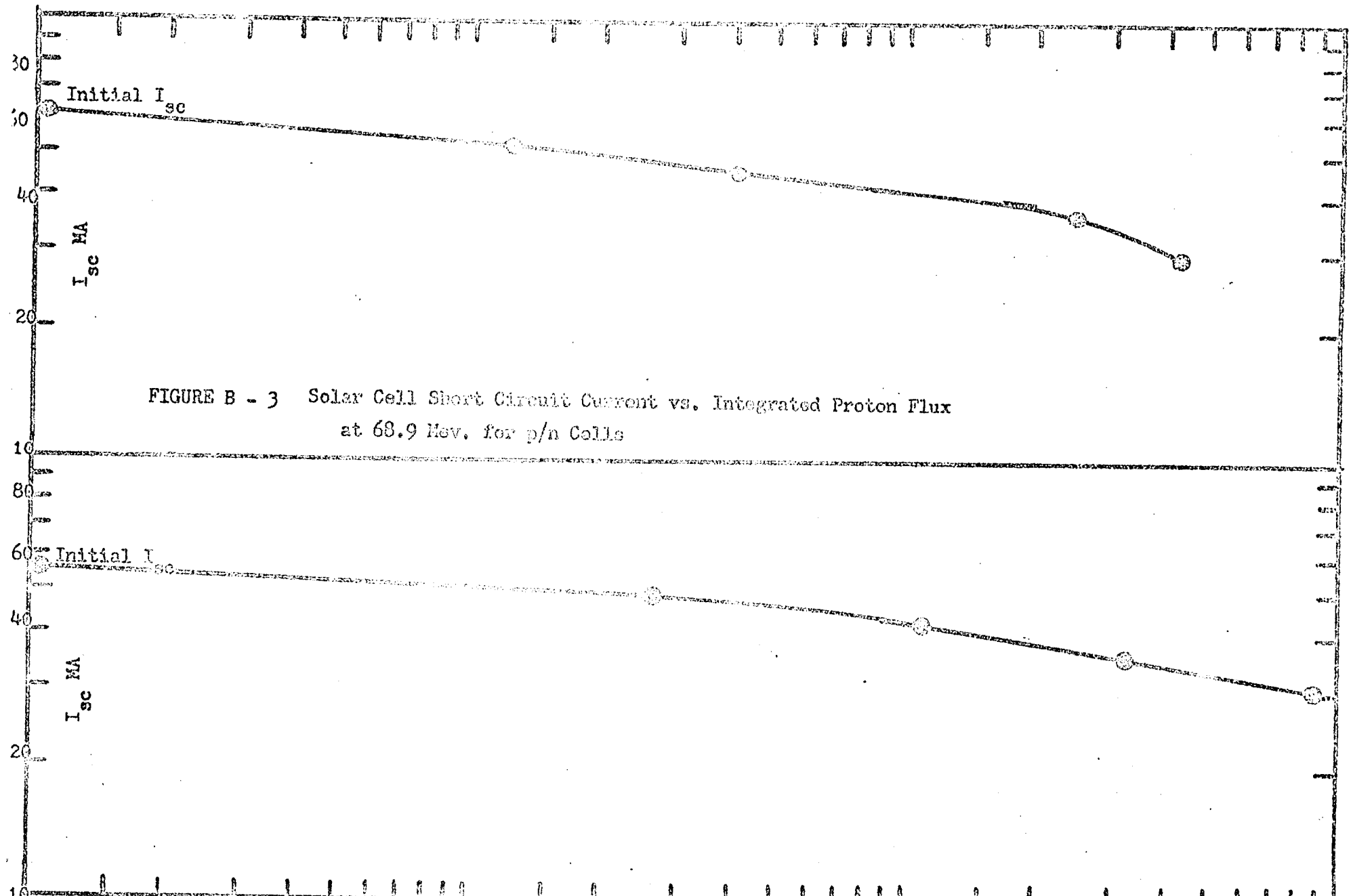

FIGURE B - 3 Solar Cell Short Circuit Current vs. Integrated Proton Flux at 68.9 Mev. for p/n Cells

FIGURE B - 4 Solar Cell Short Circuit Current Integrated Proton Flux at 68.9 Mev n/p Cells

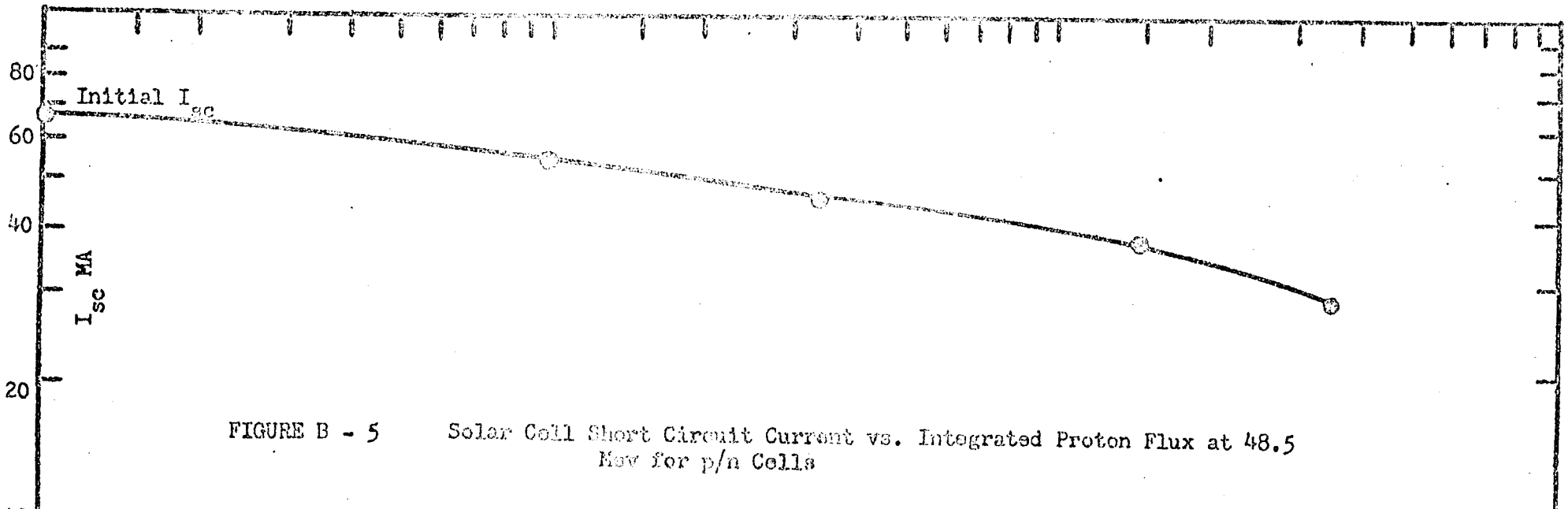

FIGURE B - 5 Solar Cell Short Circuit Current vs. Integrated Proton Flux at 48.5 Mev for p/n Cells

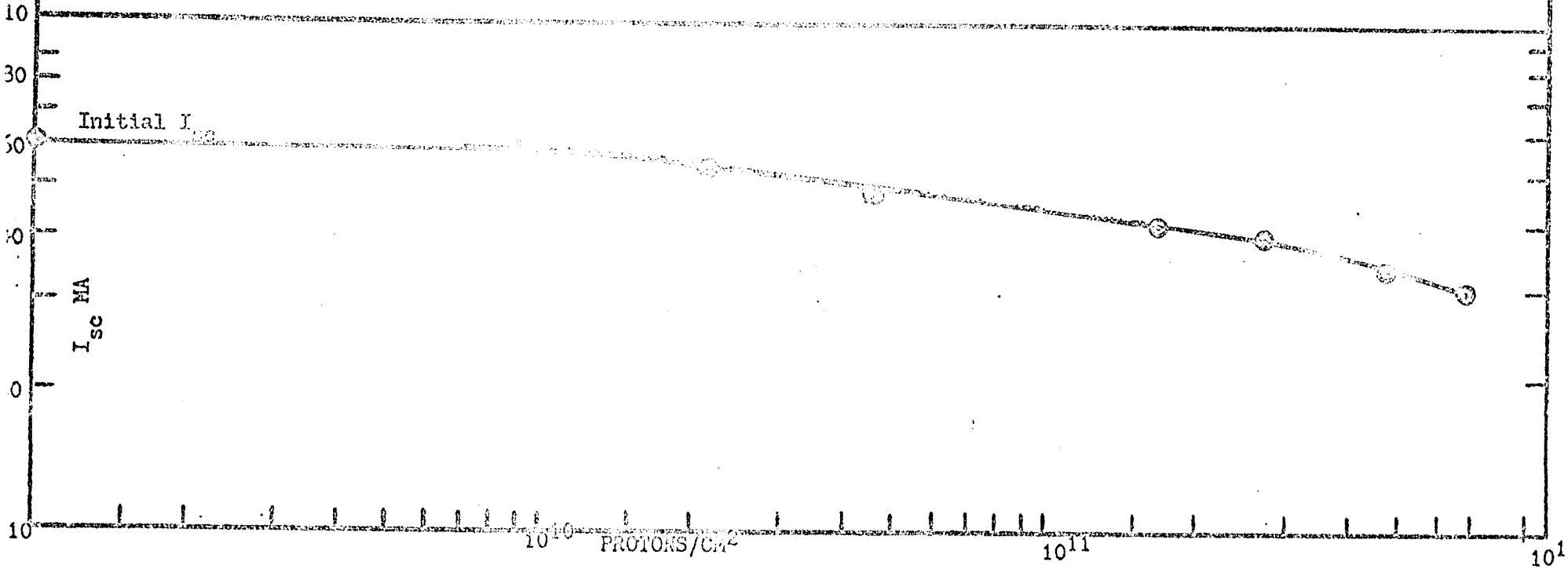

FIGURE B - 6 Solar Cell Short Circuit Current vs. Integrated Proton Flux at 48.5 Mev for n/p Cells

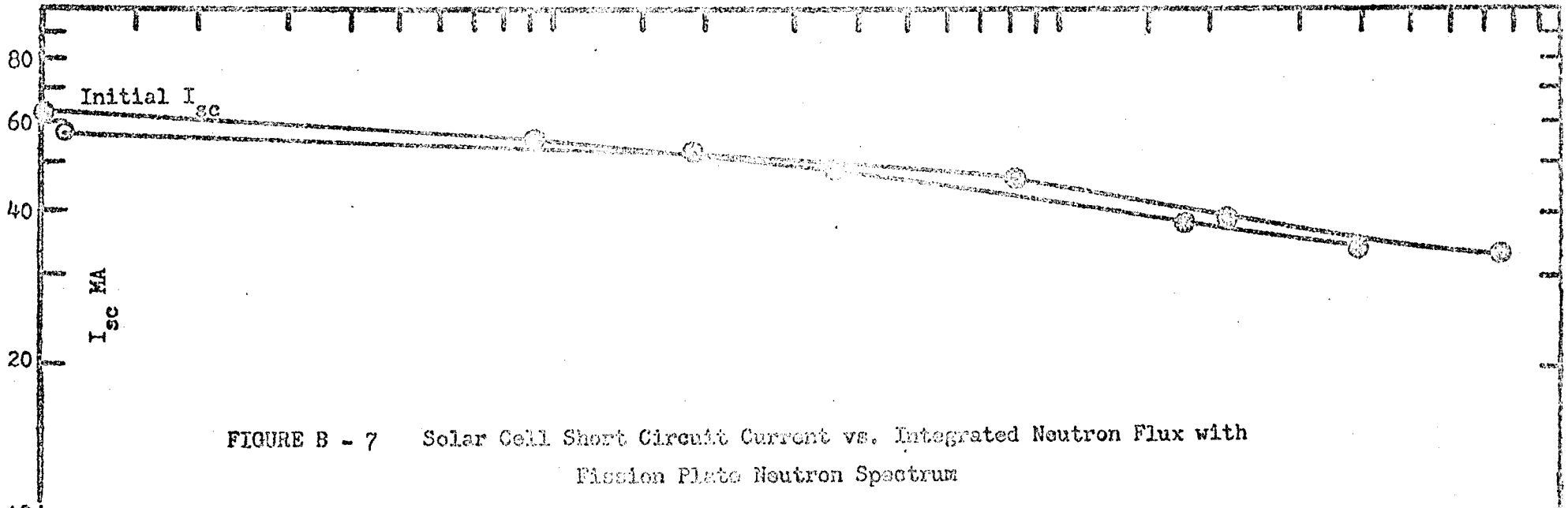

FIGURE B - 7 Solar Cell Short Circuit Current vs. Integrated Neutron Flux with Fission Plate Neutron Spectrum

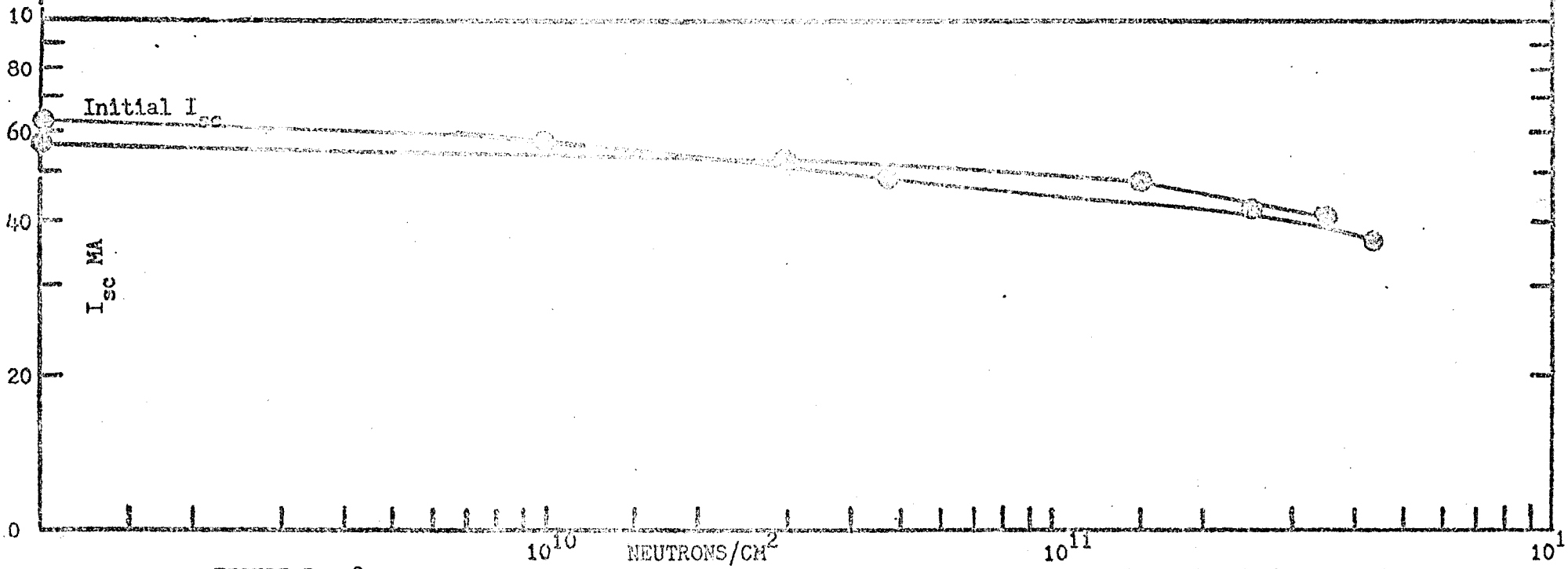

FIGURE B - 8 Solar Cells Short Circuit Current vs. Integrated Neutron Flux with Moderated Neutron Spectrum

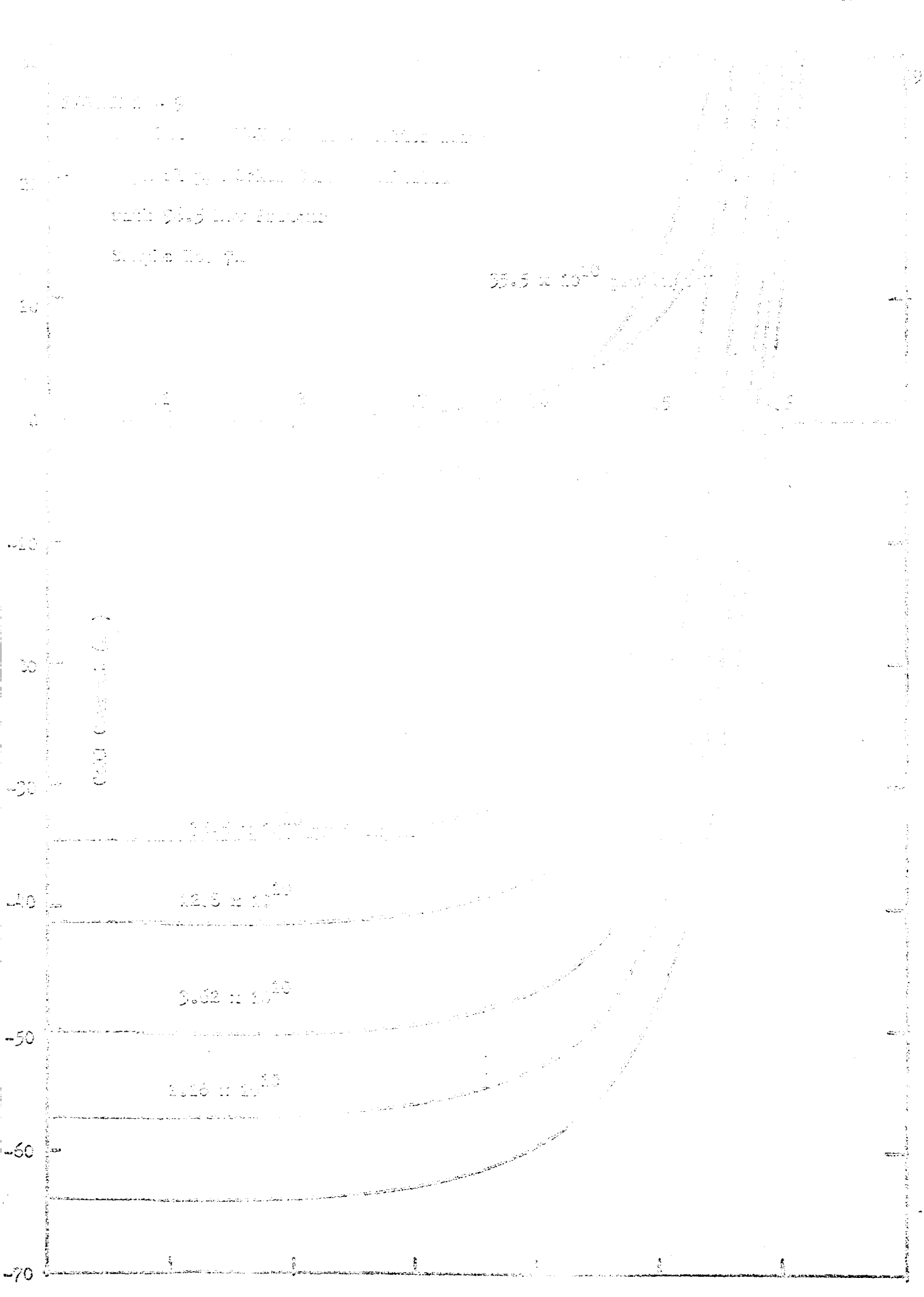
-10
-30
-40
-50
-60
-70

Figure B-10

Dark V-I Characteristics for a Typical Solar Cell Irradiated

Sample No. 7R

35.5×10^{10} proton/cm^2

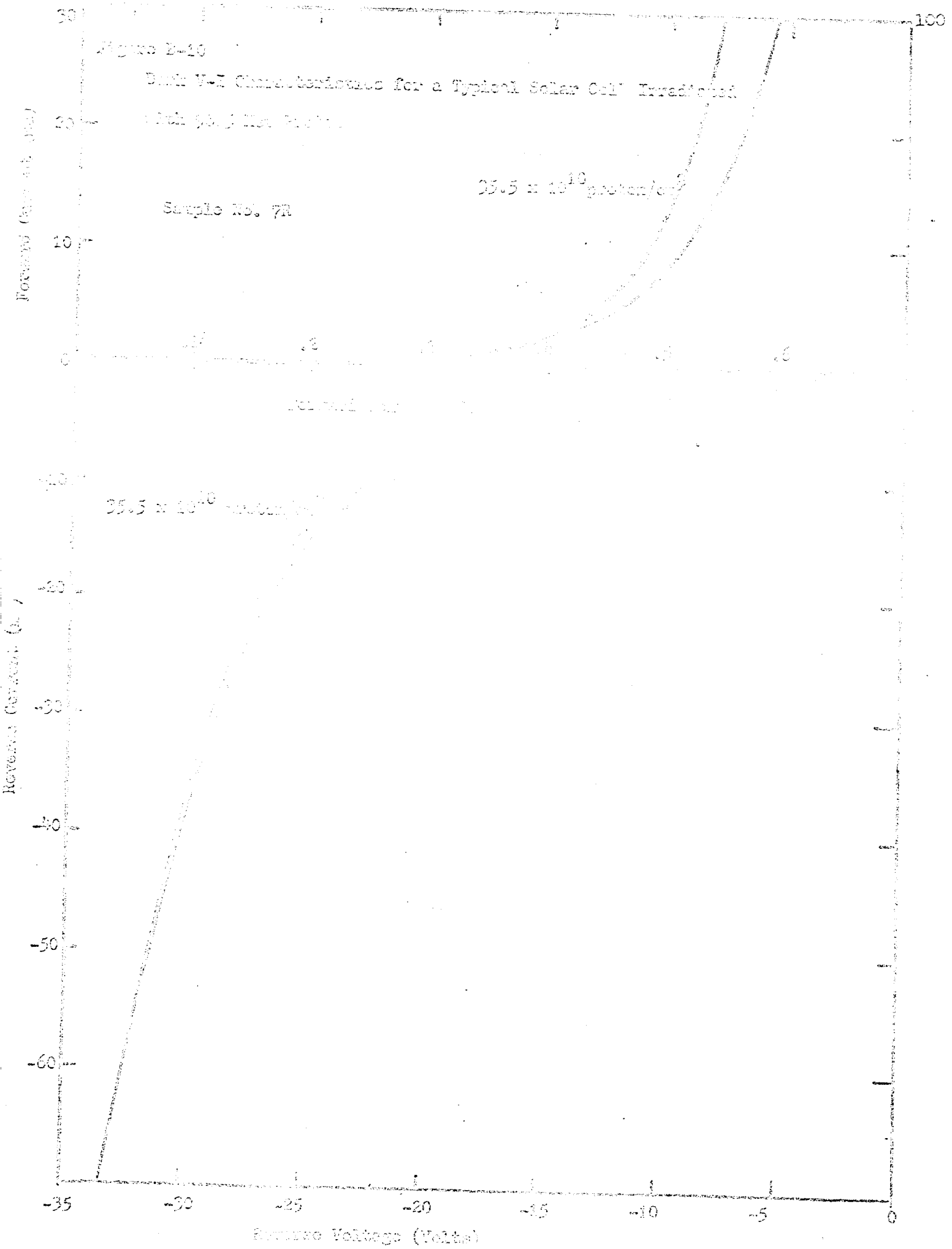

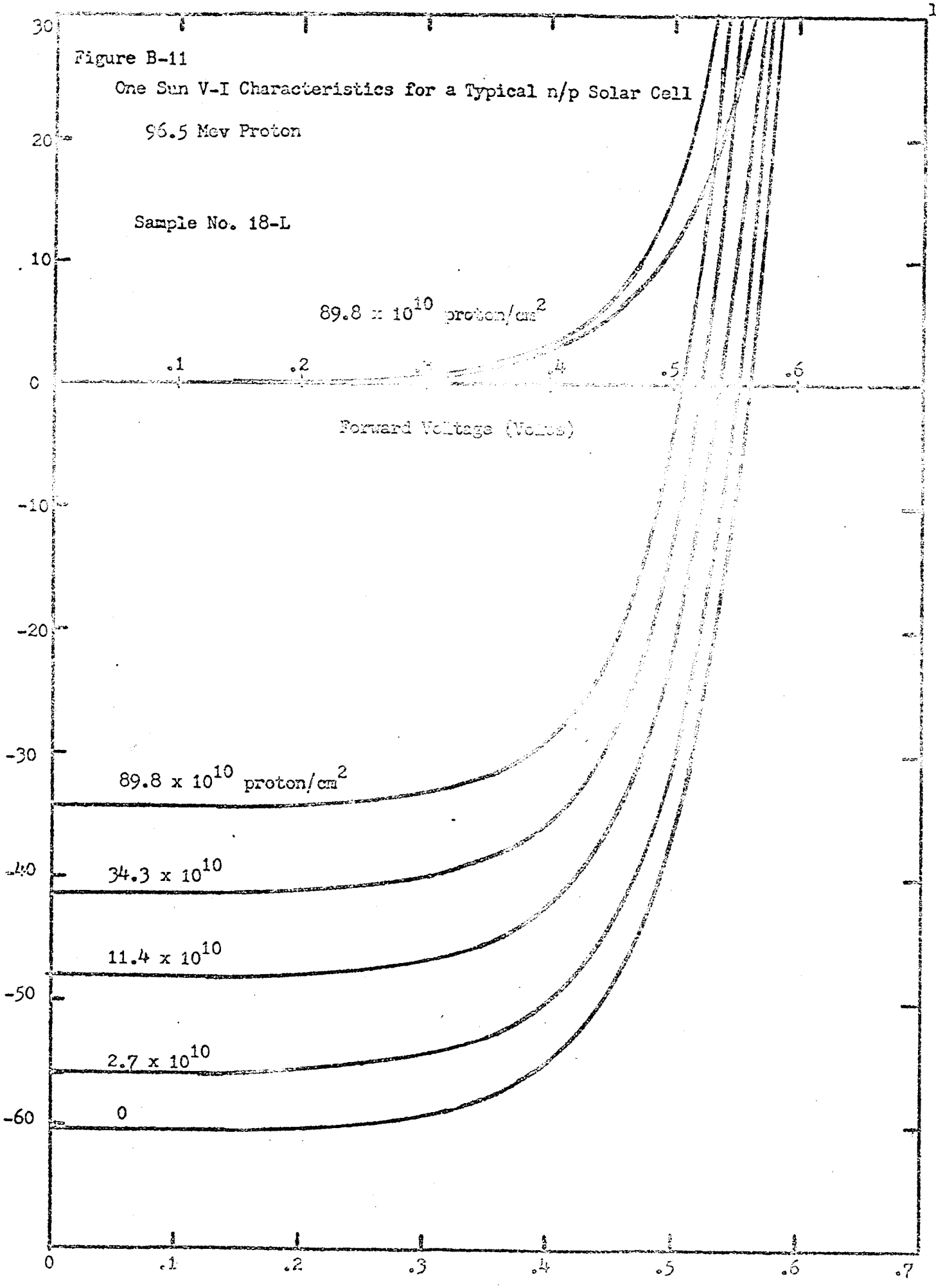
Figure B-11
One Sun V-I Characteristics for a Typical n/p Solar Cell
96.5 Mev Proton
Sample No. 18-L
89.8 x 10^10 proton/cm^2
Forward Voltage (Volts)
89.8 x 10^10 proton/cm^2
34.3 x 10^10
11.4 x 10^10
2.7 x 10^10
0
30
20
10
0
-10
-20
-30
-40
-50
-60
.1
.2
.3
.4
.5
.6
.7

Figure B-12

Dark V-I Characteristics for a Typical n/p Solar Cell

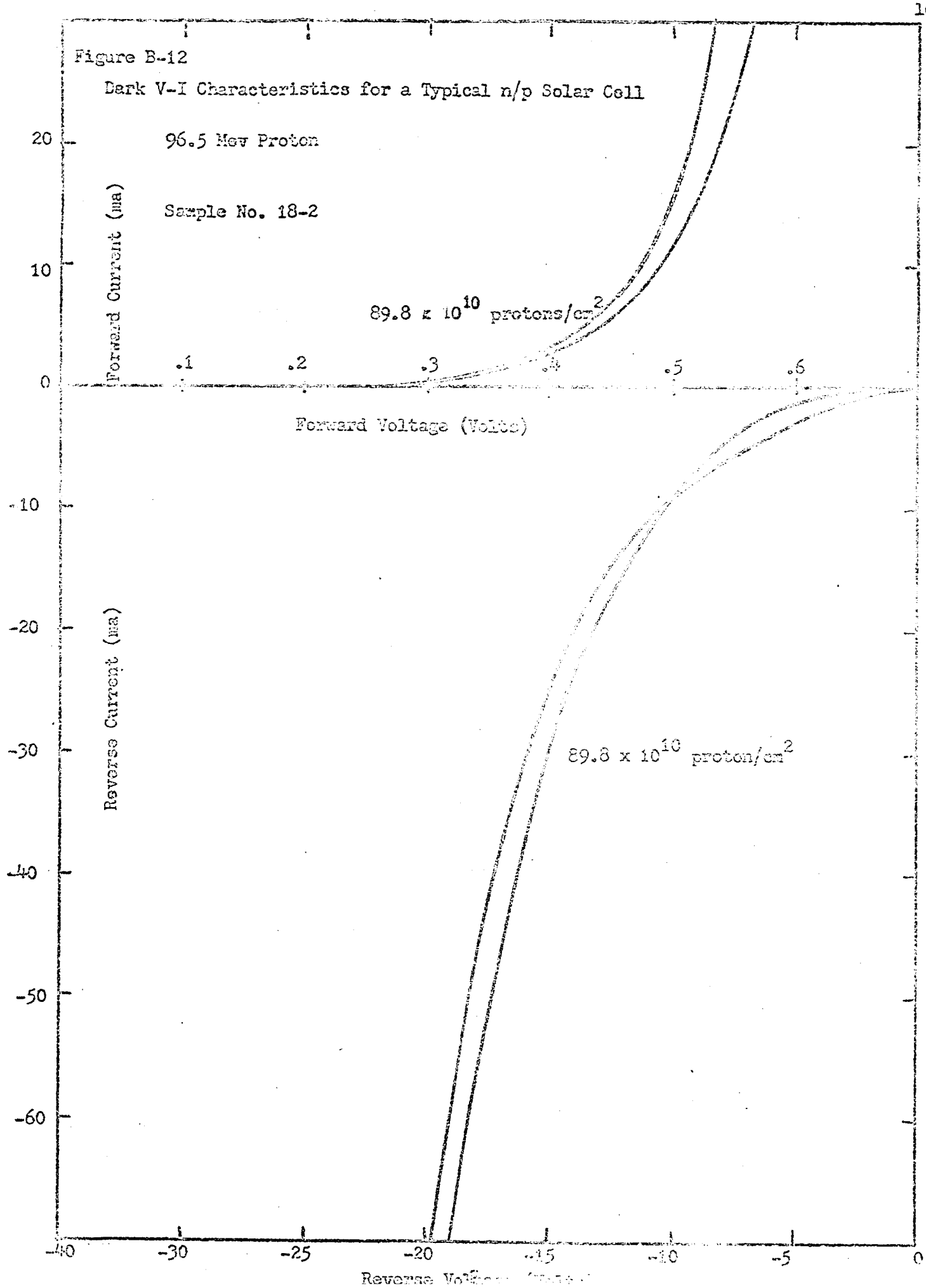

Figure B-13

One Sun V-I Characteristics for a Typical p/n Solar Cell Irradiated with a Fission Plate Neutron Spectrum

(Sample 30R)

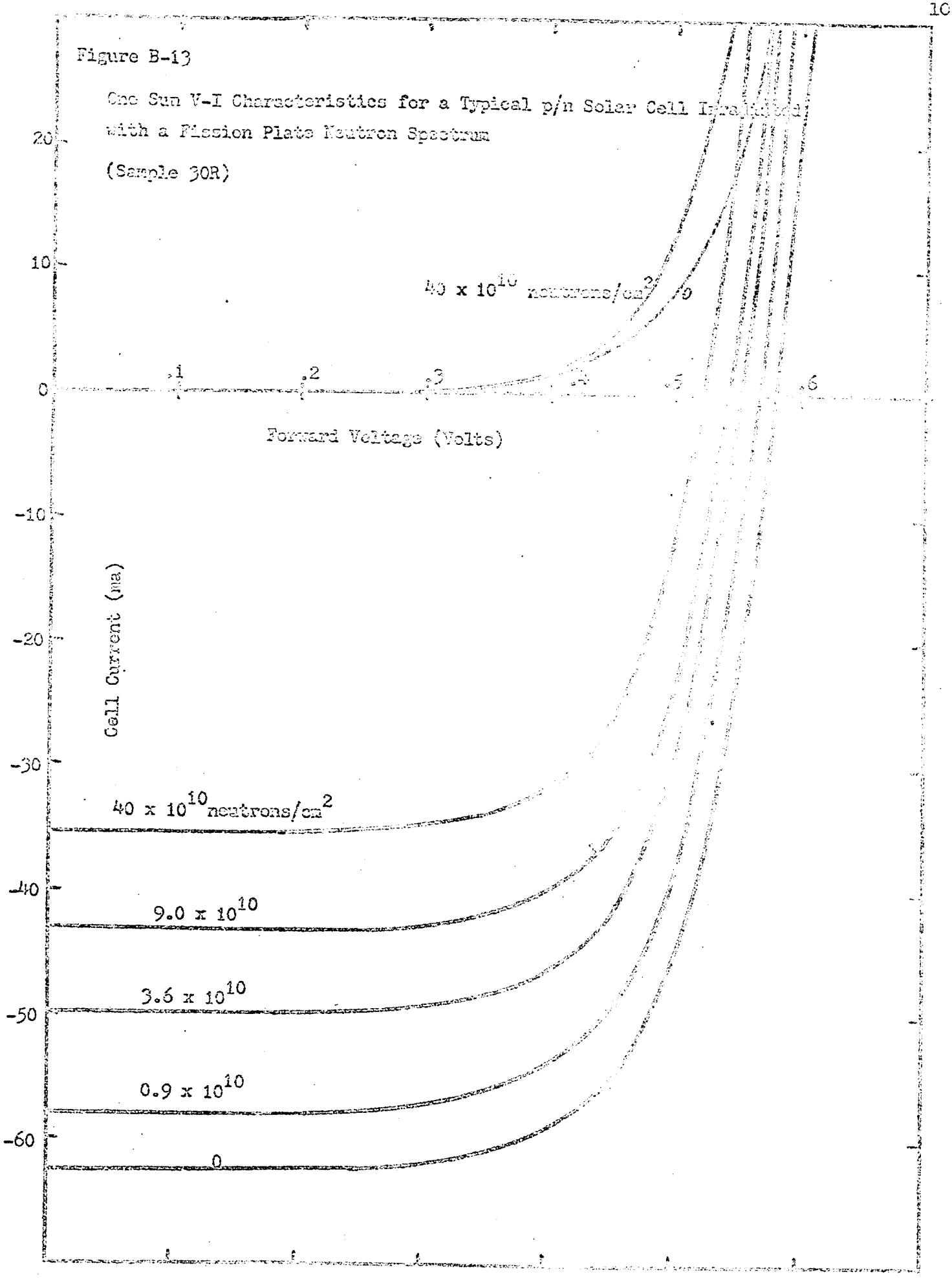

Figure B-14
Dark V-I Characteristics for a Typical p/n Solar Cell Irradiated with Fission Plate Neutron Spectrum

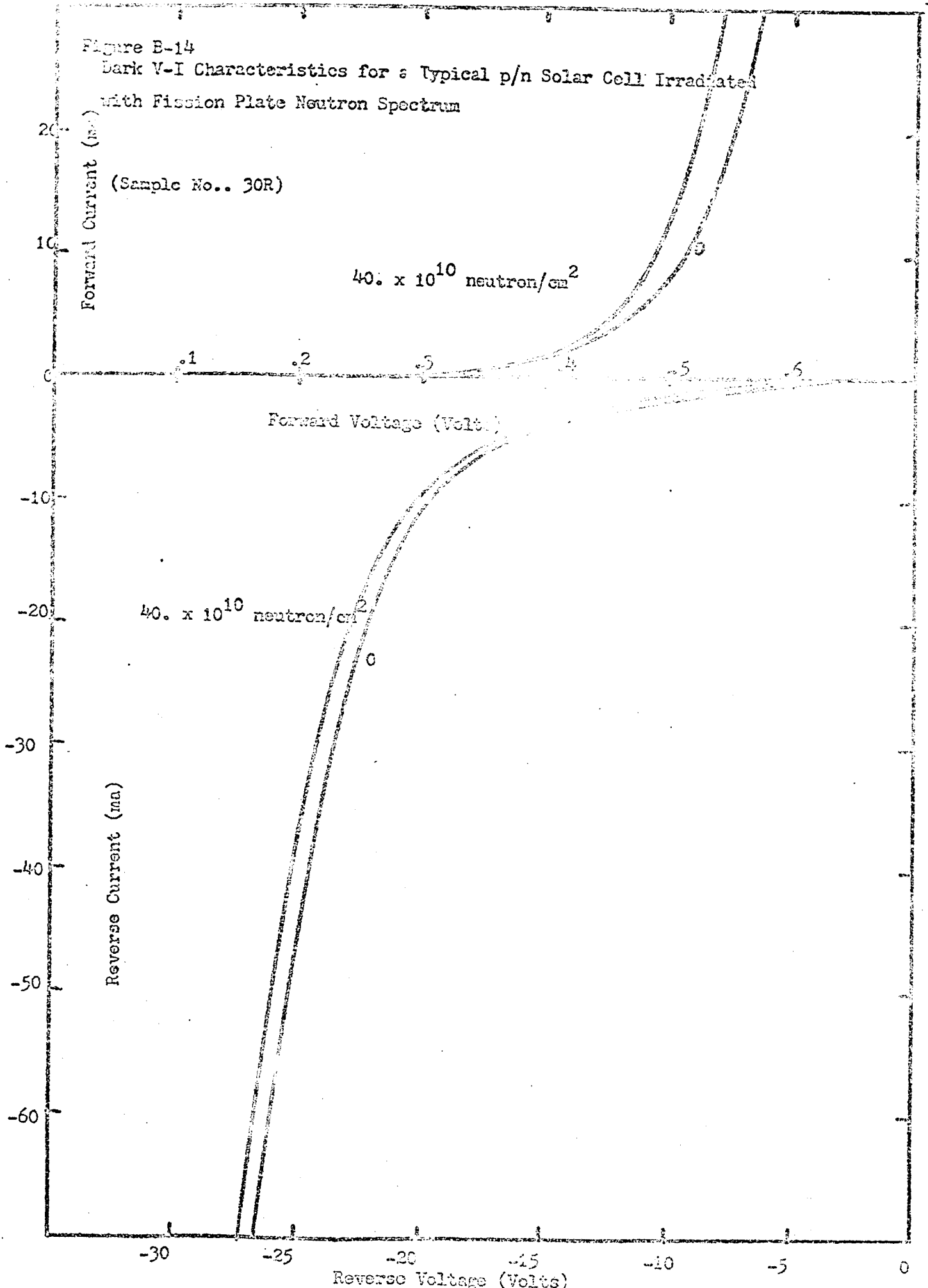

Figure B-15
One Sun V-I Characteristics for aTypical n/p Solar Cell
Irradiated with a Fission Plate Neutron Spectrum

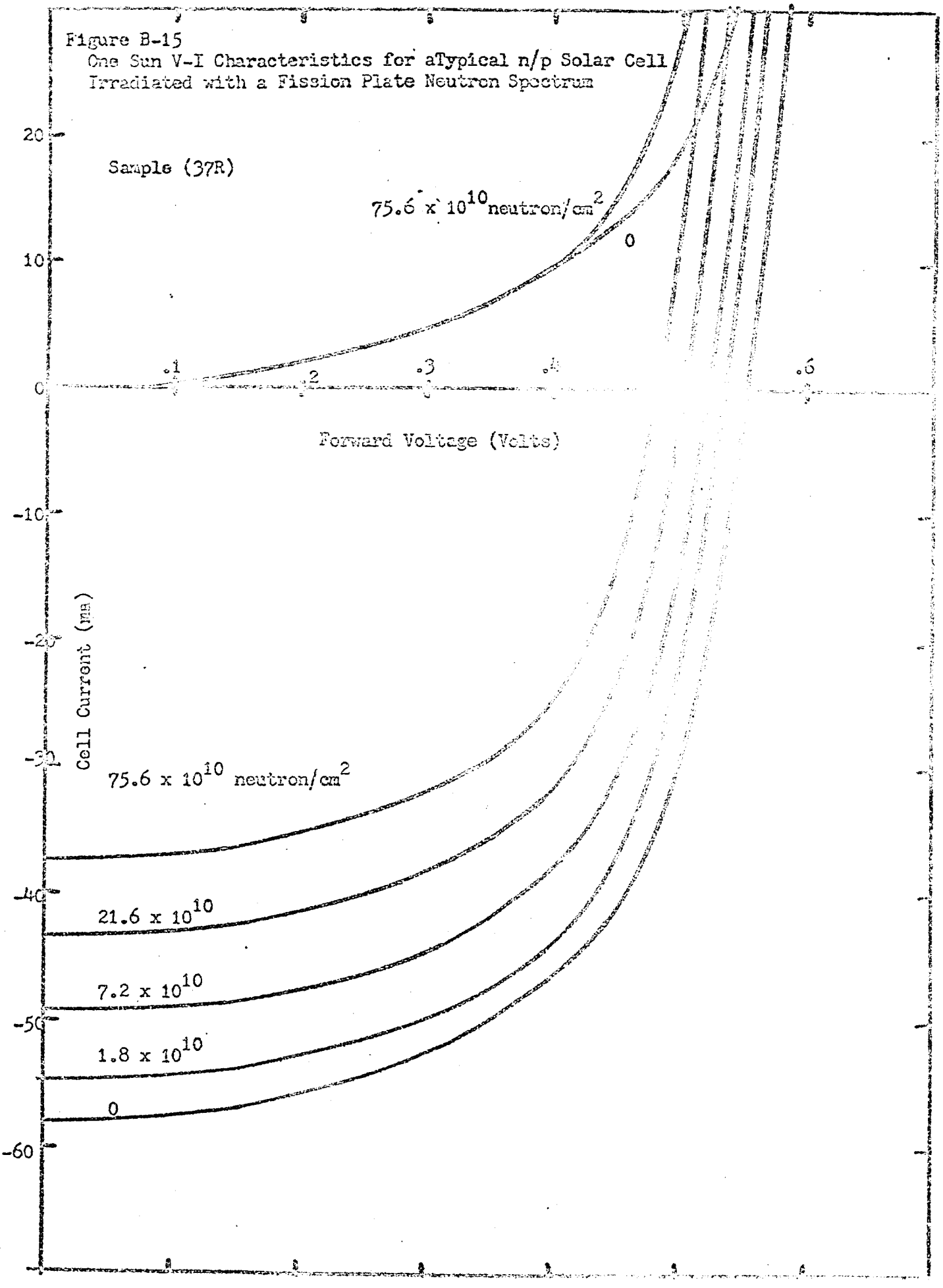

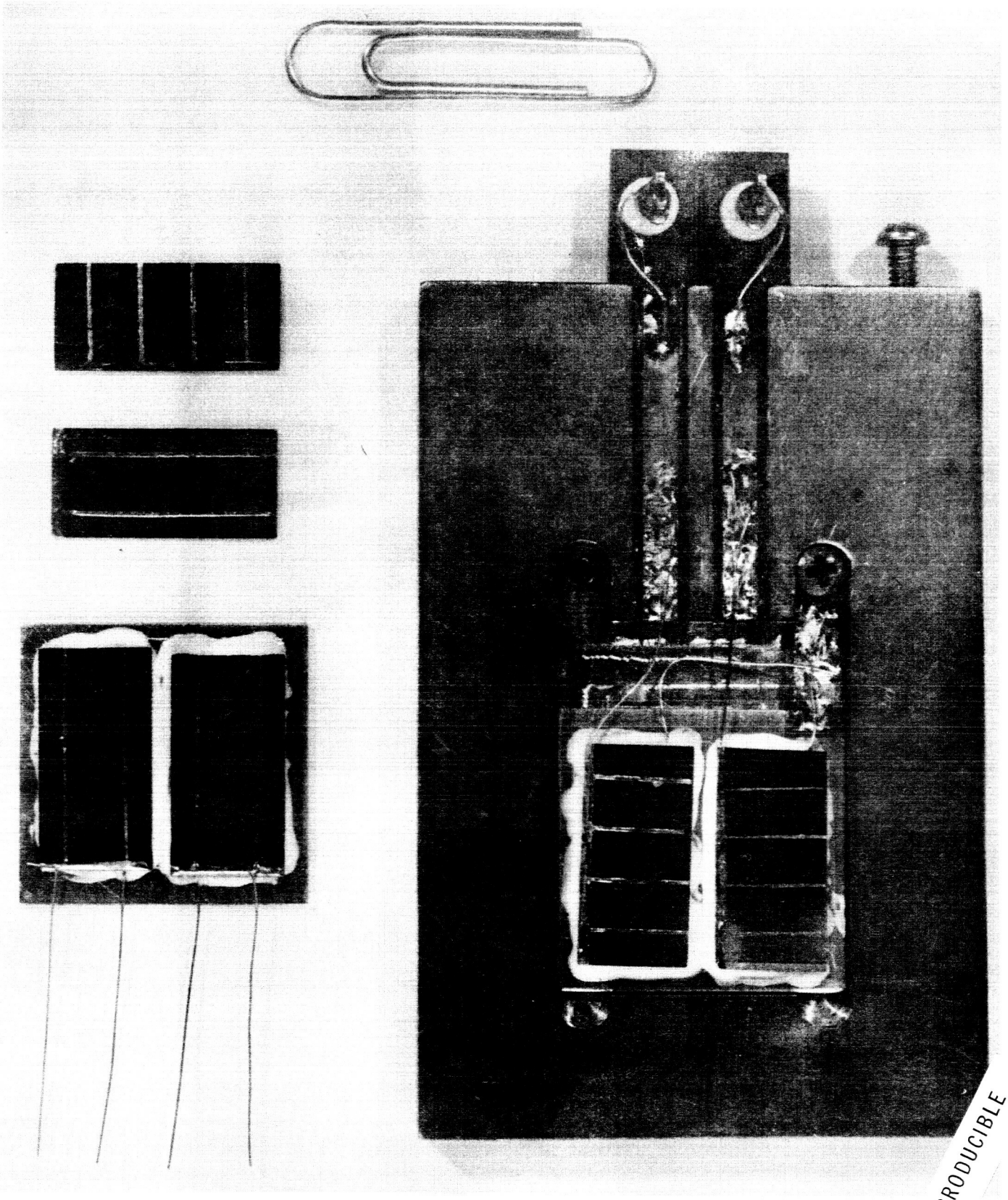

FIGURE 7. SOLAR CELLS AND MOUNTING HARDWARE

NOT REPRODUCIBLE

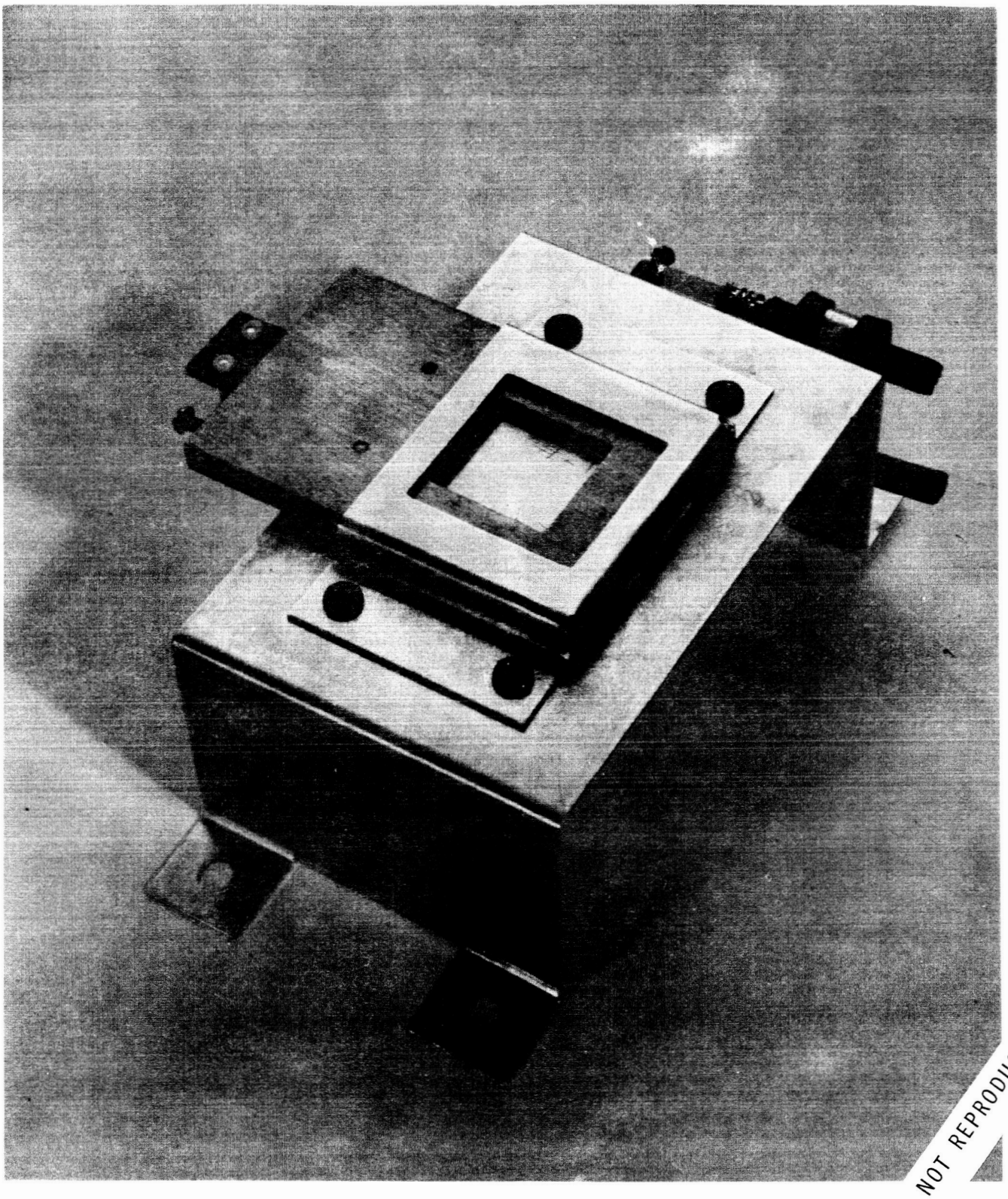

NOT REPRODUCIBLE

FIGURE 9. SAMPLE HOLDER FOR PROTON IRRADIATIONS

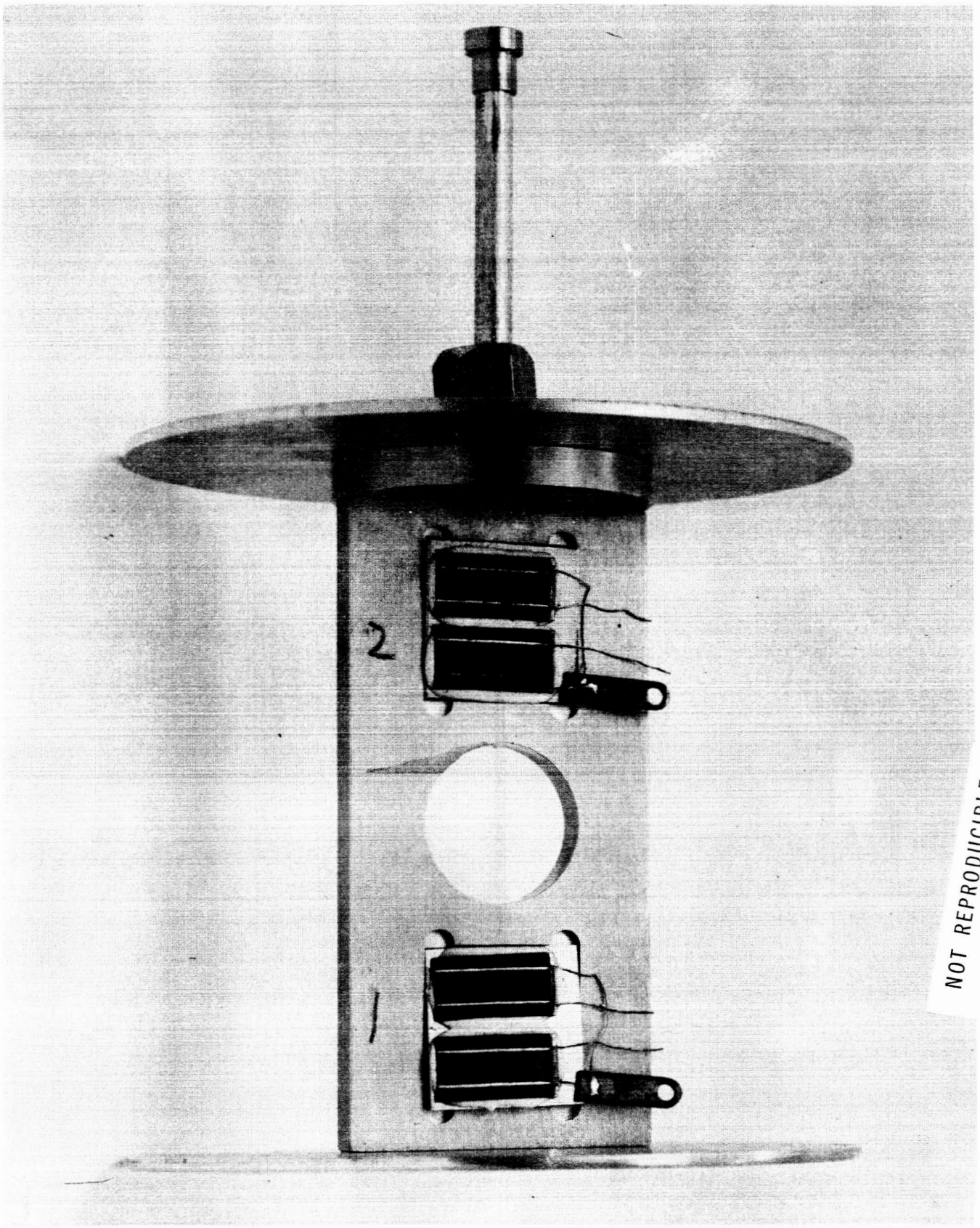

NOT REPRODUCIBLE

FIGURE 10. SAMPLE HOLDER FOR NEUTRON IRRADIATIONS

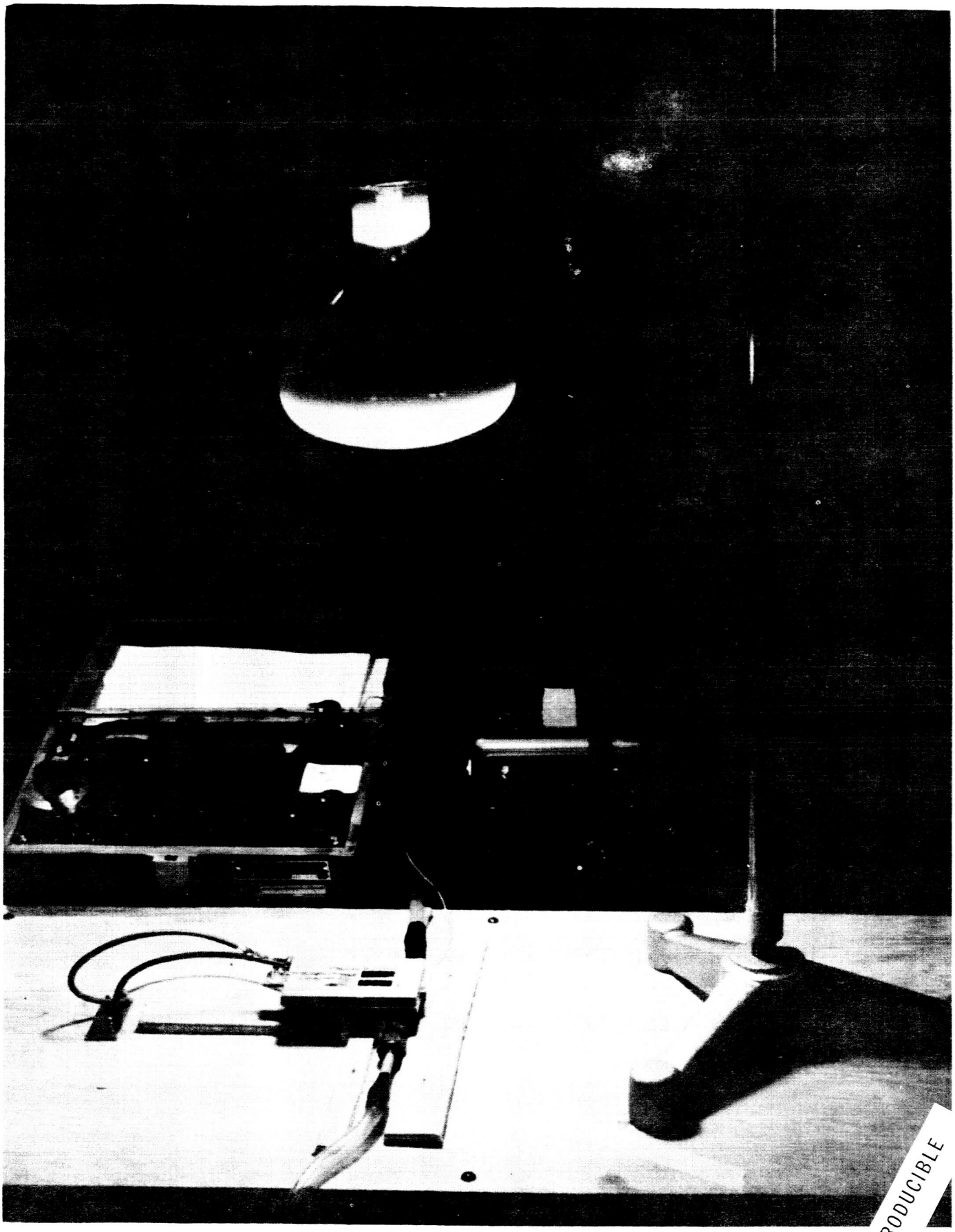

FIGURE 12. ONE SUN SOURCE

NOT REPRODUCIBLE

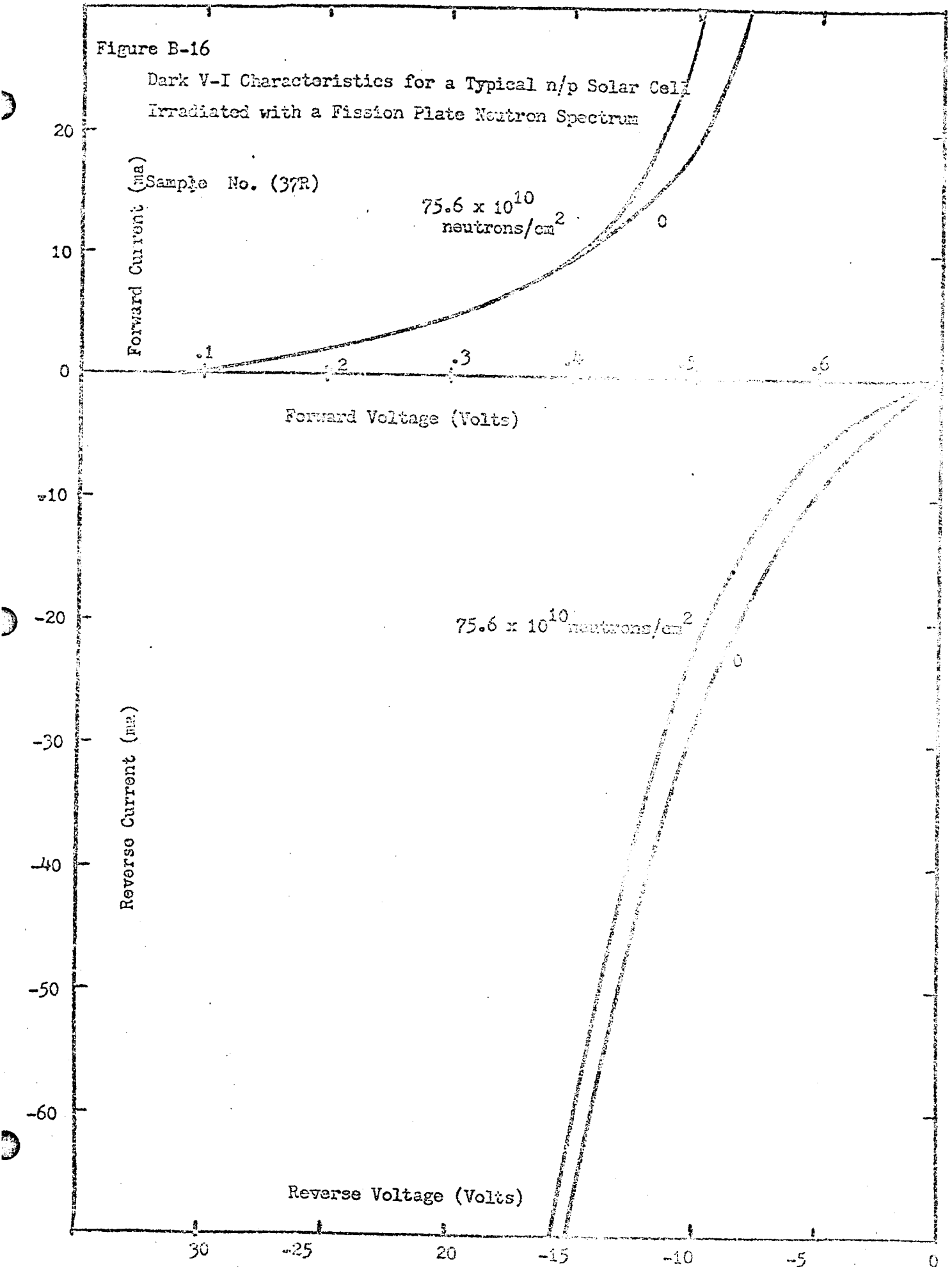

Figure B-16

Dark V-I Characteristics for a Typical n/p Solar Cell Irradiated with a Fission Plate Neutron Spectrum

Figure B-17

One Sun V-I Characteristics for a Typical p/n Solar Cell Irradiated with a Moderated Neutron Spectrum

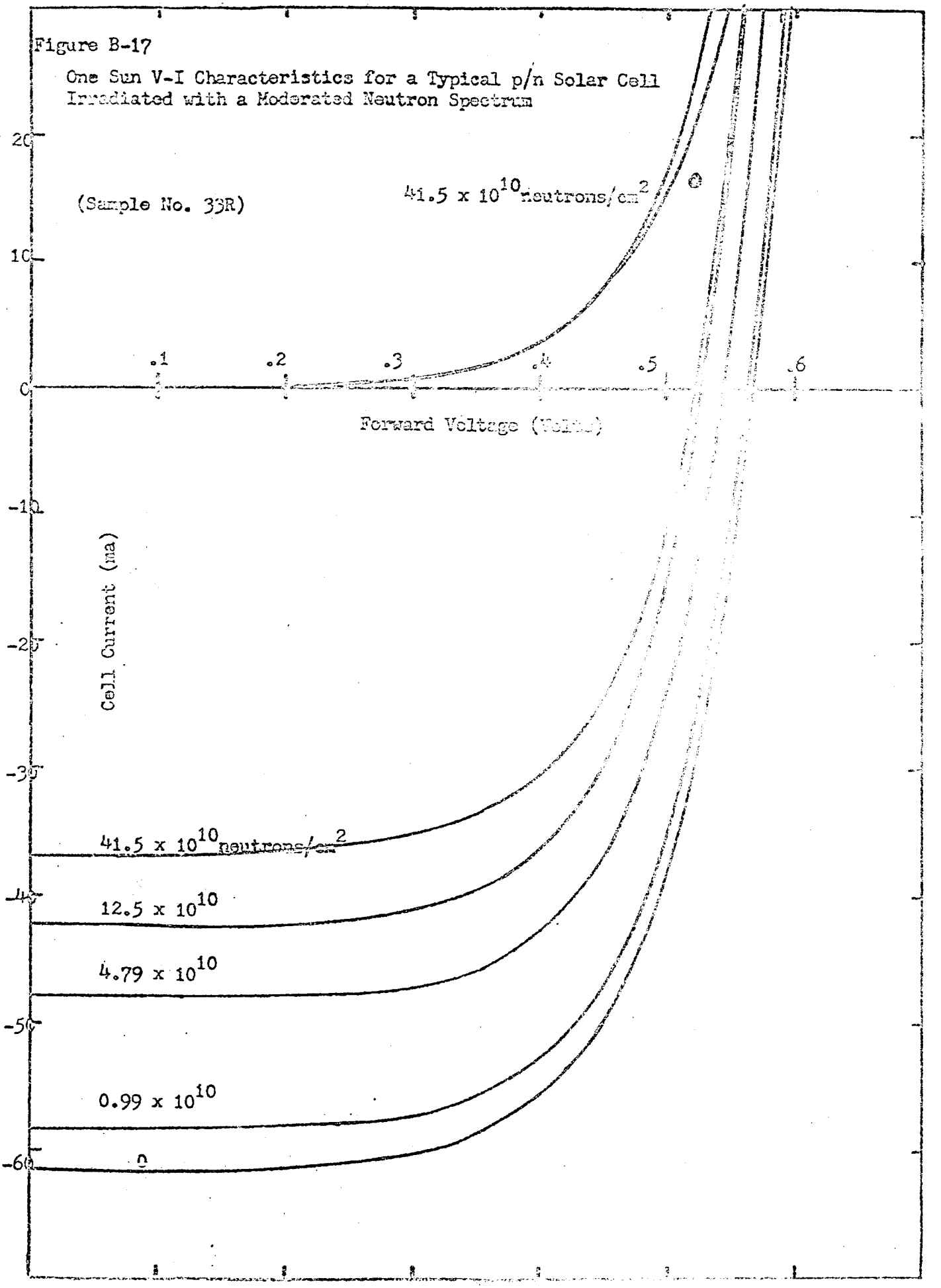

Figure B-18
Dark V-I Characteristics for a Typical p/n Solar Cell
Irradiated with a moderated neutron spectrum

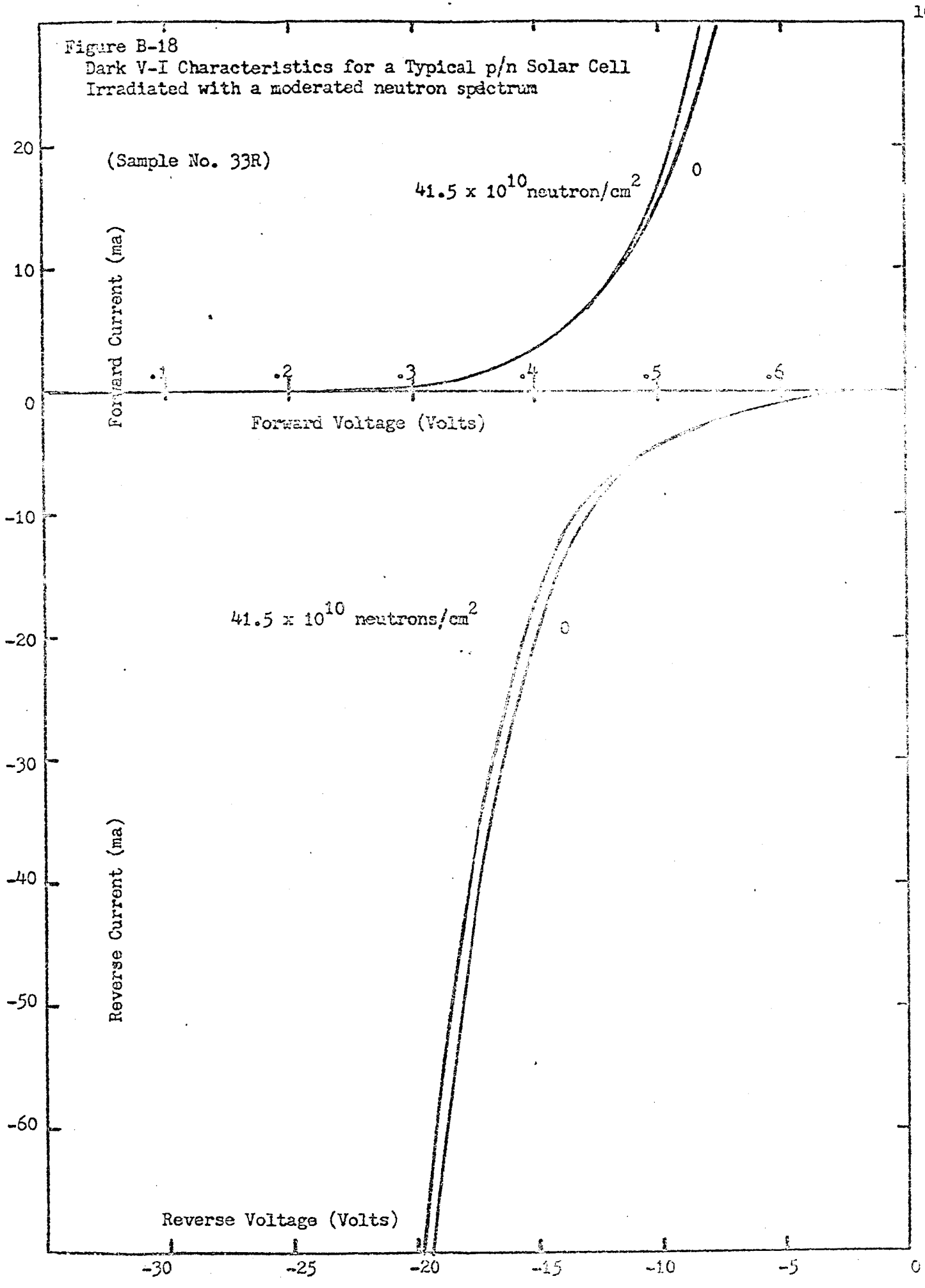

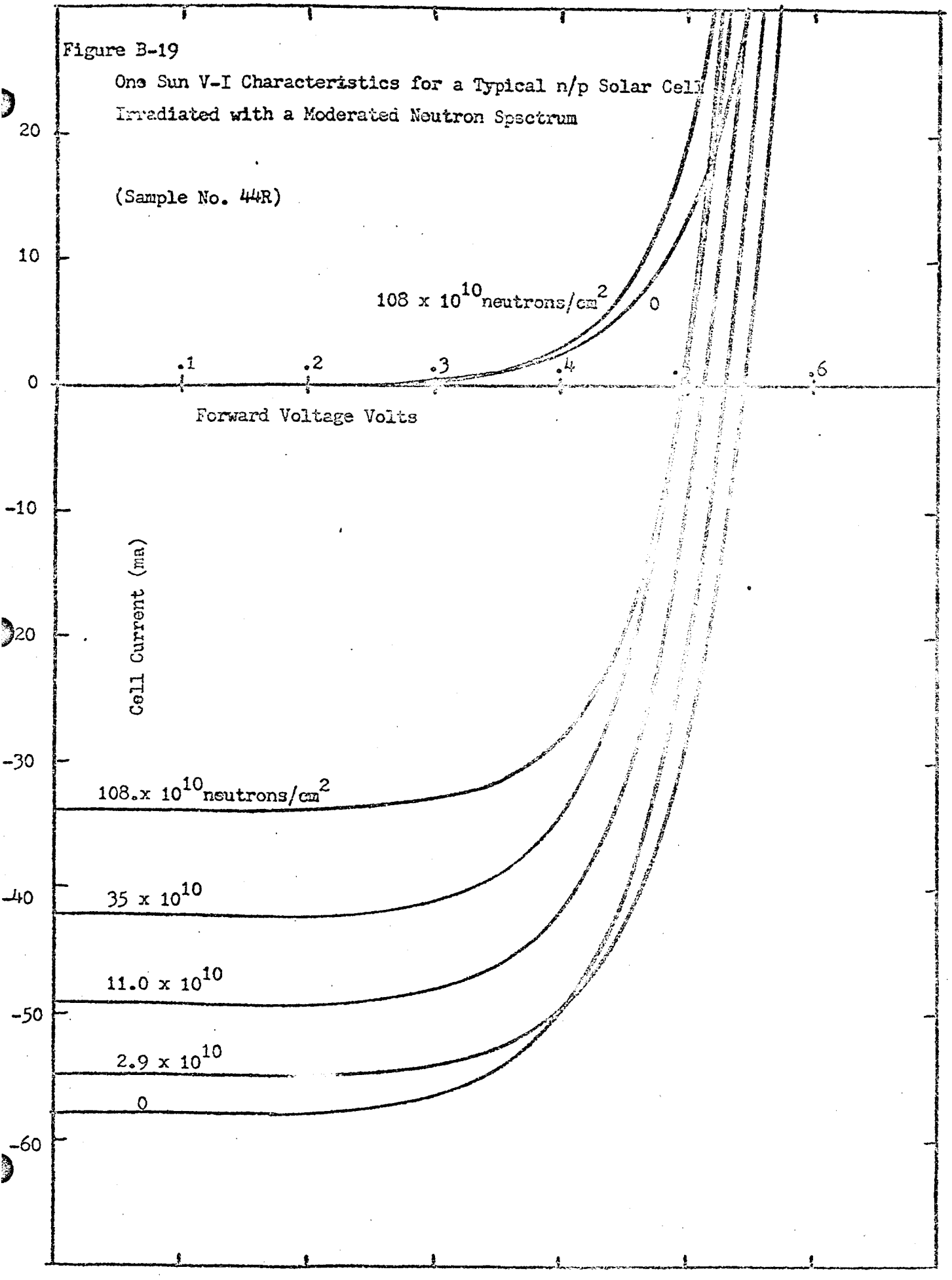
Figure B-19
One Sun V-I Characteristics for a Typical n/p Solar Cell
Irradiated with a Moderated Neutron Spectrum
(Sample No. 44R)
108 x 10^10 neutrons/cm^2
0
.1
.2
.3
.4
.5
.6
Forward Voltage Volts
Cell Current (ma)
20
10
0
-10
-20
-30
-40
-50
-60
108.x 10^10 neutrons/cm^2
35 x 10^10
11.0 x 10^10
2.9 x 10^10
0

Figure B-20

Dark V-I Characteristics for a Typical n/p Solar Cell Irradiated with Moderated Neutron Spectrum

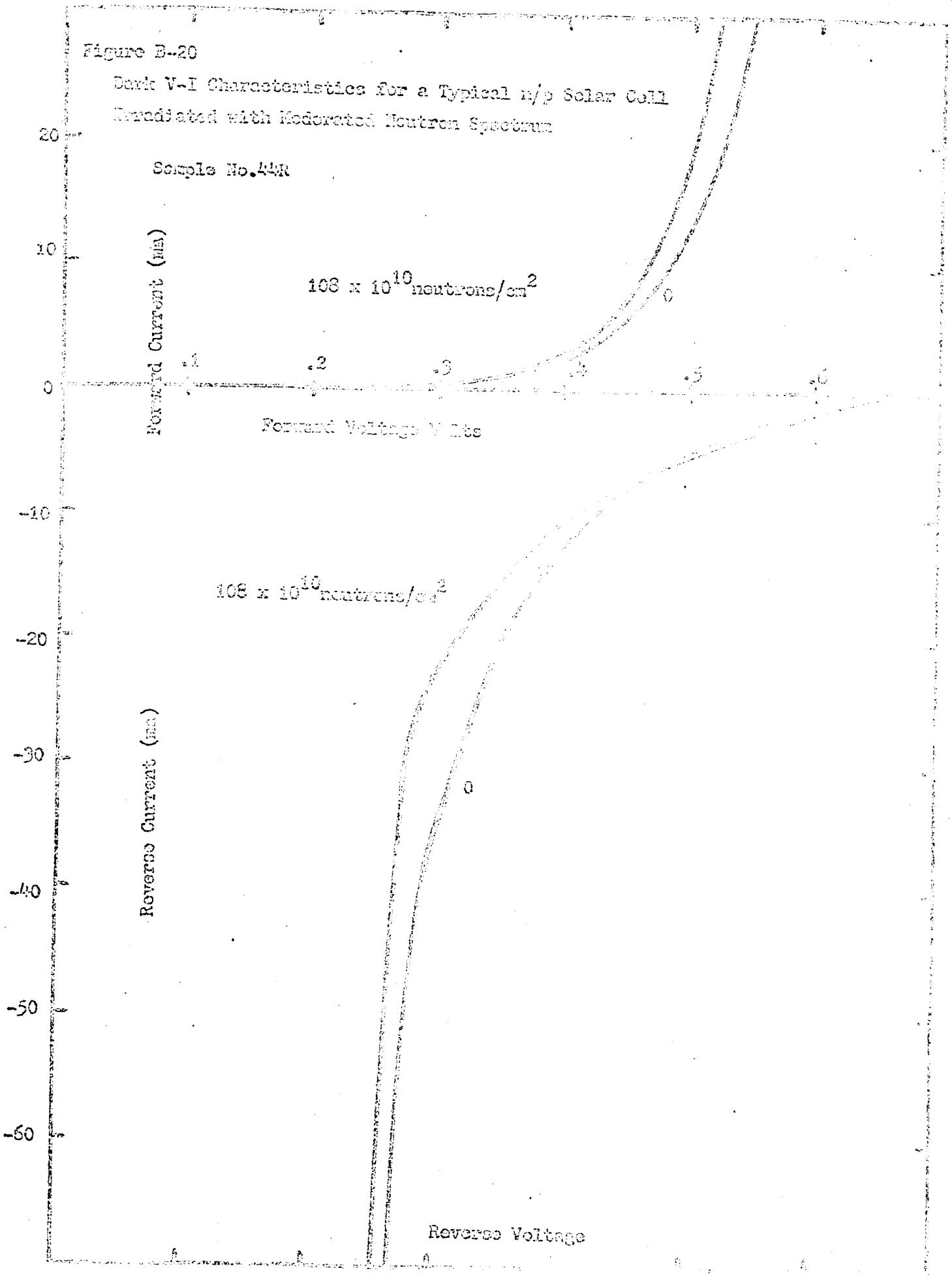

VIII. REFERENCES

A. REPORT REFERENCES

1. G. H. Kinchin and R. S. Pease, "The Displacement of Atoms in Solids by Radiation," Reports on Progress in Physics, Vol. 18, p. 1, (1955).

2. Dienes, G. J. and Vineyard, G. H., "Radiation Effects in Solids," Interscience Publishers, Inc.

3. Schreinler, H. C., "Theory of Particle [illegible] Nuclear Particle Detectors, Nuclear [illegible] Series, [illegible] 32, pp. 91-92.

4. Seitz, F. and Koehler, J. [illegible], "Displacement [illegible] Solid State Physics, Vol. 11, pp. [illegible].

5. Davies, J. A., et al, Canadian Journal [illegible] 1535 (1960); 39, pp. 601, 611 (1961); and [illegible]

6. Holmes, D. K., Robinson, M. T., and Oen, O. S., [illegible] of Energetic Atoms in Solids I Random Model," Paper [illegible], "Ranges of Energetic Atoms in Solids II Lattice Model," 1962 March meeting of the American Physical Society in Baltimore, Md., (Bull. Am. Phys. Soc. 7, 171 (1962), and private communication.

7. Bernski, G., "Paramagnetic Resonance in Electron Irradiated Silicon," J. App. Phys., Vol. 30, p. 1195 (1959).

8. Watkins, G. D., Corbett, J. W. and Walker, R. M., "Spin Resonance in Electron Irradiated Si," J. App. Phys., Vol. 30, p. [illegible] (1959).

9. Watkins, G.D. and Corbett, J.W., "Defects in Irradiated Silicon I Electron Spin Resonance of the SiA Center," Physical Review, Vol. 121, No. 4,

10. Corbett, J. W., Watkins, G. D., Chrenko, R. M., and McDonald, R. S., "Defects in Irradiated Silicon II Infrared Absorption of the Si-A Center," Physical Review, Vol. 121, No. 4, 1015-1022, February 15, 1961.

11. Klein, C. A., "Radiation-Induced Energy Levels in Silicons," Journal of Applied Physics, 30, 1222, (1959).

12. Delaney, J. A. and Beller, J. R., "Single Vacancy Migration in a Simple Cubic Lattice," Paper G-11, 9962 Annual Meeting of the American Physical Society in New York (Bull. Am. Phys. Soc. 7,28, (1952).

13. Wertheim, G. K., "Recombination Properties of Dependent Defects," J. App. Ph 30, 1166 (1959).

14. Watkins, G. D. and Corbett, J. W., "Electron Paramagnetic Resonance of Defects in Irradiated Silicon," General Electric Report [illegible] 2629E.

15. Brown, W. L., "Semiconductor Damage in Space," Nuclear Electronic Effects Program, Seventh Triannual Note, Bell Telephone Labs.

16. Borcher, J. A. and Fanghan, B. W., "Radiation Damage to Silicon Solar Cells," Contract NAS 5-457, RCA.

17. Wertheim, G. K., "Neutron Bombardment Damage in Silicon," Physical Review 111, 1500 (1958).

18. Cronemeyer, Physical Review, January 15, 1957.

19. Baicker, J. A., Abrahams, M., and Faughnan, B. W. "Radiation Damage to Silicon Solar Cells," RCA, Third Quarterly Report, Contract NAS 5-457, April 30, 1961.

20. Denney, J. M. and Downing, R. G., Final Report, "Charged Particle Radiation Damage in Semiconductors I: Experimental Proton Irradiation of Solar Cells," STL Report 8987-0001-RU-000, 15 September 1961.

21. "Radiation Damage to Silicon Solar Cells," RCA, Summary Report, Contract NAS 5-457, July 31, 1961

22. Brown, W. L., "Semiconductor Radiation Damage in Space," Nuclear Electronic Effects Program, Seventh Triannual Technical Note, Bell Telephone Laboratories.

23. Hulten, W. C., et. al., NASA, Langley Field, Virginia, Unpublished.

24. Loferski, J. J., "Analysis of the Effect of Nuclear Radiation on Transistors", J.A.P. Vol. 29, January 1958.

25. Moll, J. C., and Ross, I. M., "The Dependence of Transistor Parameters on the Distribution of Base Layer Resistivity", Proc. IRE, Vol. 44, January 1956.

26. Easley, J. W., and Dooley, J. A., "On the Neutron Bombardment Reduction of Transistor Current Gain," J. App. Phys., Vol. 31, No. 6, June, 1960 (1024-8).

27. Battelle Memorial Institute. Radiation Effects Information Center, Report No. 23, April, 1962.

28. Hulten, W. C., Wenaker, W. C., and Patterson, J. L., "Irradiation Effects of 22 and 240 Mev Protons on Several Transistors and Solar Cells," NASA Technical Note D-718.

29. Hulten, W. C., et al, Unpublished.

30. Messenger, G. C., and Spratt, J. P., "The Effects of Neutron Irradiation on Germanium and Silicon," Proc. IRE, Vol. 46, p. 1038 (1958).

31. Wertheim, G. K., "Neutron Bombardment Damage in Silicon," Bulletin of the American Physical Society, Vol. 3, No. 2, March, 1958.

32. Easley, J. W., "Comparison of Neutron Damage in Germanium and Silicon Transistors", Third Semi-Annual Radiation Effects Symposium, October 28-30, 1958, Lockheed Nuclear Products, Vol. 4.

33. Hicks, D. A., Keller, D. V., et al, "Radiation Damage to Transistors," Boeing Airplane Company Boeing Document D5-2380, December 1958.

34. Blair, R. R., "The Effects of Fast-Neutron Bombardment on Types 2N1675 and PT901 Silicon Power Transistors," Bell Telephone Laboratories, Inc., Nuclear Electronic Effects Program, Sixth Triannual Technical Note, 15 March 1961, pp. 89-118.

35. Sri Ram Kavipurapu, "Minority Carrier Lifetime Measurements in Neutron-Irradiated Silicon Diodes," Bell Telephone Laboratories Inc., Nuclear Electronic Effects Program, Sixth Triannual Technical Note, 15 March 1961, pp. 35-62.

36. Beck, R. W., Paskell, E.; and Peet, C. S. "Some Effects of Fast Neutron Irradiation on Carrier Lifetimes in Silicon", J. Appl. Phys., Vol. 30, Sept. 1959, (1437-1439).

37. Easley, J. W., and Dooley, J. A., "Irradiation of Germanium Alloy Transistors," AGET Symposium on Nuclear Radiation Effects on Semiconductor Devices and Materials, N.Y., February, 1957.

38. Curtis, O. L., "Effects of 14-Mev Neutron Irradiation Upon Carrier Lifetime and Germanium," Oak Ridge National Laboratory Solid State Division, Annual Progress Report for Period Ending August 31, 1958.

39. Curtis, Cleland, Crawford and Pigg, "Effect of Irradiation on the Hole Lifetime in n-Type Germanium," Bulletin of the American Physical Society, Vol. 3, No. 1, January 1958.

40. Curtis, O. L., and Cleland, J. W., "Investigation of Minority Carrier Recombination in Irradiated Germanium, Bulletin of APS.

41. XDC 59-8-228, Data Report and Analysis of Battelle Pool Mapping, by A. W. Casper, General Electric Co., Nuclear Materials and Propulsion Operation.

11. Denney, J. M., Downing, R. G., Lackman, S. R., and Oliver, J. W., "Estimate of Space Radiation Effects on Satellite Solar Cell Power Supplies," STL Report EM 10-21, MR-13, 20 October, 1961.

12. Brown, W. L., and Pearson, G. L., "Proton Radiation Damage in Silicon Solar Cells," WADD-TN-60-241, 15 July 1960,

13. Donnelly, M. M., "Van Allen Radiation Damage in Solar Cells," Nuclear Electronics Effects Program, Fifth Triannual Technical Note, Bell Telephone Laboratories.

14. Loferski, J. J., Rappaport, P., et al, "Radiation Damage to Silicon Solar Cells," RCA, First Quarterly Report, Contract NAS 5-457, October 31, 1960.

15. Loferski, J. J., Rappaport, P., et al, "Radiation Damage to Silicon Solar Cells," RCA, Second Quarterly Report, Contract NAS 5-457, January 31, 1961.

16. Czachor, A. and Piefoszewski, J., "Effect of Reactor Fast Neutrons on Electron-Hole Recombination in Germanium," J. App. Phys. Vol. 32, No. 10, October 1961.

17. Closser, W. H., "Drift Mobility in Neutron Irradiated n-type Germanium," J. App. Phys. Vol. 31, No. 2, February, 1960.

18. Curtis, O. L., and Cleland, J. W., "Monoenergetic Neutron Irradiation of Germanium," J. Appl. Phys. Vol. 31, No. 2, February, 1960.

19. Vavilov, V. S., Plotnikov, A. F., and Zakhvatkin, G. V., "Infrared Absorption of Silicon of High Resistivity Containing Radiation Defects," Soviet Physics Solid State, Vol. 1, No. 6, December, 1959.

B. General References

1. Walse, M. C., Physical Review 88, 1283; (1952); 949, (1956).

2. Rupprecht, G. and Klein, C. A., "Energy Levels in Neutron Irradiated n-Type Silicon," Phys. Rev. 116, 342 (1958).

3. Beeler, J. R. and McGurn, J. L., "Single Vacancy Migration in a Square Planar Lattice," Paper G-10, 1962 Annual Meeting of the American Physical Society in New York (Bull. Am. Phys. Soc. 7, 22 (1962).

4. Hem, F. S., and Segall, B., "Energy Bands in Periodic Lattices," Green's Function Method.

5. Besco, D. G. and Beeler, J. R., Paper [illegible] of the Dimensional BeO with Iodine," 1963 Annual Meeting of APS in New York City, (Bull. Am. Phys. Soc. 7, 52, (1962), and private communication.

6. Billington, D. S. and Crawford, J. H., "Irradiation Damage in Solids," Princeton University Press.

7. Troubetzkoy, E. S., "Fast Neutron Cross Section of Iron, Silicon, Aluminum, and Oxygen," Final Report covering period 17 December 1958 to 30 September 1959, NDA 2111-3, Volume C.

8. "Charged Particle Cross Sections Neon to Chromium," prepared by Los Alamos, LA-2424.

9. Loferski, J. J., and Wysocki, J. J., "Spectral Response of Photovoltaic Cells," RCA Review, Vol. XXIII, No. 1, March 1961.

10. Chow, K. T., and Lodi, E. A., "Proton Damage to Solar Cells," Lockheed Aircraft Corp. Technical Memorandum LMSD-703[illegible], July 1960.

20. Smits, F. M., Smith, K. D. and Brown, W. L., "Solar Cells for Communications Satellites in the Van Allen Belt," Brit. Inst. Rad. Engr. J., Vol. 22, August, 1961 (161-9).

21. Vavilov, V. S. and Plotnikov, A. F., "The Photoconductivity of Neutron Irradiated P-Type Silicon," Soviet Physics - Solid State, Vol. 3, No. 8, February, 1962 (1783-4).

22. Konoplova, R. F., Mashovets, T. V. and Ryvkin, S. M., "The Effect of Defects Produced by Neutron Irradiation on the Process of Recombination in Germanium," Fiz. tverdogo Tela, Sbornik (Supplement) II, 1959 (11-12).

23. Buras, B. and Suwalski, J., "In-pile Hall Coefficient Measurements of Germanium Bombarded by Fast Neutrons," Acta. Phys. Polon, Vol. 19, No. 1, 1960 (15-18).

24. Easley, J. W. and Blari, R. R., "Fast Neutron Bombardment of Germanium and Silicon Esaki Diodes," J. Appl. Phys. Vol. 31, No. 10, October, 1960. (1772-4).

25. Vavilov, V. S., Patskevich, V. M., B. Ya. and Glazunov, P. Ya.," The Effects of Bombardment with High Energy Electrons on the Electrical Conductivity of Silicon and the Dependence of the Rate of the Defect Formation on the Orientation of the Crystal with Reference to the Electron Beam.," Soviet Physics - Solid State, Vol. 2, No. 7, January, 1961.

26. Yurkov, B. Ya., "The Dependence of the Number of Radiation Defects in Silicon on the Initial Electron Energy," Soviet Physics - Solid State Vol. 2, No. 11, May, 1961 (2412-14).

27. Galkin, G. N., Rytova, N. S., Vavilov, V. S., "Volume Recombination of Carriers in N-Type Silicon Containing Radiation Defects," Soviet Phys. - Solid State, Vol. 2 No. 9, March, 1961 (1819-23).

28. Binder, D., "Effect of Fission Spectrum Neutrons on N-Type Germanium," Phys. Rev., Vol. 122, No. 14, May 15, 1961. (1147-8).

29. Ruby, S. L., Schupp, F. D., Wolley, E. D., "Effect of Monoenergetic Fast Neutrons on N-Type Germanium," Phys. Rev., Vol. 111, No. 6, September 15, 1958. (1493-6).

30. Wertheim, G. K., "Neutron Bombardment Damage in Silicon," Phys. Rev. Vol. 111, No. 6, September 15, 1958. (1500-5).

31. Vook, F. L. and Balluffi, R. W., "Length and Resistivity Changes in Germanium Upon Low Temperature Deuteron Irradiation and Annealing," Phys. Rev., Vol. 113, No. 1, January 1, 1959 (68-9).

32. Simmons, R. O., "Lattice Parameter Changes in Deuteron Irradiated Germanium," Phys. Rev., Vol. 113, No. 1, January 1, 1959(70-1).

33. Vook, F. L., and Balluffi, R. W., "Structure of Deuteron Irradiated Germanium," Phys. Rev. Vol. 113, No. 1, January 1, 1959 (72-8).

34. Loferski, J. J. and Rappaport, P., "Radiation Damage in Ge and Si Detected by Carrier Lifetime Changes: Damage Thresholds," Phys. Rev. Vol. 111, No. 2, July 15, 1958. (432-9).

35. Fan, H. Y. and Ramdas, A. K., "Infrared Absorption and Photoconductivity In Irradiated Silicon." J. Appl. Phys. Vol. 30, No. 8 August, 1959, (1127-34).

36. Wertheim, G. K., "Recombination Properties of Bombardment Defects in Semiconductors," J. Appl. Phys. Vol. 30, No. 8, August, 1959. (1166-74).

37. Geballe, T. H., "Radiation Effects in Semiconductors: Thermal Conductivity and Thermoelectric Power," J. Appl. Phys., Vol. 30, No. 8, August, 1959 (1153-7).

38. Curtis, O. L., "Radiation Effects on Recombination in Germanium," J. Appl. Phys. Vol. 30, No. 8, August, 1959 (1174-80).

39. Crawford, J. H. and Cleland, J. W., "Nature of Bombardment Damage and Energy Levels in Semiconductors," J. Appl. Phys. Vol. 30, No. 8 August, 1959 (1204-13).

40. Gossick, B. R., "Disordered Regions in Semiconductors Bombarded by Fast Neutrons," J. Appl. Phys. Vol. 30, No. 8, August, 1959 (1214-18).

41. Sonder, E., "Magnetic and Electrical Properties of Neutron-Irradiated Silicon," J. Appl. Phys. Vol. 30, No. 8, August, 1959 (1188-94).

42. Klein, C. A., "Radiation Induced Energy Levels in Silicon," J. Appl. Phys. Vol. 30 No. 8, August, 1959 (1222-31).

43. Holmes, D. K. and Leibfried, G., "Range of Radiation Induced Primary Knock-ons in the Hard Core Approximation," J. App. Phys. Vol. 31, June, 1960 (1046-56).

44. Loferski, J. J. and Rappaport, P., "Effect of Radiation on Silicon Solar Energy Converters," RCA Review, Vol. 19, December, 1958 (536-54).

45. Curtis, O. L., "Radiation Induced Recombination Centers in Germanium," J. Appl. Phys., Vol.29, December, 1958 (1722-9).

46. Schweinler, H. C., "Some Consequences of Thermal Neutron Capture in Silicon and Germanium," J. Appl. Phys, Vol. 30, August, 1959 (1125-6).

47. Kleinman, D. A., "Considerations on the Solar Cell," Bell System Tech. J., Vol. 40, January, 1961 (85-115).

48. Tannenbaum, M., and Mills, A. D., "Preparation of Uniform Resistivity N-Type Silicon by Nuclear Transmutation," Electrochem Soc J., Vol. 108, February, 1961 (171-6).

49. Shockley, W. and Quesser, H. J., "Detailed Balance Limit of Efficiency of P-N Junction Solar Cells," J. Appl. Phys. Vol. 32, March 1961 (510-19).

50. Dale, B. and Smith, F. P., "Spectral Response of Solar Cells," J. App. Phys., Vol. 32, No. 7, July, 1961 (1377-81).

51. Terman, L. M, "Spectral Response of Solar Cell Structures," Stanford Electronics Laboratories Technical Report No. 1605-1, September 21, 1959.

52. Lucovsky, G., "Photoeffects in Nonuniformly Irradiated P-N Junctions," J. Appl. Phys., Vol 31, No. 6, June, 1960 (1088-1095).

53. Murphy, J. A., "Biblioabstract on Effects of Nuclear Radiation on Semiconductors," General Electric Report No. 56GL209, August 1, 1956.

54. Junga, F. A., and Enslow, G. M. "Radiation Effects in Silicon Solar Cells," IRE Transactions on Nuclear Science, June, 1959 (49-53).

55. Thompson, J. C., "Survey of Nuclear Reactors and Irradiation Facilities and Bibliography of Research on Effects of Nuclear Radiation on Electronic Components and Materials," U. S. Navy Electronics Laboratory Research Report 1001, 4 November 1960.

56. Bobone, R., Langdon, W. R. and Merchant, B. W., "Summary Report: ADVENT Power System," GEL Report No. 61 GL205, November 30, 1961.

57. Bobone, R. and Torhune, J. H., "Spectral, Integrated and Local Response of Silicon Solar Cells," GEL Report on Advent Power System, APS Memo #119, December 6, 1960.

58. Mandelkorn, G. et al., "A New Radiation-Resistant High-Efficiency Solar Cell," USASRDL, Technical Report 2162, October, 1960.

59. Kallander, J. W. and Weller, J. F., "Radiation Behavior of Electrical Materials and Components for Space Vehicles," U.S. Naval Research Laboratory, Paper presented at Fifth Navy Science Symposium, Annapolis, Md., April 18, 1961.

60. Wysocki, J. J. et al, "High Temperature Dynamical Efficiency Photovoltaic Solar Energy Converter," RCA, Sixth Quarterly Progress Report, Contract DA-36-039-sc-78184, July 31, 1960.

61. Slater, J. C., "The Effects of Radiation on Materials," Journal of Applied Physics, Vol. 22, No. 3, March, 1951.

62. Harwood, J. J., Hausner, H. H., Morse, J. G., and Rauch, W. G., "The Effects of Radiation on Materials," Reinhold Publishing Corporation, New York, 1958.

63. Fraser, J. C., and Langdon, W. R., "The Correlation of Radiation Effects in Inorganic Materials," GEL Report for WSVD, 31 May 1961.